

DISSERTATION

THE VASCULATURE OF THE PARAVENTRICULAR NUCLEUS OF THE HYPOTHALAMUS:
INFLUENCE OF DEVELOPMENT, GAMMA-AMINOBUTYRIC ACID (GABA) RECEPTORS,
AND PRENATAL GLUCOCORTICIDS

Submitted by

Krystle A Frahm

Graduate Degree Program in Cell and Molecular Biology

In partial fulfillment of the requirements

For the Degree of Doctor of Philosophy

Colorado State University

Fort Collins, Colorado

Spring 2014

Doctoral Committee:

Advisor: Stuart Tobet

Michael Tamkun
Shane Hentges
Deborah Garrity

Copyright by Krystle Anne Frahm 2014

All Rights Reserved

ABSTRACT

THE VASCULATURE WITHIN THE PARAVENTRICULAR NUCLEUS OF THE HYPOTHALAMUS: INFLUENCE OF DEVELOPMENT, GAMMA-AMINOBUTYRIC ACID (GABA) RECEPTORS, AND PRENATAL GLUCOCORTICOIDS

The paraventricular nucleus of the hypothalamus (PVN) is a critical brain region that regulates many homeostatic and stress responses. In addition to its dense cytoarchitecture, it also contains a vast network of blood vessels. These blood vessels within the mouse PVN have a higher density than other brain regions, which develops postnatally. Loss of gamma aminobutyric acid (GABA) signaling or prenatal dexamethasone (dex) treatment decreased the blood vessel density. Dex also decreased blood brain barrier (BBB) competency while increasing desmin-immunoreactive pericytes at postnatal day (P)20. Long-term consequences included a decrease in GFAP contact with blood vessels selectively in dex-treated females, and an increase in depression-like behaviors in dex-treated males.

Chapter 2 examines the blood vessel density within the PVN. Initially the blood vessel density is similar than surrounding brain regions, then after P8 there was an increase that resulted in a highly vascularized network around P20. The highest densities were restricted to the rostral and mid regions of the PVN, where the neuroendocrine neurons are housed. In addition, mice lacking a functional GABA_B receptor had a significant decrease in blood vessel density in the mid region at P20.

The protein endocan has been proposed to be a “tip cell” marker, indicating angiogenesis. To further characterize the postnatal angiogenic period within the PVN, recently developed antibodies against endocan were used. Chapter 3 provides evidence that endocan is normally

expressed in the mouse brain but not restricted to tip cells. In addition, prior perfusion with fluorescein isothiocyanate (FITC) prevents endocan-immunoreactivity (ir) and provides a novel method for identifying non-functional blood vessels.

Chapters 4 and 5 show that excess fetal glucocorticoids alters the BBB within the PVN at two time points. At P20, there was a loss of BBB integrity accompanied by an increase in desmin-ir pericytes on a reduced blood vessel network due to dex-treatment for both prepubertal males and females. In contrast at P50, the blood vessel density and BBB were no longer disrupted following fetal dex-treatment. However, there was a decrease in glial fibrillary acidic protein (GFAP)-ir astrocytes in dex-treated females and an increase in desmin-ir pericytes in dex-treated males.

In conclusion, the work set forth in this dissertation indicates that the dense vascular network within the PVN develops postnatally and is susceptible to regulation by both exogenous and endogenous factors.

ACKNOWLEDGEMENTS

To my family: my parents Suzanne and Thomas, Gma Anna, Aunt Debbie and father Martin. Thank you for shaping me into who I am and supporting me along this path. Cameron and Kayla, my “real” friends, thank you for always being there for me and not letting the distance allow us to grow apart.

To Drs. Marilyn McGinnis, Augustus Lumia, Rebecca Cunningham, and James Roberts for introducing me to the field of research. I would also like to thank my committee members Michael Tamkun, Shane Hentges, and Deborah Garrity for their time and support. Also, Karen Solomon, Nancy Graham, Lori Williams, Erin Bisenius, Shazette Pierce for your help along the way.

To my mentor Dr. Stuart Tobet who worked tirelessly to improve my writing and critical thinking skills. I was lucky enough to sit at your lunch table at the Society for Neuroscience annual meeting and forever changed my life. Current and former members of the Tobet Lab, including but not limited to, Kristy McClellan, Gabe Knoll, Matthew Stratton, Cheryl Hartshorn, Chad Eitel, Pankaj Kumar, Brian Searcy, Chad Eitel, Qian Zhang, Melanie Schow, Connor Nash, Michelle Staros, Circe McDonald, and Colleen McCollum.

In no particular order, Reagan Pennock, Philip Fox, Elizabeth Akin, Shawna Matthews, Alejandro Trujillo, Christina Dennison, Rebecca Lossing, Krysta Chapin, Mallory Shields, An Dang, Albert Gonzales, Sara Neys, Brett Beal, Matthew Dicken, Caitlin Kelly, Krysta Chapin, Heather Hall for making my time at CSU thoroughly enjoyable.

TABLE OF CONTENTS

ABSTRACT.....	ii
ACKNOWLEDGEMENTS.....	iv
CHAPTER 1. INTRODUCTION.....	1
CHAPTER 2. GABAB RECEPTORS AND THE DEVELOPMENT OF THE PVN	
VASCULATURE	13
Overview.....	13
Introduction.....	14
Materials and Methods	16
Results.....	18
Discussion	20
References	29
CHAPTER 3. ENDOCAN IMMUNOREACTIVITY IN THE MOUSE BRAIN: METHOD FOR IDENTIFYING NONFUNCTIONAL BLOOD VESSELS	32
Overview.....	32
Introduction.....	33
Materials and Methods	35
Results.....	37
Discussion	38
References	46
CHAPTER 4. DEVELOPMENT OF THE BLOOD-BRAIN BARRIER WITHIN THE PARAVENTRICULAR NUCLEUS OF THE HYPOTHALAMUS: INFLUENCE OF FETAL GLUCOCORTICOID EXCESS	48
Overview.....	48
Introduction.....	49
Materials and Methods	51
Results.....	54
Discussion	58
References	70
CHAPTER 5. PRENATAL DEXAMETHASONE ALTERS THE COMPOSITION OF THE BLOOD-BRAIN BARRIER WITHIN THE PARAVENTRICULAR NUCLEUS OF THE HYPOTHAMUS OF ADULT MICE	73
Overview.....	73
Introduction.....	74
Materials and Methods	77
Results.....	81
Discussion	83
References	94
CHAPTER 6. DISCUSSION	99
REFERENCES	108

APPENDIX..... 121

LIST OF FIGURES

Figure 1.1 Image of blood vessels, pericytes and astrocytic endfeet in the mouse brain.....	7
Figure 1.2. Proposed model of postnatal blood vessel development along with alterations due to changes during embryonic development	12
Figure 2.1 Blood vessels within the paraventricular nucleus of the hypothalamus (PVN) across development and region.....	25
Figure 2.2. Changes in total length of blood vessels as a function of age, sex, paraventricular nucleus of the hypothalamus (PVN) region and GABA _B receptor function	26
Figure 2.3. Changes in blood vessels density in the paraventricular nucleus of the hypothalamus (PVN) as a function of GABA _B receptors.....	27
Figure 2.4. Changes in blood vessel length in the mid region of the paraventricular nucleus of the hypothalamus (PVN) and the cortex (CTX) at the lateral edge of the section as a function of GABA _B receptors	28
Figure 3.1. Immunoreactive endocan was distributed throughout the mouse brain at postnatal day 12	42
Figure 3.2. Immunoreactive endocan was distributed throughout the brain in C57BL/6J background mice on postnatal day 20	43
Figure 3.3. Immunoreactive endocan was distributed throughout the brain in FVB/N but not mixed C57BL/6J /S129/CBA background mice on postnatal day 20.....	44
Figure 3.4. Vascular perfusion of FITC allowed identification of cerebral vasculature, but blocked detection of endocan immunoreactivity	45
Figure 4.1. Postnatal blood-brain barrier development in the mouse cortex (CTX), lateral hypothalamus (LH) and paraventricular nucleus of the hypothalamus (PVN) at P12, P22 and P52.....	63
Figure 4.2. Postnatal desmin-immunopositive pericyte coverage in the mouse cortex (CTX), lateral hypothalamus (LH) and paraventricular nucleus of the hypothalamus (PVN) at P12, P22 and P52.....	64
Figure 4.3. Blood vessels in the paraventricular nucleus of the hypothalamus (PVN) were wider than in the mouse cortex (CTX) at P12 and P52	65
Figure 4.4. Prenatal exposure to dexamethasone (dex) impacted blood vessel density in the postnatal mouse paraventricular nucleus of the hypothalamus (PVN) at P20.....	66

Figure 4.5. Prenatal exposure to dexamethasone (dex) impacted blood-brain barrier development in the mouse cortex (CTX) and paraventricular nucleus of the hypothalamus (PVN) at P20	67
Figure 4.6. Prenatal exposure to dexamethasone (dex) impacted desmin-immunoreactive pericyte coverage in the mouse paraventricular nucleus of the hypothalamus (PVN) at P20	68
Figure 4.7. Regions selected for analysis	69
Figure 4.8. Analysis of vascular permeability	69
Figure 5.1. Prenatal exposure to dexamethasone (dex) does not impact blood vessel density within the mouse paraventricular nucleus of the hypothalamus (PVN) at P50	88
Figure 5.2. Prenatal exposure to dexamethasone (dex) impacted desmin-immunoreactive pericyte coverage in the male mouse paraventricular nucleus of the hypothalamus (PVN) at P50.....	89
Figure 5.3. Prenatal exposure to dexamethasone (dex) impacted total GFAP-immunoreactive astrocytes in the female mouse paraventricular nucleus of the hypothalamus (PVN) at P50	90
Figure 5.4. Prenatal exposure to dexamethasone (dex) impacted ir-GFAP surrounding blood vessels in the female mouse paraventricular nucleus of the hypothalamus (PVN) at P50.....	91
Figure 5.5. Prenatal exposure to dexamethasone (dex) does not impact the blood-brain barrier development in the mouse paraventricular nucleus at P50.....	92
Figure 5.6. Testing for depression-like behavior using the tail suspension test	93
Figure 6.1. Blood vessels maintained <i>in vitro</i>	105
Figure 6.2. Current model of postnatal blood vessel development along with alterations due to excess glucocorticoids during embryonic development in the paraventricular nucleus of the hypothalamus (PVN)	107

CHAPTER 1. INTRODUCTION

Currently, cardiovascular disease (CVD) is the leading cause of death in the United States and worldwide (Thayer et al., 2010). Individuals suffering from CVD are more likely to have the most prevalent mental disorder major depressive disorder (MDD; The World Health Report, 2001). This co-morbidity constitutes an approximate 20% population prevalence (Reviewed in Goldstein et al., 2014) and by 2020 is postulated to be the number one cause of disability worldwide (The World Health Report, 2001). To understand the etiology with hopes of reducing the incidence of MDD and CVD, independently and collectively, studies are needed to identify potential mechanisms.

A key brain region that may be involved in the comorbidity of CVD and MDD is the paraventricular nucleus of the hypothalamus (PVN; Baune et al., 2012; Goldstein et al., 2014). The PVN is an important locus for understanding disorders of the hypothalamic-pituitary-adrenal (HPA) axis with potential impact for mood disorders and other comorbid disorders with ties to PVN functions, including obesity and CVD (Brunton, 2010; Tobet et al., 2013). HPA axis activity is regulated through secretion of corticotropin-releasing hormone (CRH) and arginine vasopressin (AVP) from the PVN that act on the pituitary to release adrenocorticotrophic hormone (ACTH), which then stimulates the secretion of glucocorticoids from the adrenal cortex (Pariante, 2009). In addition to the HPA axis, neurons in the PVN integrate peripheral signals into a succinct neuronal response important for maintaining homeostasis, vasomotor tone, energy balance, and behavioral functions (Ferguson et al., 2008; Handa & Weiser, 2013; Swanson & Sawchenko, 1983). In a recent review, glucocorticoids were shown to change the neural circuitry within the PVN resulting in HPA dysregulation, similar to the effects observed in patients with depression (Levy & Tasker, 2012). The PVN also contains neurons that attenuate hypertension (Braga et al., 2011; Ferguson et al., 2008; Sriramula et al., 2011). For example,

an increase of the Na(+)-K(+)-2Cl(-) cotransporter-1 decreases gamma aminobutyric acid (GABA)ergic synaptic inhibition and increases the sympathetic drive from the PVN, which contribute to the development of hypertension (NKCC1; Ye et al., 2012). Therefore, the PVN may provide a site for cell-based mechanisms that underlie the co-morbidity of CVD and MDD.

The PVN is comprised of a number of different neuronal phenotypes that are critical for regulating many important functions that range from initiating flight or fight responses, maintaining homeostasis (Ferguson et al., 2008; Swanson et al., 1983) and regulating the physiological response to energetic challenges (Hill, 2012). The PVN is located in the anterior region of the hypothalamus situated along the dorsal portion of the third ventricle (Herman et al., 2005; Swanson & Sawchenko, 1983). In the rat it has a volume of approximately 0.5mm³ and contains approximately 100,000 neurons (Handa & Weiser, 2013). The PVN has a dense three-dimensional clustering of cells adjoining the dorsal portion of the third ventricle (Simmons & Swanson, 2009). The neurons of the PVN are characterized by their neuropeptides, including CRH, AVP, oxytocin (OT), thyrotropin-releasing hormone (TRH), somatostatin, and angiotensin (Armstrong et al., 1980; Biag et al., 2012; Ford-Holevinski et al., 1991; Handa & Weiser, 2013; Simmons & Swanson, 2009; Swanson and Sawchenko, 1983). Neurons within the PVN contain receptors for GABA, estrogens, androgens, glucocorticoids, and angiotensin II type 1 and many other signaling systems (Bingham et al., 2006; Fan et al., 2012; Lund et al., 2004; McClellan et al., 2010; Mitra et al., 2003). Individually and collectively these cell types and expressed receptors distinguish extensive cellular heterogeneity in the PVN. This emphasizes the need to understand the relationships among the diverse cellular elements of the PVN in maintaining homeostasis and initiating stress responses.

Neurons within the PVN can be grouped by their function (Biag et al., 2012; Handa & Weiser, 2013). One such group, referred to as neurosecretory parvocellular neurons, project their axons

to the median eminence and release CRH, AVP, TRH and somatostatin into the portal vasculature targeting the anterior pituitary. A second group is comprised of neurosecretory magnocellular neurons that have terminals that secrete OT and AVP into general circulation through fenestrated capillaries of the posterior pituitary. A third group of neurons are long-projecting and directly innervate the brainstem and spinal cord. The location of these neurons in the mouse varies throughout the PVN and parvocellular and magnocellular neurons are indistinguishable (Biag et al., 2012). By contrast in rats, they are grouped into subdivisions dependent on cell type and can be distinguished based on size (Handa & Weiser, 2013). In the mouse, the rostral and mid regions house the majority of the neurosecretory parvocellular and magnocellular CRH, OT, AVP, TRH and somatostatin neurons and the caudal portion holds the majority of long-projection neurons that provide autonomic innervation (Biag et al., 2012).

During fetal development, there are high levels of GABA_A and GABA_B receptors within the PVN, while surrounding the PVN are cells and fibers containing immunoreactive GABA (McClellan et al., 2010). Global deficiencies in GABA signaling through the loss of heterodimeric G protein coupled GABA_B receptors in mice results in decreased female reproductive function (Catalano et al., 2005), altered glucose homeostasis (Bonaventura et al., 2008), generalized epilepsy (Prosser et al., 2001), severe memory impairment (Schuler et al., 2001), increased anxiety-like behavior (Jacobson et al., 2007; Mombereau et al., 2005), and antidepressant-like behavior (Mombereau et al., 2005). These behavioral changes have been linked to inappropriate development of brain cytoarchitecture, including several hypothalamic components (McClellan et al., 2006; McClellan et al., 2008). Region-specific changes in cell position and the level of protein expression have been observed in a sex-dependent manner in mice lacking a functional GABA_B receptor. For example, within the PVN, mice lacking functional GABA_B receptors through a gene disruption of the R1 subunit (GABA_BR1) showed significant alterations in the locations of cells containing immunoreactive estrogen receptor alpha selectively in females and

a more widely distributed spread of immunoreactive neuronal nitric oxide synthase (nNOS) (McClellan et al., 2010). Changes in levels of immunoreactive proteins within the PVN have also been observed in GABA_BR1 knockout (KO) mice. There was decreased immunoreactive brain-derived neurotrophic factor (BDNF; McClellan et al., 2010) and an increase in immunoreactive CRH in the rostral PVN region in females (Stratton et al., 2011). GABA signaling within the PVN can also control sympathetic vasomotor tone and contribute to CVD (Li & Pan, 2007). These findings suggest that GABA is important to the development and regulation of neurons that come to reside in the PVN.

Among its dense cytoarchitecture, the PVN contains a 3-fold denser blood vessel matrix compared to surrounding brain regions across multiple species (Ambach & Palkovits, 1974; Finley, 1938; van den Pol, 1997). There is a lack of studies focused on the development of this dense vascular bed. Increases in PVN vascular density have been shown during postnatal development in male rats and differences in density were observed as a function of location within the nucleus rather than strictly aligning with magnocellular and parvocellular divisions (Menendez & Alvarez-Uria, 1987). While this dense vascular matrix has been known for some time (e.g. (Ambach & Palkovits, 1974; Basir 1931; Craigie, 1940; Finley, 1938; Poppi, 1928), its development and function have not been well characterized. Currently whether this unique vasculature plays a role in the development of CVD, MDD, or any other disorder remains unknown.

If the blood vessels within the PVN experience a postnatal angiogenic period in mice, when this occurs should be identified. Previous studies have shown endocan as a potential marker for angiogenesis (Roudnicky et al., 2013; Sarrazin et al., 2010). Endocan is a secreted proteoglycan and has been proposed as a biomarker for cancer. Recently, antibodies have

been developed for endocan, which may identify when the postnatal angiogenic period is occurring in the PVN (Frahm et al., 2013).

The blood vessels in the brain vary from those in the periphery. The brain receives 20% of cardiac output yet accounts for only 2% of body mass (Quaegebeur et al., 2011). These complex and highly regulated cerebral blood vessels exist to supply oxygen and nutrients to the brain while protecting it from potentially harmful items such as toxins and pathogens (Chip et al., 2013). What sets brain blood vessels apart is that a large portion of them maintain a restrictive barrier known as the blood-brain barrier (BBB). The purpose of the BBB is to regulate a microenvironment necessary for reliable neuronal signaling by protecting the brain from potentially harmful items such as toxins. The BBB consists of a continuous layer of endothelial cells, which form the walls of blood vessels, connected to one another through tight junctions. These tight junction proteins are the initial barrier and restrict permeability by forming a physical barrier composed of several different proteins including, but not limited to, the transmembrane claudins and occludins that are stabilized by linking to zonula occludens (Reviewed in Abbott et al., 2006; Hawkins & Davis, 2005; Iadecola, 2004; Saunders et al., 2013). Other components of the BBB include pericytes and astrocytic endfeet that surround endothelial cells (Hawkins & Davis, 2005). Changes in any of these components that together form the BBB could compromise its functional integrity.

Pericytes, first described in 1873, are also referred to as Rouget cells (Reviewed in Dore-Duffy & Cleary, 2011) and play a role in tight junction formation, structural stability, angiogenesis (Armulik et al., 2010; Daneman et al., 2010) as well as regulate vascular stability (Winkler et al., 2011). Pericytes have contractile properties that can regulate capillary diameter and blood flow through their finger-like processes that ensheath capillary walls (Iadecola, 2004; Winkler et al., 2011). Loss of pericytes results in an increased permeability of the BBB (Daneman et al.,

2010). Studies imply that during early prenatal development cross-talk between pericytes and astrocytes is essential but *in vivo* work is needed to corroborate this hypothesis (Bonkowski et al., 2011).

Astrocytes are glial cells that detect and modulate neuronal activity and blood vessel function through regulation of endothelial cells junctions and transport (reviewed in Daneman, 2012). Astrocytes have an enrichment of connexin 30 and 43, which form gap junction channels allowing ion and small molecule exchange between cells, which develop postnatally in the mouse (Ezan et al., 2012). Inhibition of astrogliogenesis during early postnatal development results in increased endothelial cell proliferation, blood vessel diameter and pericyte coverage (Ma et al., 2012). Astrocytic endfeet in close proximity to microvessel walls are specialized and contain aquaporin 4 and the Kir4.1 K(+) channel, which are important for maintaining ion and volume regulation (Abbott et al., 2006).

Recently, there has been a focus on expanding our understanding of the BBB in the context of communication with neurons. There are coordinated interactions that exist between neurons, astrocytes, and pericytes that are essential for the health and function of the central nervous system, referred to as the neurovascular unit (NVU; Hawkins & Davis, 2005). In adulthood, the NVU is formed by astrocytic endfeet and pericytes in close proximity to blood vessels (Saunders et al., 2013). Decreases in blood vessel density result in neuronal loss (Bell et al., 2010) and within the PVN this loss could potentially result in a wide range of diseases and disorders (Quaegebeur et al., 2011).

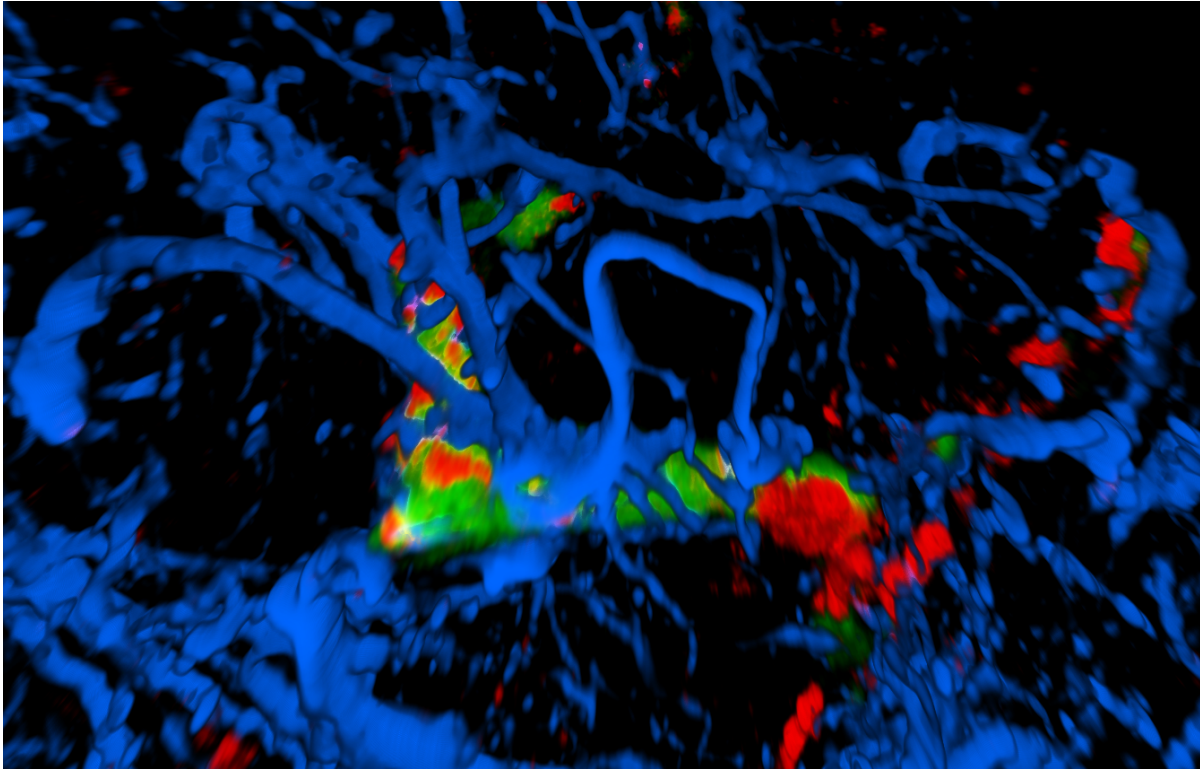


Figure 1.1. Image of blood vessels, pericytes and astrocytic endfeet in the mouse brain. High magnification of a blood vessel (green), surrounded by a pericyte (red) and ensheathed with astrocytic endfeet (blue).

Many assume that the BBB is uniform throughout the brain; however, markers for the BBB in rat endothelial cells show differential expression between venules and capillaries as well as between capillaries themselves (Saubamea et al., 2012). Some brain regions, such as the circumventricular organs (CVO), do not have a typical BBB. It is frequently stated that these regions lack a BBB (Norsted et al., 2008), but this is likely misleading. There are differences in vascular permeability to dye extravasation among the CVO (Morita & Miyata, 2012). One subset of CVOs had different vascular permeability for both low- and high-molecular-mass molecules than the others. Furthermore, all CVOs have a decrease in permeability compared to peripheral organs, indicating some maintenance of barrier function (Morita & Miyata, 2012). The CVOs have the ability to modulate their permeability. A recent study showed that changes in feeding state, such as fasting, increased permeability in a CVO known as the median

eminence (Langlet et al., 2013). Therefore, there is much work to be done to look at the BBB in a region-dependent manner and how it can vary.

The BBB can be modulated and its breakdown has been implicated in disease onset and progression (Dalkara et al., 2011; Gosselet et al., 2011; Hawkins & Davis, 2005; van Sorge & Doran, 2011). During inflammation, tight junctions can open, increase BBB permeability and contribute to edema (Abbott et al., 2006) while in patients with disease such as multiple sclerosis (Waubant, 2006), HIV, Parkinson's disease and Alzheimer's disease there is an associated BBB breakdown (Abbott et al., 2006). During adulthood in mice, loss of pericytes diminished cerebral blood flow and increased BBB breakdown resulted in neuronal degeneration (Bell et al., 2010). Spontaneously hypertensive rats exhibit increased BBB permeability allowing circulating angiotensin II to leak into the PVN (Biancardi et al., 2013). To determine if the physiological relevance of these findings, more context-dependent *in vivo* studies are needed.

One factor that contributes to CVD is prenatal stress (Maccari et al., 2003; Baum et al., 2003). In rodent studies, the synthetic glucocorticoid dexamethasone (dex) has been suggested to mimic at least one component of maternal stress (O'Regan et al., 2004). Prenatal exposure to dex has been shown to increase anxiety-like (Hossain et al., 2008) and depressive-like behaviors in adulthood (Roque et al., 2011). There are multiple ways that the developing brain can be exposed to excess levels of glucocorticoids. First, the glucocorticoid metabolizing enzyme 11 β -hydroxysteroid dehydrogenase type 2 (11 β -HSD2) is highly expressed in the placenta and fetus, and normally allows approximately 20% of maternal glucocorticoids to reach the fetus in an active form (Wyrwoll & Holmes, 2012; Zandi-Nejad et al., 2006). High levels of maternal stress, however, may decrease 11 β -HSD2 in the placenta and allow excess active glucocorticoids to reach the developing brain. Second, a low protein diet reduces 11 β -HSD2

increasing the ratio of active to inactive glucocorticoids reaching the developing fetus (Bertram & Hanson, 2002). Next, glucocorticoids are administered during early gestation (5-6 weeks) to mothers whose children are at high risk for congenital adrenal hyperplasia to prevent ambiguous genitalia if the fetus is female (Vos & Bruinse, 2010). Finally, the synthetic glucocorticoid dex (Liggins & Howie, 1972) has been administered since 1972 prior to preterm delivery to promote lung development and is currently administered in 12% of pregnancies (Damsted et al., 2011; Karemaker et al., 2008). Dex has high glucocorticoid receptor (GR) activity, low mineralocorticoid receptor activity, and a 90% bioavailability that peaks in plasma within 2 hours (Damsted et al., 2011). Concerning 11 β -HSD2, dex is a poor substrate and therefore not metabolized or affected by it (Holmes et al., 2006; Zandi-Nejad et al., 2006). While another synthetic glucocorticoid betamethasone has become the suggested standard (Lee et al., 2008), the key is that past, present and future patients have exposure to excess glucocorticoids during prenatal development. Therefore, increased glucocorticoids can and do reach the fetus, and impact normal development with long-lasting consequences for humans although the mechanisms are not well understood.

Prenatal stress has been implicated in causing long-term functional consequences such as depression-like behavior (Bale, 2005), hypertension (Levitt et al., 1996) and in humans alterations in HPA axis function (Wyrwoll & Holmes, 2012). More specifically, prenatal stress in rodents alters GR expression in the hippocampus, elevates levels of basal corticosterone (Levitt et al., 1996) and increases CRH mRNA within the PVN (Welberg et al., 2001). In humans, neonatal dex treatment blunts the cardiovascular stress response in children (Karemaker et al., 2008), but it is unknown if blood vessels in the PVN are also affected. If so, this could be a potential mechanism for dysfunction.

Glucocorticoids have been proposed to underlie adult disorders like depression (Wyrwoll & Homes, 2012) and at the level of the PVN results in HPA dysregulation (Levy & Tasker, 2012). Steroid hormones, like glucocorticoids, transmit extracellular signals into changes in gene activity (DeFranco, 1997). Glucocorticoids and dex bind to GR, and when the complex forms can then bind specific DNA sequences and trans-activate particular genes (reviewed in Forster et al., 2005). Glucocorticoids provide negative feedback for HPA axis regulation. This occurs through GR binding to negative glucocorticoid response element (nGRE) sites on the promoter of the proopiomelanocortin gene, which represses ACTH (Reviewed in Heitzer et al., 2007).

Concerning the vasculature, excess glucocorticoids modify the molecular composition of the BBB *in vivo* (Malaeb et al., 2007; Sadowska et al., 2009) and *in vitro* (Forster et al., 2005; Gu et al., 2009). Dex inhibits neovascularization (Nakamura et al., 1992) and alters the BBB by increasing tight junction proteins (Forster et al., 2005; Malaeb et al., 2007; Sadowska et al., 2009). After dex administration, BBB permeability rapidly decreases (Gu et al., 2009; Hedley-Whyte & Hsu, 1986). There is an increase in mRNA synthesis for the tight junction protein occludin in the presence of glucocorticoids. This is due to the presence of a putative GRE in the occludin promoter (Forster et al., 2005). Another tight junction protein claudin-5 in cell culture increases promoter activity and mRNA levels in response to dex (Burek & Forster, 2009). Dex treatment of brain endothelial cells increases expression of the drug efflux transporter P-glycoprotein in a development-dependent manner (Iqbal et al., 2011). Prenatal dex also changes the vascular area fraction in the hippocampus while increasing it in the amygdala (Neigh et al., 2010). Therefore, glucocorticoids can impact components of the BBB and blood vessel density but have not been studied in the context of the PVN. These findings may provide a novel mechanism related to the development of MDD and CVD as observed in humans.

To examine the dense PVN vasculature and whether it is susceptible to changes, Chapter 2 focuses on the postnatal blood vessel development of the PVN in the mouse. In addition, mice lacking functional GABA_B receptors were also studied and showed a decrease in vascular density providing evidence of vascular regulation for this region.

In trying to identify potential markers of angiogenesis, Chapter 3 examines endocan using recently developed monoclonal antibodies. Instead of being a marker for angiogenesis, immunoreactive endocan was present globally throughout the blood vessels in the brain. This is the first study to identify endocan in a non-disease state and suggests endocan is normally present within the brain. Also, prior perfusion with fluorescein isothiocyanate (FITC) prevents endocan-immunoreactivity (ir) and provides a novel method for identifying non-functional blood vessels.

To determine if excess glucocorticoids during development impacts the vascular network in the PVN, pregnant mice were treated with dex (E11-17) and their offspring were examined at P20 and P50. For both males and females there was a significant decrease in blood vessel density and an increase in extravascular FITC leakage and desmin immunoreactive (ir) pericyte coverage indicating a disrupted BBB at P20 within the PVN in Chapter 4. To establish if these were transient or maintained into adulthood, Chapter 5 examined blood vessel density, BBB competency, GFAP-ir astrocytes and desmin-ir pericytes within the PVN. There was a female-specific decrease in GFAP-ir in dex-treated females and an increase in desmin-ir in dex-treated males. However, there were no differences in density or BBB competency observed at P50. Therefore, prenatal exposure to excess glucocorticoids impacted the vasculature within the PVN in a sex-specific manner. In addition, both male and female mice exposed to excess glucocorticoids during prenatal development also displayed an increase in depression-like behavior demonstrating there are long-lasting behavioral consequences.

Overall, the work presented in this dissertation demonstrates that in addition to changes in neurons, PVN blood vessels are also regulated by GABA and glucocorticoids.

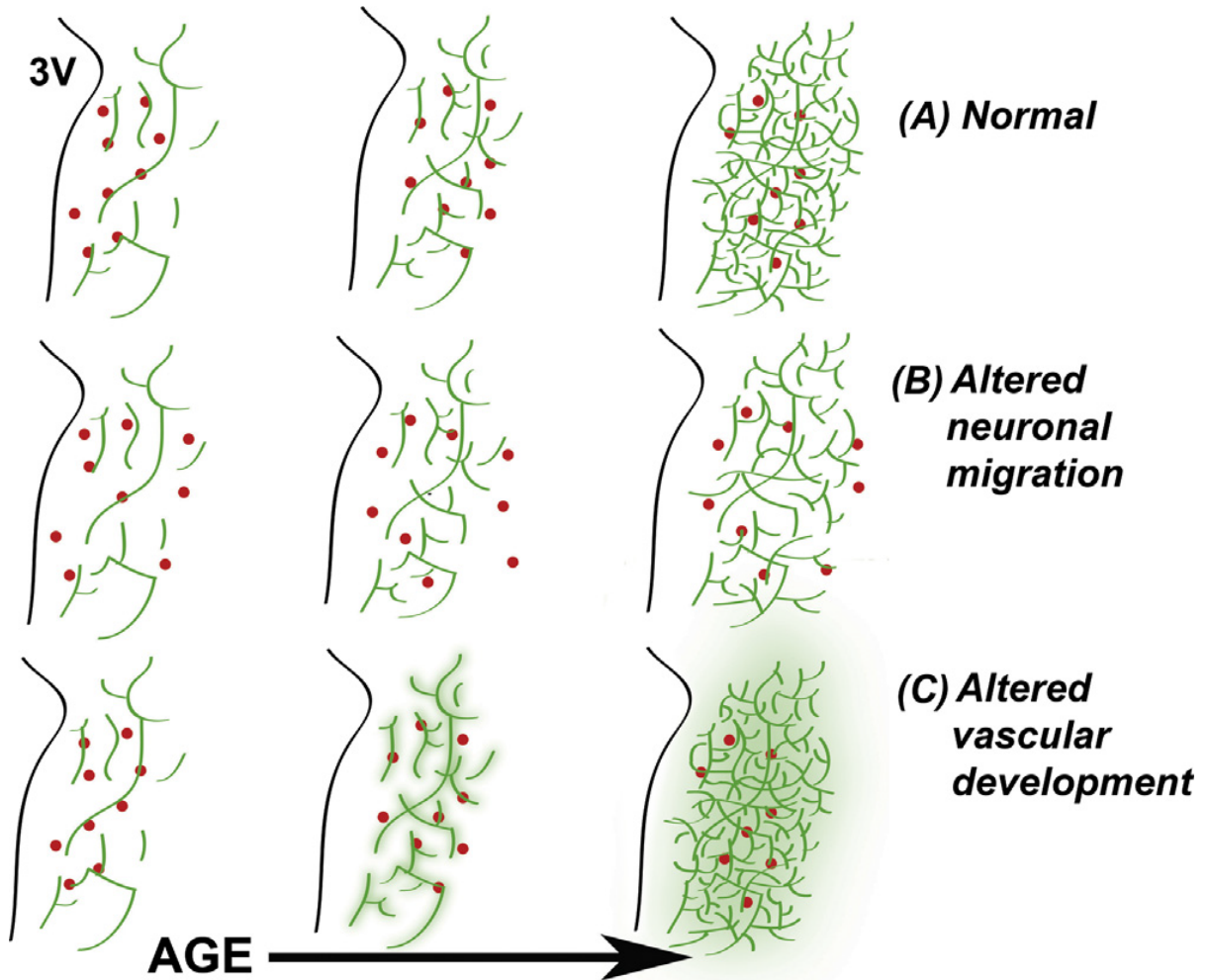


Figure 1.2. Proposed model of postnatal blood vessel development along with alterations due to changes during embryonic development. Neurons within the paraventricular nucleus of the hypothalamus (PVN) migrate laterally from the proliferative zone of the third ventricle (3V) with age followed by a postnatal angiogenic period that increases the blood vessel density by 40% (A). Changes in neuronal migration during development may impact the postnatal angiogenic period (B) and subsequently change in the vascular network (green lines) and blood-brain barrier in adulthood (C).

CHAPTER 2. THE VASCULATURE WITHIN THE PARAVENTRICULAR NUCLEUS OF THE HYPOTHALAMUS VARIES AS A FUNCTION OF DEVELOPMENT, SUB-NUCLEAR LOCATION, AND GABA SIGNALING

Overview

The paraventricular nucleus of the hypothalamus (PVN) is a cell group that plays important roles in regulating sympathetic vasomotor tone, food intake, neuroendocrine and autonomic stress responses and cardiovascular function. The developing PVN is surrounded by neuronal elements containing, and presumably secreting, gamma-aminobutyric acid (GABA). The vasculature of the adult PVN is notably denser than in other brain regions or in the PVN during perinatal development. To characterize the postnatal angiogenic process in mice, blood vessels were analyzed at P8, 20 and 50 in rostral, mid, and caudal divisions of the PVN in males and females. Vascular changes relative to disruption of the R1 subunit of the GABA_B receptor were evaluated at P8 and P20. For defined regions of interest within the PVN there were age dependent increases in blood vessel lengths and branching from P8 to 20 to 50 with the most notable increases in the middle region. Loss of GABA_B receptors did not influence vascular characteristics at P8 in any region, but by P20 there was significantly (20%) less blood vessel length and branching in the mid-PVN region versus wild type. These findings suggest that the loss of GABA_B signaling may lead to a late developing defect in angiogenesis. The loss of vascularity with defective GABA_B signaling suggests that neurovascular relationships in the PVN may be an important locus for understanding disorders of the hypothalamic-pituitary-adrenal axis with potential impact for psychiatric mood disorders along with other comorbid disorders that may be regulated by cells in the PVN.

Introduction

The paraventricular nucleus of the hypothalamus (PVN) is critically involved in regulating a number of homeostatic and behavioral functions. These include stress responses, energy balance, as well as autonomic nervous system regulation and neuroendocrine functions (Swanson & Sawchenko, 1983; Ferguson et al., 2008). Neurons located within the PVN have been characterized as containing a number of neuropeptides including corticotropin-releasing hormone (CRH), oxytocin (OT), thyrotropin-releasing hormone (TRH), and arginine vasopressin (AVP; Armstrong et al., 1980; Ford-Holevinski et al., 1991; Swanson & Sawchenko, 1983; Simmons & Swanson, 2009). Receptors for gamma aminobutyric acid (GABA), estrogens, androgens and glucocorticoids are also expressed throughout the brain and heavily within the PVN (Mitra et al., 2003; Lund et al., 2004, Bingham et al., 2006; McClellan et al., 2010). Individually and collectively these cell types and expressed receptors distinguish extensive cellular heterogeneity in the PVN.

Brain nuclei are characterized by the clustering of neurons into groups, which is the predominant organization for the hypothalamus. The PVN has a unique three-dimensional clustering of cells adjoining the dorsal portion of the third ventricle (Simmons & Swanson, 2009). Interestingly, the PVN can also be characterized by its dense vascularization (Ambach & Palkovitz, 1974; van den Pol, 1997). While this dense vascular matrix has been known for some time (e.g. Finley, 1938), its development and function has not been well characterized. One report using male rats indicated that the extensive vascularization occurs during postnatal development and may differ by region within the PVN (Menendez & Alvarez-Uria, 1987). The development of PVN vascular density has not been investigated in other species to our knowledge. The importance of examining multiple species is underscored by the several well-characterized differences in neuronal organization for the PVN between rats and mice (Kádár et

al., 2010; Biag et al., 2012). Given the potential that vascular developmental processes are susceptible to alterations, the current study examined the vascular development in the mouse PVN in the context of a disruption of GABA signaling as described below.

In adulthood, GABA is the major inhibitory neurotransmitter throughout the brain, however, during development GABA is usually excitatory and often morphogenetic (McClellan et al., 2006, 2008, 2010; Davis et al., 2002). Heterodimeric G protein coupled GABA_B receptors have been shown to be important for appropriate development of brain cytoarchitecture, including several hypothalamic components (McClellan et al., 2006, 2008). Recent studies have shown that loss of GABA signaling within the PVN through the GABA_B R1 leads to a decrease in levels of immunoreactive brain-derived neurotrophic factor (BDNF; McClellan et al., 2010) and region-specific differences in immunoreactive CRH levels (Stratton et al., 2011). In addition, mice lacking a functional GABA_B receptor show significant alterations in the locations of cells containing immunoreactive estrogen receptor alpha and neuronal nitric oxide synthase (nNOS; McClellan et al., 2010). Other developmental events are more dependent on GABA_A signaling (chloride channel) rather than GABA_B signaling, such as the migration of neurons containing gonadotropin releasing hormone (GnRH) from the nasal compartment into the brain (Tobet et al., 2001).

The current study examined the postnatal development of the vasculature within the PVN in mice. Rostral-to-caudal analysis showed differences in vascular density within the PVN that increased strongly in the second postnatal week. Finally, mice lacking a functional GABA_B receptor showed a decreased blood vessel density most strongly within the mid region of the PVN.

Materials and Methods

Animals

All mice were bred on a C57BL/6J background. GABA_B R1 subunit disrupted mice were generated through the insertion of a gene encoding β -galactosidase into the coding region of the R1 subunit (Prosser et al., 2001; McClellan et al., 2008). Mice were maintained in plastic cages with aspen bedding (autoclaved Sani-chips, Harlan Teklad, Madison, WI, USA) in the Painter Building of Laboratory Animal Resources at Colorado State University. Food (#8640, Harlan Teklad, Madison, WI, USA), tap water and environmental enrichment were provided ad libitum in a 14/10h light/dark cycle. Procedures for animal care and handling were approved by, and conducted in accordance with, the Colorado State University Institutional Animal Care and Use Committee guidelines.

The day of birth was designated postnatal day (P)0. Mice were deeply anesthetized by inhaling isoflurane (Vet One). Brains for analysis were removed and immersion fixed with 10 ml (P8) or 20 ml (P20) 4% paraformaldehyde in 0.1M phosphate buffer (pH 7.4) overnight. Brains were changed into 0.1M phosphate buffer for storage at 4°C prior to sectioning and processing for immunohistochemistry. Body weights were measured and sex determination was confirmed by PCR analysis for the *SRY* gene on the Y chromosome. Mice were genotyped for the GABA_B R1 knockout allele using a standard Taq polymerase PCR kit (Qiagen, Valencia, CA).

Animals per group are as follows: n=3 (P8 female KO, P8 male KO, P20 male KO) and n=4 (P8 female WT, P8 male WT, P20 female WT, P20 male: WT, P20 female KO).

Immunohistochemistry

Brains were embedded in 5% agarose and 50 μ m coronal sections were cut using a vibrating microtome (Leica VT1000S) at 4°C. Free-floating serial sections were processed as previously reported (Davis et al., 2002; Tobet et al., 1996) with slight modifications. Briefly, sections were collected in 0.05M phosphate-buffered saline (PBS), pH 7.5 and excess unreacted aldehydes were neutralized in 0.1M glycine for 30 minutes followed by 0.5% sodium borohydride for 15 minutes. Sections were washed in PBS then incubated in a PBS blocking solution (5% normal goat serum (NGS), 0.5% Triton X-100 (Tx), and 1% hydrogen peroxide) for at least 30 minutes. Sections were then incubated in primary antiserum directed against platelet endothelial cell adhesion molecule (PECAM also known as CD31, 1:30; BD Biosciences, San Jose, CA) in 1% BSA and 0.5% Tx. Sections were incubated for 2 nights at 4°C in primary antisera. Sections were then washed at room temperature with 1% NGS and 0.02% Tx in PBS. Sections were incubated for 2 hrs in a secondary biotin conjugated donkey anti-rat antiserum (1:1000; Jackson Immunoresearch, West Grove, PA) in PBS containing 1% NGS and 0.32% Tx. As a tertiary reaction, sections were incubated in a Vectastain reagent (3 μ l/ml solutions A and B - Vectastain ABC Elite kit; Vector Laboratories, Burlingame, CA) at room temperature for 1 hr. After 1 hr of washing in Tris-buffered saline (pH 7.5), reaction product was developed over 5min in Tris-buffered saline containing 0.025% diaminobenzidine, 0.02% nickel, and 0.02% hydrogen peroxide.

Analysis

Sections were viewed and images digitized using an Olympus BH2 microscope with an Insight QE digital camera in Spot Advanced Software. Using a 40x objective, 300 μ m x 224 μ m serial bilateral images were collected throughout the entire PVN. Images were processed to improve contrast using Adobe Photoshop (version CS for Macintosh). Total blood vessel length and the

number of branches were used to characterize the vasculature in each region of interest either within the PVN or in a lateral cortical control region. Branch points were manually counted and a bilateral average was calculated for each distinct PVN region (rostral, mid, and caudal). There was an average of 2 sections per region with a range of 1 to 3. There was no consistency in an increase or decrease in number of sections for a specific age, sex or genotype. For blood vessel length, images were light corrected (Image J, version 1.43u), analyzed for length using Angiogenesis Tube Formation (Metamorph, version 7.7.0.0, Molecular Devices, Inc.) For each animal both sides of the PVN and parietal cortex were quantified in each section. For each region a bilateral average was generated (rostral, mid, caudal) and the average value was taken for analysis. Statistical significance was determined by ANOVA as sex X genotype (wild type vs. knock out) X age (P8 vs. P20) X region as a repeated measure using SPSS software (SPSS Inc., Chicago, IL.). Values are reported as mean \pm SEM and $p < 0.05$ was considered significant.

Results

A few days after birth (P4) the vascular pattern of the PVN was similar in density to the surrounding hypothalamus and then proceeded to expand over the next 3 weeks as shown in females (Fig. 2.1A-E). Even approximately one week after birth (P8) the vasculature of the PVN was difficult to distinguish from the surrounding hypothalamus (Fig. 2.1B). However, by P12 there was a discernible increase in the vasculature within the PVN compared to surrounding brain regions (Fig. 2.1C). This increase in blood vessel density was expanded by weaning at P20 (Fig. 2.1D) and maintained past puberty into young adulthood on P50 (Fig. 2.1E).

Since there was a visible increase in blood vessel density within the PVN throughout development, we quantified two aspects of this density, vascular length and branching, throughout the rostral (Fig. 2.1F), mid (Fig. 2.1G), and caudal (Fig. 1H) aspects of the nucleus. The vascular pattern shown in a representative female clearly differed from rostral-to-caudal and the densest region was in the middle of the Nissl-defined nucleus at P12 (Fig 1G). There was a notable disparity in the most caudal region where the vasculature within the nuclear pattern discernible by Nissl-stain was not notably denser than in the surrounding hypothalamus (Fig. 1H).

Through development, there was an increase in blood vessel lengths within the PVN. Within the rostral, mid and caudal regions, collectively, there were notable increases in blood vessel length on P20 compared to P8 for both males and females (Fig. 2.2; $F(1,19) = 136.7$ $p < 0.001$). On P20, there was a significant 30% greater blood vessel length in the mid region as compared to the rostral and caudal ($F(2,13) = 23.7$, $p < 0.001$). In mice lacking a functional GABA_B receptor, there was a significantly greater blood vessel length within the total PVN on P20 as compared to P8 ($P < 0.05$). However, the mid region of the KO did not have the same increased level of blood vessel lengths in the mid region on P20 as observed in WT (Fig. 2.2). There was 20% less blood vessel length within the mid region in GABA_BR1 KO mice as compared to WT ($F(2,13)=4.95$, $p < 0.05$). This contrasts with a non-significant 13% decrease rostrally and a slight 4% increase caudally. This suggests that ineffective GABA_B signaling may have had an impact on the postnatal vascular pattern within the PVN.

There was an apparent decrease in blood vessel density at P20 in mice lacking a functional GABA_B receptor (Fig. 2.3B) compared to wild type (Fig. 2.3A). Blood vessel branch points were counted as another measure of vascular patterning at P20 between male and female wild type versus mice lacking a functional GABA_B receptor (Fig. 2.3C). There were a greater number of

blood vessel branch points in the mid region compared to the rostral or caudal regions ($F(2,10) = 4.8, p < 0.05$). Mice lacking a functional $GABA_B$ receptor had significantly less blood vessel branching within the mid region as compared to WT ($F(1,10) = 3.4, p < 0.05$). Results for branch points complemented the data for total blood vessel lengths. There were no significant differences in either parameter by sex.

To determine if blood vessel density was only altered locally or was impacted more globally, an identically sized region of interest was defined and analyzed in the parietal cortex (CTX) in the same sections (Fig. 2.4A-D). For CTX, there was a small (~10%), but significant, overall decrease in blood vessel length in both male and female mice lacking functional $GABA_B$ receptors (Fig. 2.4D) compared to male and female wild type (Fig. 2.4B; $F(1,10) = 27.9, p < 0.01$).

In addition to impacting the blood vessel density within the PVN, both male and female $GABA_B R1$ KO mice were 25% lighter when weighed prior to sacrifice on P20 with no evidence of a sex difference (WT = 8.1 ± 0.37 (n=8), KO = 6.03 ± 0.47 (n=7), $p < 0.05$) as previously observed (Prosser et al., 2001). There was no difference in body weight at P8 for sex or genotype (WT = 4.4 ± 0.21 (n=8), KO = 4.4 ± 0.37 (n = 6)).

Discussion

The PVN contains a number of different neuronal phenotypes that are critical for regulating many important functions that range from initiating flight or fight responses to maintaining homeostasis (Swanson & Sawchenko, 1983; Ferguson et al., 2008). The current study characterizes the development of the vasculature within the PVN in C57BL/6 mice. There is a

postnatal angiogenic period within the PVN that results in increased blood vessel density that is maintained into adulthood. Importantly, this increase is likely regulated by neural factors such as GABA. PVN vasculature was much less developed in mice in which GABA_B signaling was deficient. Such regulated changes in vascular patterning may lead to altered function in adulthood that can be traced back to PVN function.

PVN vasculature comparison: Rats versus Mice

A number of studies have characterized the dramatic blood vessel density within the adult PVN (e.g. van den Pol, 1997). In rats, there are 3-fold more blood vessels in the PVN (van den Pol, 1997) than in other brain regions. Increases in PVN vascular density have been noted during postnatal development in rats and differences in density were observed as a function of location within the nucleus rather than strictly aligning with magnocellular and parvocellular divisions (Menendez & Alvarez-Uria, 1987). This is consistent with results of the current study in mice where there was a postnatal increase in blood vessels, specifically the mid region, of the PVN. Though mice do not have distinct magnocellular/parvocellular divisions as in rats, the mid region does contain more neurons compared to rostral or caudal (Biag et al., 2012).

As a number of characteristics differ between rats and mice (Bonthuis et al., 2010), so too are their differences in PVN vascular development. Rats were reported to have a dramatic increase in blood vessel density (5 times) in the PVN on the day of birth that decreased quickly by P2 (1.5 times). This was followed by a more persistent increase that resulted in a final 3-fold difference compared to other brain regions (Menendez & Alvarez-Uria, 1987). Based on the results of the current study, mice do not have an initial increase followed by a decrease in blood vessel density around postnatal day 2 (Menendez & Alvarez-Uria, 1987) suggesting the factors responsible for the postnatal angiogenic period in mice that starts around P8 may be delayed compared to the expression in rats.

Potential Consequences

The physiological roles of this postnatal increase in blood vessel density within the PVN remain unknown. It has been suggested that the greater vascularization of the PVN does not lead to a high basal metabolic capacity of the neurons (Badaut et al., 2000). The level of blood flow through the PVN is similar to surrounding brain regions even though related to other regions it has a high vascular network that is hypothesized to serve as a large reserve capacity for blood flow (Badaut et al., 2000). However, significantly fewer blood vessels within the PVN as seen in GABA_BR1 KO mice may reduce accessibility to oxygen and nutrients and impact a neurons ability to effectively relay its metabolic needs (Gyurko et al., 2002). It has been hypothesized that the vast blood vessel network of the PVN may be used to detect plasma osmotic pressure by magnocellular neurons (Badaut et al., 2000) that are abundant in the mid region in mice (Biag et al., 2012). A decrease in vasculature may result in PVN neurons not being able to provide proper feedback resulting in dysfunction. It is unclear whether other mechanisms altered in the GABA_BR1 KO mice may be responsible for this decrease in blood vessel development. However, examining the development of the PVN from neuronal to vascular may provide insight to function as well as help delineate dysfunction.

In the current study the loss of GABA_B function through deletion of the R1 subunit resulted in decreased vascular density within a restricted portion of the PVN and a region of the parietal cortex. For the PVN, it is notable that this decrease in blood vessel density was spatially restricted to the mid region, which has the densest neuronal packing viewable by Nissl-stain (Biag et al., 2012). Changes in cell position and the level of protein expression in a region-specific manner have been observed in mice lacking a functional GABA_B receptor (McClellan et al., 2010; Stratton et al., 2011). GABA modulates immunoreactive CRH specifically in the rostral PVN based on GABA_BR1 KO female mice having increased levels of immunoreactive CRH compared to controls (Stratton et al., 2011). For the central, or mid PVN, GABA_BR1 KO

mice had immunoreactive nNOS that was more widely distributed spatially than in controls (McClellan et al., 2010). Interestingly, there has been no indication of an influence of genetic disruption of nNOS itself on neuronal or vascular characteristics in the PVN (unpublished observations) in mice for which the loss of NOS activity is complete (Gyurko et al., 2002). Since the mid region of the mouse houses the majority of CRH, OT, AVP, TRH and somatostatin neurons as compared to the rostral or caudal regions (Biag et al., 2012), changes in vascular characteristics may alter their ability to respond properly to signals from the periphery.

Decreases in blood vessel density in the cortex of GABA_BR1 KO mice show the potential global importance of the neurovascular relationship. These mice are lighter than wild type and have changes in reproduction (Catalano et al., 2005), altered glucose homeostasis (Bonaventura et al., 2008), develop generalized epilepsy (Prosser et al., 2001), demonstrate an increase in anxiety-like behavior (Jacobson et al., 2007; Mombereau et al., 2005), and show antidepressant-like behavior (Mombereau et al., 2005). Whether these are direct or indirectly tied to changes in brain vascular function remains to be determined.

GABA impacts the second angiogenic period

The initial vascular development of the PVN was not disturbed due to altered GABA_B signaling. On P8, there were no significant differences for blood vessel lengths or the number of branch points between the Nissl-defined PVN in the rostral, mid or caudal region of the PVN compared to the surrounding hypothalamus. This might suggest that the most important period for GABA_B signaling is during the postnatal period when vessel expansion normally begins. However, it is too early to rule out fetal antecedent events that could still play important roles. Cells containing estrogen receptor alpha, nNOS and BDNF are already disrupted to differing extents at birth (McClellan et al., 2010) and malfunctions in these cells (or others) may interact with specific angiogenic factors selectively at the later time points. Studies are needed to examine changes

in factors known to influence vascular development and plasticity, such as vascular endothelial growth factor, to shed light on why GABA_BR1 KO mice do not undergo a robust angiogenic period as compared to wild type.

In summary, the results of the current study show a progressive postnatal angiogenic period with the greatest increase in blood vessel density occurring in the mid region in the mouse PVN. In addition, the data suggest that the loss of GABA_B signaling may lead to a late developing defect in PVN angiogenesis. The relative decrease of vascularity with defective GABA_B signaling suggests that neurovascular relationships in the PVN may be an important locus for understanding disorders of the hypothalamic-pituitary-adrenal axis with potential impact for mood disorders and other comorbid disorders with ties to PVN functions, including obesity and cardiovascular disease (Brunton, 2010).

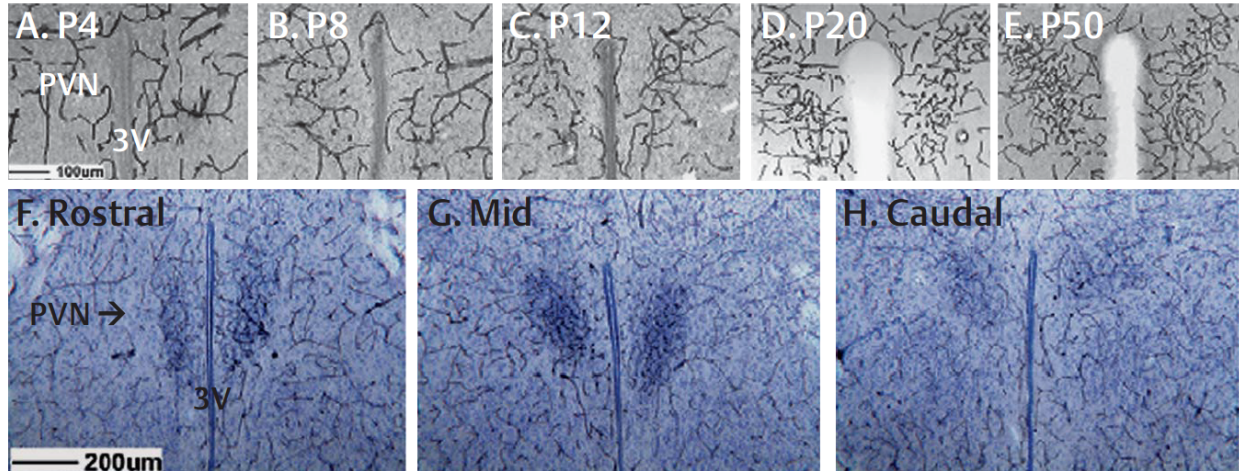


Figure 2.1. Blood vessels within the paraventricular nucleus of the hypothalamus (PVN) across development and region. Digital images in females (A-E) show that during early postnatal development, on P4 (A) and P8 (B), the blood vessel pattern was indistinguishable from the surrounding regions. By P12 (C) there was a dramatic increase in blood vessel density within the PVN compared to the surrounding regions. On P20 (D) and into young adulthood on P50 (E), the increase in vasculature was maintained. Representative digital images (F-G) of 50µm sections from a P12 female illustrate that the rostral (F) and mid (G) PVN were dense in neuronal elements (Nissl-stain) and blood vessels (PECAM immunoreactive) compared to surrounding brain regions. For the caudal region (H) of the PVN, the density of neuronal elements easily illuminates the nucleus, but the vascular density was more similar to the surrounding hypothalamus. The scale bar (100µm) shown in lower left corner panel A applies to panels A-E. The scale bar (200µm) in the lower left corner of panel F applies to panels F-H.

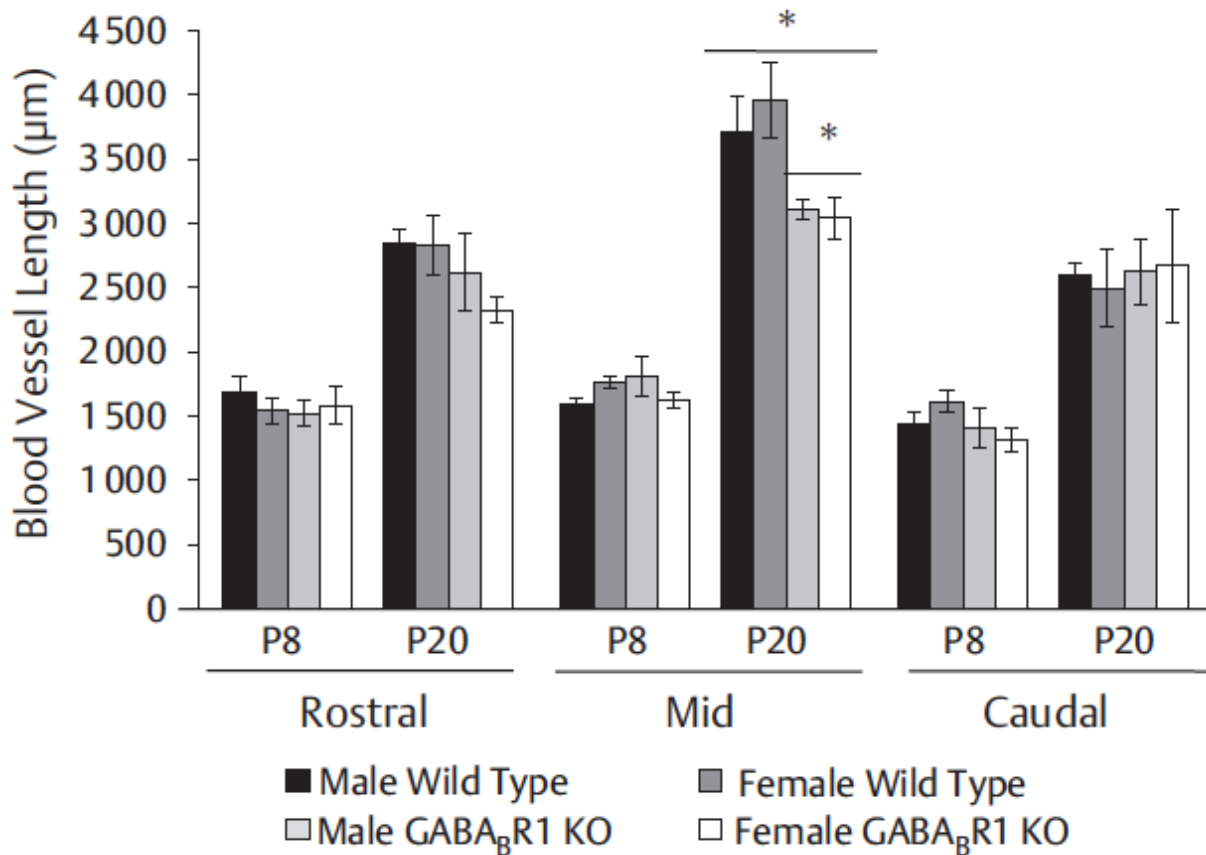


Figure 2.2. Changes in total length of blood vessels as a function of age, sex, paraventricular nucleus of the hypothalamus (PVN) region and GABA_B receptor function. The graph illustrates changes in total length of blood vessels as a function of age, sex, PVN region, and GABA_B receptor status. For WT, there were significantly greater blood vessel lengths in rostral, mid, and caudal regions at P20 as compared to P8 ($p < 0.05$). On P20, there was also a significantly greater blood vessel length in the mid region of the PVN as compared to the rostral or caudal regions ($p < 0.05$). Mice lacking a functional GABA_B receptor had significantly less blood vessel length in the mid region compared to wild type ($p < 0.05$). There was no significant difference in total blood vessel length on P8 for genotype or PVN region.

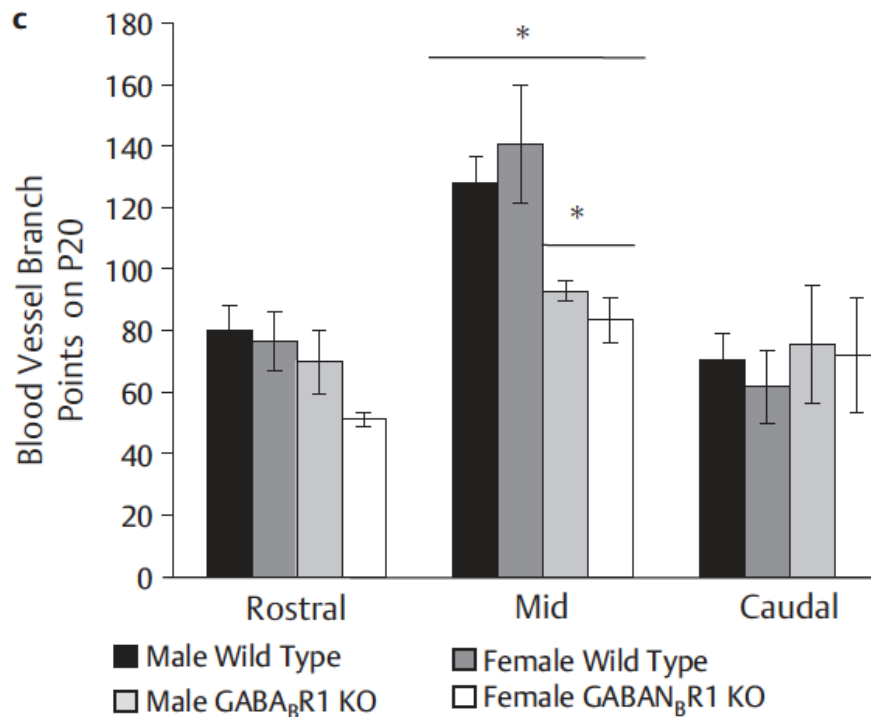
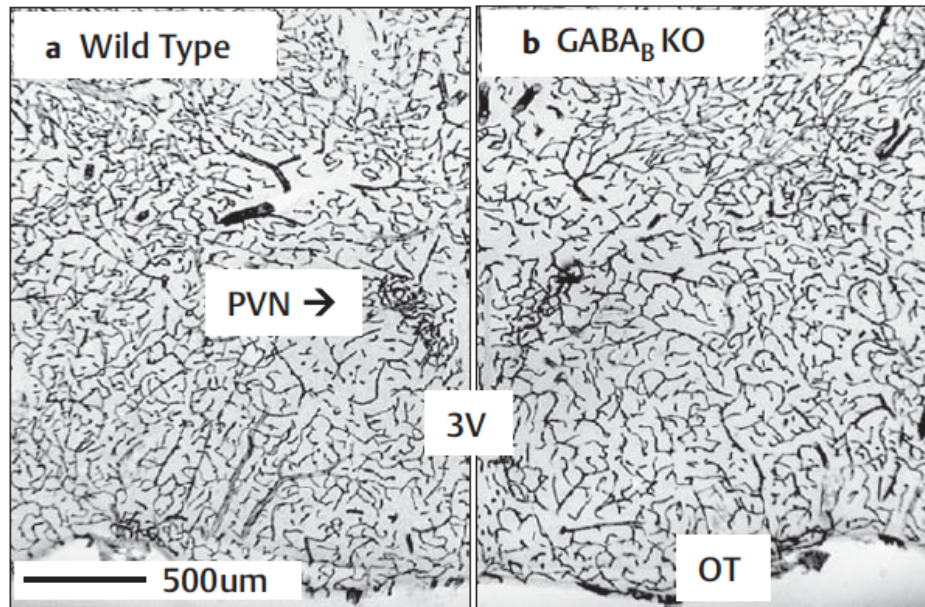


Figure 2.3. Changes in blood vessels density in the paraventricular nucleus of the hypothalamus (PVN) as a function of GABA_B receptors. Images (A-B) show a representative mid PVN region in wild type (A) and in mice lacking a functional GABA_B receptor (B) on P20. Matched sections using immunoreactive platelet endothelial cell adhesion molecule (PECAM) to visualize blood vessels show a decrease in blood vessel density for mice lacking functional GABA_B receptors compared to wild type. The graph (C) shows on P20 there was significantly greater blood vessel branching in the mid region as compared to rostral or caudal for both males and females ($p < 0.05$). Mice lacking a functional GABA_B receptor had significantly less blood vessel branching in the mid region compared to wild type ($p < 0.05$). The scale bar (500µm) shown in lower left corner panel A applies to panels A-B.

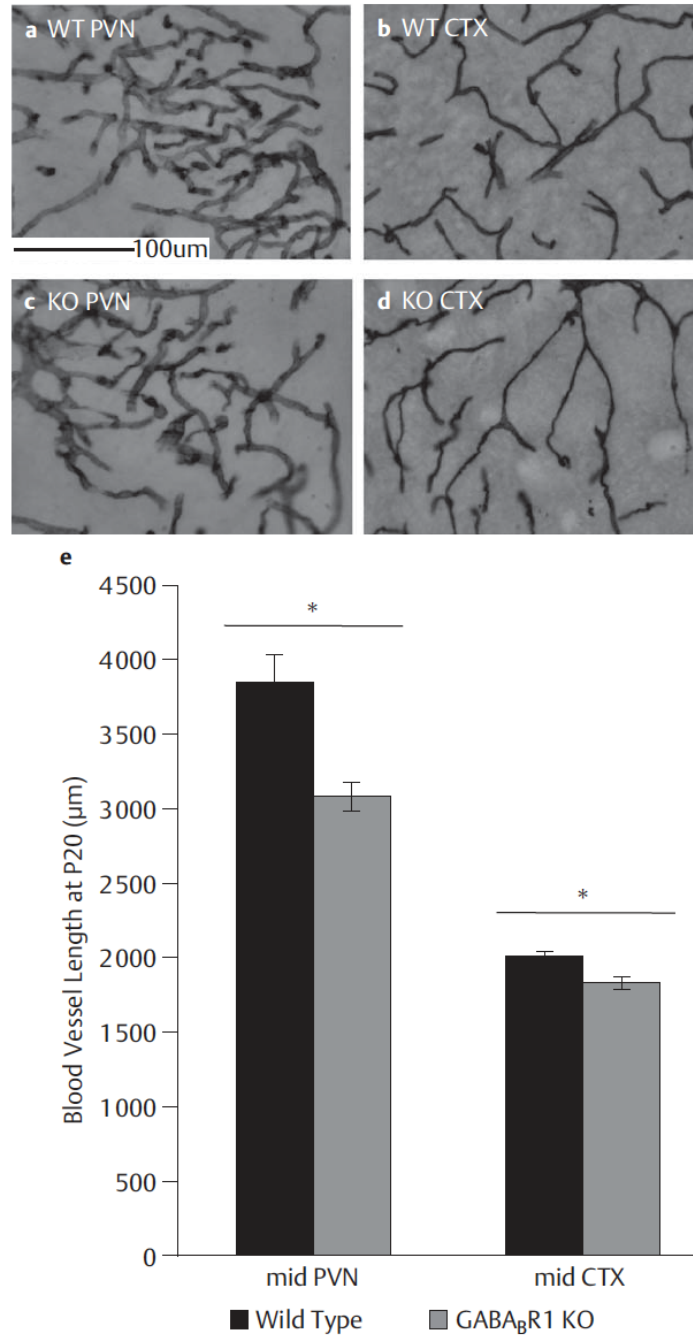


Figure 2.4. Changes in blood vessel length in the mid region of the paraventricular nucleus of the hypothalamus (PVN) and the cortex (CTX) at the lateral edge of the section as a function of GABA_B receptors. Images (A-D) on P20 show a decrease in blood vessel density for mice lacking functional GABA_B receptors (C-D) compared to wild type (A-B) in mid sections of the PVN (A, C), and CTX (B, D). The graph (E) shows on P20, there were significantly less blood vessel lengths in mice lacking a functional GABA_B receptor in the PVN and CTX compared to wild type ($p < 0.05$). In the mid region, the PVN contains more blood vessels than the CTX. The decrease in blood vessel length in GABA_B R1 subunit KO mice was twice as great in the PVN compared to the CTX. The scale bar (100 μm) shown in lower left corner panel A applies to panels A-D.

References

- Ambach G, Palkovits M. Blood supply of the rat hypothalamus. II. Nucleus paraventricularis. *Acta Morphol Acad Sci Hung*. 1974; 22: 311-320
- Armstrong WE, Warach S, Hatton G I, McNeill TH. Subnuclei in the rat hypothalamic paraventricular nucleus: a cytoarchitectural, horseradish peroxidase and immunocytochemical analysis. *Neuroscience* 1980; 5: 1931-1958
- Badaut J, Nehlig A, Verbavatz J, Stoeckel M, Freund-Mercier M, Lasbennes F. Hypervascularization in the Magnocellular Nuclei of the Rat Hypothalamus: Relationship with the Distribution of Aquaporin-4 and Markers of Energy Metabolism. *J Neuroendocrinol* 2000; 12: 960-969
- Biag J, Huang Y, Gou L, Askarinam A, Hahn JD, Toga AW, Hintiryan H, Dong HW. Cyto- and chemoarchitecture of the hypothalamic paraventricular nucleus in the C57BL/6J male mouse: A study of immunostaining and multiple fluorescent tract tracing. *J Comp Neurol* 2012; 520
- Bingham B, Williamson M, Viau V. Androgen and estrogen receptor-beta distribution within spinal-projecting and neurosecretory neurons in the paraventricular nucleus of the male rat. *J Comp Neurol* 2006; 499:911-923
- Bonaventura MM, Catalano PN, Chamson-Reig A, Arany E, Hill D, Bettler B, Saravia F, Libertun C, Lux-Lantos VA. GABAB receptors and glucose homeostasis: evaluation in GABAB receptor knockout mice. *Am J Physiol Endocrinol Metab* 2008; 294: 157-167
- Bonthuis PJ, Cox KH, Searcy BT, Kumar P, Tobet S, Rissman EF. Of mice and rats: key species variations in the sexual differentiation of brain and behavior. *Front Neuroendocrinol* 2010; 31: 341-358
- Brunton PJ. Resetting the dynamic range of hypothalamic-pituitary-adrenal axis stress responses through pregnancy. *J Neuroendocrinol* 2010; 22: 1198-121
- Catalano PN, Bonaventura MM, Silveyra P, Bettler B, Libertun C, Lux-Lantos VA. GABA(B1) knockout mice reveal alterations in prolactin levels, gonadotropic axis, and reproductive function. *Neuroendocrinology* 2005; 82: 294-305
- Davis AM, Henion TR, Tobet SA. Gamma-aminobutyric acidB receptors and the development of the netromedial nucleus of the hypothalamus. *J Comp Neurol* 2002; 449: 270-280
- Ferguson AV, Latchford, KJ, Samson WK. The paraventricular nucleus of the hypothalamus – a potential target for integrative treatment of autonomic dysfunction. *Expert Opin Ther Targets* 2008; 12: 717-721
- Finley KH. The capillary bed of the paraventricular and supraoptic nuclei of the hypothalamus. *Res Publ Assoc Res Nerv Ment Dis* 1938, 18: 94-109

- Ford-Holevinski TS, Castle MR, Herman JP, Watson SJ. Microcomputer-based three-dimensional reconstruction of in situ hybridization autoradiographs. *J Chem Neuroanat* 1991; 4:373-385
- Gyurko R, Leupen S, Huang PL. Deletion of exon 6 of the neuronal nitric oxide synthase gene in mice results in hypogonadism and infertility. *Endocrinology* 2002; 143: 2767-2774
- Jacobson LH, Bettler B, Kaupmann K, Cryan JF. Behavioral evaluation of mice deficient in GABA(B(1)) receptor isoforms in tests of unconditioned anxiety. *Psychopharmacology* 2007; 190: 541-553
- Kádár A, Sánchez E, Wittmann G, Singru PS, Füzesi T, Marsili A, Larsen PR, Liposits Z, Lechan RM, Fekete C. Distribution of hypophysiotropic thyrotropin-releasing hormone (TRH)-synthesizing neurons in the hypothalamic paraventricular nucleus of the mouse. *J Comp Neurol* 2010; 518: 3948-3961
- Lund TD, Munson DJ, Haldy ME, Handa RJ. Androgen inhibits, while oestrogen enhances, restraint-induced activation of neuropeptide neurones in the paraventricular nucleus of the hypothalamus. *J Neuroendocrinol* 2004; 16: 272-278
- McClellan KM, Calver AR, Tobet SA. GABAB receptors role in cell migration and positioning within the ventromedial nucleus of the hypothalamus. *Neuroscience* 2008; 151: 1119-1131
- McClellan KM, Parker KL, Tobet SA. Development of the ventromedial nucleus of the hypothalamus. *Front Neuroendocrinol* 2006; 27: 193-209
- McClellan KM, Stratton MS, Tobet SA. Roles for gamma-aminobutyric acid in the development of the paraventricular nucleus of the hypothalamus. *J Comp Neurol* 2010; 518: 2710-2728
- Menendez A, Alvarez-Uria M. The development of vascularization in the postnatal rat paraventricular nucleus: a morphometric analysis. *J Hirnforsch* 1987; 28: 325-329
- Mitra SW, Hoskin E, Yudkovitz J, Pear L, Wilkinson HA, Hayashi S, Pfaff DW, Ogawa S, Rohrer SP, Schaeffer JM, McEwen BS, Alves SE. Immunolocalization of estrogen receptor beta in the mouse brain: comparison with estrogen receptor alpha. *Endocrinology* 2003; 144: 2055-2067
- Mombereau C, Kaupmann K, Gassmann M, Bettler B, van der Putten H, Cryan JF. Altered anxiety and depression-related behaviour in mice lacking GABAB(2) receptor subunits. *Neuroreport* 2005; 16: 307-310
- Prosser HM, Gill CH, Hirst WD, Grau E, Robbins M., Calver A, Soffin EM, Farmer CE, Lanneau C, Gray J, Schenck E, Warmerdam BS, Clapham C, Reavill C, Rogers DC, Stean T, Upton N, Humphreys K, Randall A, Geppert M, Davies CH, Pangalos MN. Epileptogenesis and enhances prepulse inhibition in GABA(B1)-deficient mice. *Mol Cell Neurosci* 2001; 17: 1059-1070
- Quaegebeur A, Lange C, Carmeliet P. The neurovascular link in health and disease: molecular mechanisms and therapeutic implications. *Neuron* 2011; 71: 406-424
- Simmons DM, Swanson LW. Comparison of the spatial distribution of seven types of neuroendocrine neurons in the rat paraventricular nucleus: toward a global 3D model. *J Comp Neurol* 2009; 516:423-441

Stratton MS, Searcy BT, Tobet SA. GABA regulated corticotropin releasing hormone levels in the paraventricular nucleus of the hypothalamus in newborn mice. *Physiol Behav* 2011; 104: 327-333

Swanson LW, Sawchenko PE. Hypothalamic integration: organization of the paraventricular and supraoptic nuclei. *Annu Rev Neurosci* 1983; 6: 269-324

Tobet SA, Bless EP, Schwarting GA. Developmental aspects of the GnRH neuronal system. *Mol Cell Endocrinol* 2001; 185: 173-184

Tobet SA, Chickering TW, King JC, Stopa EG, Kim K, Kuo-Leblank V, Schwarting GA. Expression of gamma-aminobutyric acid and gonadotropin-releasing hormone during neuronal migration through the olfactory system. *Endocrinology* 1996; 137: 5415-5420

van den Pol AN. GABA immunoreactivity in hypothalamic neurons and growth cones in early development *in vitro* before synapse formation. *J Comp Neurol* 1997; 383: 178-188

CHAPTER 3. ENDOCAN IMMUNOREACTIVITY IN THE MOUSE BRAIN: METHOD FOR IDENTIFYING NONFUNCTIONAL BLOOD VESSELS

Overview

Endocan is a secreted proteoglycan that has been shown to indicate angiogenic activity: remodeling in several tumor types in humans and mice. Serum endocan levels also indicate prognosis and has been proposed as a biomarker for certain cancers. Recently, monoclonal antibodies directed against mouse endocan have been developed allowing for further characterization of endocan function and potentially as a marker for angiogenesis through immunoreactivity in endothelial tip cells. The results of the current study show that endocan immunoreactivity in the mouse brain is present in blood vascular networks including but not limited to the cortex, hippocampus and paraventricular nucleus of the hypothalamus in C57BL/6J and FVB/N mice. Endocan immunoreactivity did not vary during postnatal development or by sex. Interestingly, after vascular perfusion with fluorescein isothiocyanate (FITC), endothelial cells positive for FITC were immunonegative for endocan suggesting FITC interference with the immunohistochemistry. A small number of FITC-negative blood vessels were endocan immunoreactive suggesting the identification of new blood vessels that are not yet functional. The current study shows that endocan is normally present in the mouse brain and prior vascular perfusion with FITC may provide a useful tool for identify newly forming blood vessels.

Introduction

Endocan, previously known as endothelial cell-specific molecule-1 (ESM-1), was identified with its localization restricted to endothelial cells (Lassalle et al., 1996). Endocan is a secreted dermatan sulfate proteoglycan that has been suggested to promote angiogenesis (Chen et al., 2012). Elevated levels of endocan mRNA negatively correlate with cancer survival rates and overexpression of endocan leads to tumor formation (Scherpereel et al., 2003; Depontieu et al., 2012). High endocan mRNA levels in human tumor tissue correlates with prognosis and is proposed to serve as a biomarker for inflammatory disorders and cancer development and continues to be investigated as a target for cancer therapy (Sarrazin et al., 2006). Increased levels of endocan have been detected in the serum of sepsis patients (Sarrazin et al., 2006; Sarrazin et al., 2010; Scherpereel et al., 2003). Overall, endocan has shown promise as an indicator of angiogenesis and disease progression.

Endocan has also been studied in activated endothelial cells referred to as tip cells, which indicate newly forming blood vessels (Sarrazin et al., 2010, Del Toro et al. 2010). Endocan mRNA is upregulated on tumor-associated blood vessels and it is proposed that modification of endocan interactions with vascular endothelial growth factor receptors may inhibit tumor angiogenesis (Roudnicky et al., 2013). However, beyond its detection in endothelial cells undergoing angiogenesis, the role of endocan is not well understood.

To visualize and characterize endocan distributions, monoclonal antibodies were generated to study roles in angiogenesis, cancer, and other diseases. Antibody clones MEP14 and MEP19 were generated against the C-terminus of human endocan and recognize both rat and mouse endocan. (Depontieu et al, 2012). The generation of these antibodies may provide a useful tool

to characterize changes in the distribution or levels of immunoreactive endocan under normal or disease states, and potentially its function.

The goal of the current study was to use selective antibodies directed against endocan to study the developing blood vessel network within the paraventricular nucleus of the hypothalamus (PVN). The PVN develops an unusually dense vasculature following a postnatal angiogenic period that occurs between postnatal (P) days 8-12 in the mouse (Frahm et al., 2012). The current study examined endocan as a potential marker for angiogenesis, which within the PVN may be coordinated with the postnatal angiogenic period.

In examining blood vessels and blood-brain barrier competency, several studies have utilized the small molecule dye fluorescein isothiocyanate (FITC). When perfused through the vasculature, FITC accumulates in endothelial cell nuclei and binds covalently to cellular components (Miyata & Morita, 2011). This allows for visualization of functional blood vessels and the ability to double or triple label for other proteins of interest in relevant vasculature. Extravascular FITC leakages can also indicate a compromised blood-brain barrier (Miyata & Morita, 2011). Mouse brains were processed for endocan with or without prior vasculature perfusion of FITC.

Overall, the current experiments demonstrated that immunoreactive endocan is present in a pattern that mirrors the vasculature throughout the brain only in certain mouse strains. Prior vascular perfusion with FITC prevented detection of immunoreactive endocan. Therefore, the use of FITC may provide a novel method to identify non-functional blood vessels using immunoreactive endocan as a marker.

Materials and Methods

Animals

Male and female mice were on a mixed C57BL/6JxS129xCBA background (Solomon et al., 2012), or pure bred C57BL/6J or FVB/N backgrounds. The day of birth was designated P0. For tissue collection, mice were anesthetized by ketamine (80 mg/kg) and xylazine (8 mg/kg) and transcardially perfused with heparanized PBS with or without FITC (ThermoFisher Scientific, MW 389.38) followed by 4% paraformaldehyde in 0.1M phosphate buffer (pH 7.4; modified from Miyata & Morita, 2011). Brains were removed, post fixed overnight, then changed into 0.1M phosphate buffer for storage at 4°C.

Mice were maintained in plastic cages with aspen bedding (autoclaved Sani-chips, Harlan Teklad, Madison, WI, USA) in the Painter Building of Laboratory Animal Resources at Colorado State University. Food (#8640, Harlan Teklad, Madison, WI, USA) with filtered tap water and environmental enrichment was provided ad libitum in a 14/10h light/dark cycle. Animal care and handling was in accordance with the Colorado State University Animal Care and Use Committee guidelines.

Immunohistochemistry

Tissue was processed as previously described (Frahm et. al., 2012) in an antigen retrieval immunohistochemical protocol. Briefly, brains were embedded in 5% agarose and cut coronally into 50µm sections using a vibrating microtome (Leica VT1000S). Free-floating serial sections were collected in 0.05M phosphate-buffered saline (PBS), pH 7.5. Excess unreacted aldehydes were neutralized in 0.1M glycine followed by 0.5% sodium borohydride. Sections were washed in room temperature PBS then were washed in sodium citrate (0.05 M, pH 8.6). The sections were then placed into sodium citrate buffer preheated to 80°C to promote antigen retrieval

(Dellovade et al., 2001). They were allowed to slowly come back to room temperature after which they were returned to PBS for additional washes. Sections were washed in PBS then incubated in a PBS blocking solution (5% normal goat serum (NGS), 0.5% Triton X-100 (Tx), and 1% hydrogen peroxide). Sections were then incubated in primary monoclonal antibodies directed against endocan (either clone MEP14 or MEP19, Lunginnov, Lille, France) or platelet endothelial cell adhesion molecule (PECAM also known as CD31, 1:30; BD Biosciences, San Jose, CA, USA). All sections were incubated at 4°C overnight in primary antibodies. Sections were then washed in room temperature with 1% NGS and 0.02% Tx in PBS. Sections were incubated with the appropriate secondary antibodies for either biotin conjugated donkey anti-mouse antibodies (1:2500; Jackson ImmunoResearch, West Grove, PA), biotin conjugated donkey anti-mouse (1:1000; Jackson ImmunoResearch) or Cy3 conjugated anti-mouse (1:200, Jackson ImmunoResearch) in PBS containing 1% NGS and 0.32% Tx. For brightfield, sections were incubated in a Vectastain reagent (3µl/ml solutions A and B - Vectastain ABC Elite kit; Vector Laboratories, Burlingame, CA) at room temperature. After washing in Tris-buffered saline (pH 7.5), reaction product was developed in Tris-buffered saline containing 0.025% diaminobenzidine, 0.02% nickel, and 0.02% hydrogen peroxide.

Data Collection

Brightfield images were acquired using an Olympus BH2 microscope with an Insight QE digital camera in Spot Advanced Software. Fluorescent images were acquired on a Zeiss 510-Meta laser-scanning confocal microscope. FITC fluorescence was imaged using a 488/543 nm bandpass filter and emission detected using a 505/530 nm bandpass emission filter. Cy3 fluorescence indicating endocan was imaged using a 488/543 nm bandpass filter and emission detected using a 585/615 nm bandpass emission filter. Z-stacks were taken with 6 layers every 3µm obtained at 40x magnification using oil immersion objectives.

Results

Endocan immunoreactivity at postnatal day 12

Brains at P12 were examined for immunoreactive endocan during the postnatal angiogenic period specific to the PVN (Frahm et al., 2012). The distribution of immunoreactive endocan resembled the normal blood vessel pattern in the PVN, cortex (CTX) and Hippocampus (figure 3.1). Previous studies examining tumors showed that endocan mRNA correlated with newly forming blood vessels (Sarrazin et al., 2010, Del Toro et al. 2010). However, the current findings suggest immunoreactive endocan is detectable within virtually all of the vasculature of the brain at P12 in FVB/N mice.

Endocan immunoreactivity at postnatal day 20

To determine if the distribution of immunoreactive endocan varied by age, brains from FVB/N (figures 3.2a-c in brightfield) and C57BL/6J (figures 3.2d-g by immunofluorescence) mice were examined at P20. These strains were selected because they are commonly utilized in our laboratory and others. The distribution pattern of immunoreactive endocan again was consistent with general blood vessel patterns. There was immunoreactive signal throughout the brain, although images are specifically provided for cortex (figure 3.2a,d), hippocampus (figure 3.2b,e) and PVN (figure 3.2c, f) in C57BL/6J and FVB/N background mice. There was no labeling in the absence of primary antibody in control sections (figure 3.2g).

Endocan immunoreactivity in FVB/N and C57BL/6J xS129xCBA mixed background mice at postnatal day 20

We next determined endocan immunoreactivity at P20 in a C57BL/6J xS129xCBA mixed background mouse used in unrelated experiments due to a specific gene disruption (Solomon et al., 2012). C57BL/6JxS129xCBA mice not containing the altered allele were examined

alongside FVB/N mice. The distribution of immunoreactive endocan was similar in the cortex, hippocampus and PVN in FVB/N mice (figure 3.3a-c) compared to C57BL/6J mice (figure 3.1a-c). Matched sections demonstrate there was no endocan immunoreactivity in the cortex, hippocampus or PVN (3.3d-f) of C57BL/6J xS129xCBA mice using MEP19.

Prior vascular perfusion of FITC blocked Endocan immunoreactivity

The perfusion of FITC allows for visualization of blood vessels and the localization of its extravascular leakage that likely indicates compromise of blood-brain barrier function (Miyata & Morita, 2011). However, in C57BL/6J and FVB/N mice, vascular perfusion of FITC prior to application of antibodies directed against endocan blocked endocan immunoreactivity (figure 3.4a, 3.4g). Images in figure 4a and 4d show blood vessels labeled with FITC indicating functional blood vessels. Only restricted blood vessels or blood vessels devoid of FITC contained endocan immunoreactivity (figure 3.4b, e). Confocal microscopy showed no overlap or colocalization between FITC and endocan (figure 3.4c, f). Brightfield images also showed immunoreactive endocan in a much more restricted number of blood vessels (figure 3.4g, h). Labeling with antibodies against platelet endothelial cell adhesion molecule (PECAM), a protein also present in endothelial cells, was not impacted due to prior FITC perfusion (figure 3.4i). These studies suggest that vascular perfusion of FITC prior to endocan processing might identify developing blood vessels that are not yet functional.

Discussion

Elevated endocan has been observed in tumor endothelial cells in human glioblastomas arising from cell types such as astrocytes and oligodendrocytes (Maurage et al., 2009) and pituitary adenomas (Cornelius et al., 2012). Endocan immunoreactivity has also been found in normal

human pituitary tissue specifically in endocrine cells, demonstrating that endocan is not limited to endothelial cells (Cornelius et al., 2012). Previous studies have also identified endocan as a potential marker for angiogenesis (Sarrazin et al., 2010, Roudnicky et al., 2013). However, the recent production of antibodies directed against endocan allows a greater sensitivity for visualizing its presence and distribution, particularly in the mouse brain. Instead of being in a tip cell distribution, immunoreactive endocan was visualized in a global blood vessel pattern at P12 and P20 in brains from C57BL/6J and FVB/N mice. This identification of endocan immunoreactivity in mouse brain endothelium calls for further examination of its potential function in mouse vasculature. The presence of immunoreactive endocan in the endothelial cells of the brain vasculature may provide insight into the potential source of endocan detected in the serum of healthy humans and mice (Depontieu et al, 2012).

Prior studies using northern blot and in situ hybridization analyses of mouse brain (Abid et al., 2006) or human tissue (Lassalle et al., 1996) were unable to detect endocan. There are at least 2 potential reasons for lack of mRNA when immunoreactive protein is found. First, the sensitivity of the mRNA methods may have been lower than the sensitivity of the immunohistochemistry with the new monoclonal antibodies used in the current study. Secondly, it is possible that since endocan is a secreted proteoglycan, that immunoreactive endocan in brain is accumulated from the circulation after synthesis in peripheral sites. However, the detection of immunoreactive endocan in vessels that likely were not exposed to vascular perfusion makes this less probable. In addition, endocan present in the brain vasculature may provide a source for releasable endocan that may diffuse away and regulate other distant processes (Sarrazin et al., 2010) opening a new avenue for investigation.

The antibodies used in this study generated against endocan have been previously shown to detect immunoreactivity in C57BL/6J and 129Sv mice, but not BALB/c mice (Depontieu et al,

2012). In the current study, there was a lack of endocan immunoreactivity in C57BL/6JxS129xCBA background mice. Clearly, strain background will be important for future studies examining endocan immunoreactivity. The MEP14 monoclonal antibody used in this study recognizes the 6 last C-terminus amino acids, identical in human, mouse and rats (Depontieu et al., 2012). This antibody was selected because it has been shown that in the absence or mutation of these 6 amino acids MEP14 did not recognize the peptide while other clones did not show this specificity. For both strains in which immunoreactive endocan was seen it was globally maintained in mouse endothelial cells within the brain. Western blots further confirmed the specificity of this antibody because immunoreactive endocan was detectable in total brain but not in the pituitary (data not shown). A previous study showed a dissimilar pattern to the findings presented in this study for endocan immunoreactivity. In human brain tissue endocan was localized in neurons and not neuroglia or blood vessels (Zhang et al., 2012). The antibodies utilized were generated by injecting purified recombinant human endocan protein into BALB/c mice, and does not indicate the specificity of their antibody. This suggests that these recently commercially available antibodies may be useful to further investigating the normal and disease state expression of endocan in a variety of tissues and cells types.

In addition to visualizing endocan immunoreactivity in numerous contexts, endocan labeling in brains taken from mice perfused with FITC may provide a tool to visualize newly forming blood vessels. There was an unexpected immunoreactive pattern in brains following vascular perfusion with FITC. Initially after finding poor immunolabeling, additional sections were retested with new antibody lots (graciously donated by Lunginnov). Upon further experiments it became clear that only brains either from the C57BL/6J xS129xCBA background or perfused with FITC had this appearance. Experiments comparing FVB/N and C57BL/6J xS129xCBA with or without FITC perfusion confirmed these findings. Only non-FITC perfused brains from

C57BL/6J or FVB/N mice showed immunoreactive endocan. A preliminary experiment attempted to block endocan labeling by adding FITC to the blocking step of a western blot. Although there was a decrease, it did not result in a total loss of labeling (data not shown). To determine if FITC perfusion impacted the immunoreactivity of other proteins in endothelial cells, FITC brains were processed for immunoreactive PECAM. The labeling of antibodies against PECAM was not altered due to FITC perfusion. Although the exact mechanism for the lack of endocan immunolabeling in FITC positive vasculature remains unknown, there is a strong potential benefit of this reliable finding. FITC labels and identifies blood vessels in which blood/perfusate can flow. Only if the dye reaches the endothelial cell will they be stained. Endocan antibodies can recognize the proteoglycan, regardless of whether it is part of a functional blood vessel. Images acquired using confocal microscopy showed endocan-positive blood vessels connecting with FITC-positive blood vessels, with no colocalization. Therefore, vascular perfusion with FITC followed by examination of immunoreactive endocan may provide a tool for viewing nonfunctional blood vessels.

Overall, immunoreactive endocan was detected abundantly in a pattern consistent with the majority of cerebral vasculature in the mouse brain. At P12 and P20, C57BL/6J and FVB/N mice showed this distribution pattern, while immunoreactive endocan was absent in a C57BL/6J xS129xCBA mixed background. Brains perfused with FITC only had endocan immunoreactivity where FITC was not present, perhaps indicating locations where blood vessels are not yet functional. In conclusion, immunoreactive endocan provides another tool for examining cerebral vasculature and in the presence of FITC perfusion may also provide a tool to visualize newly forming blood vessels.

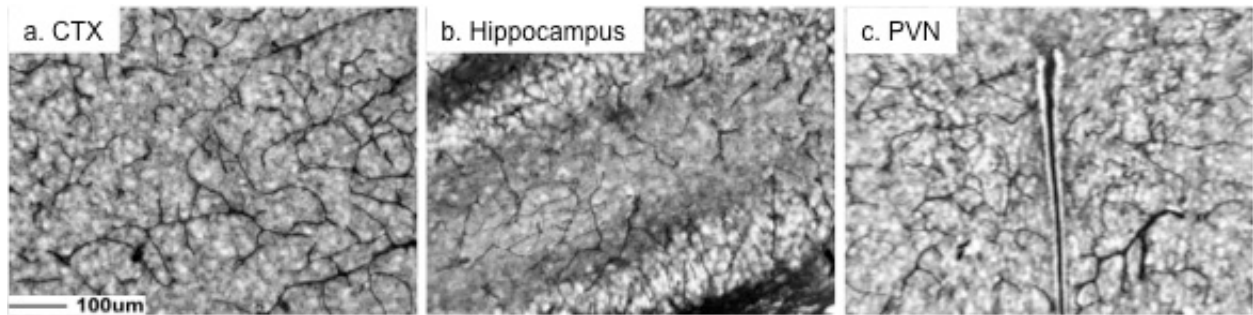


Figure 3.1. Immunoreactive endocan was distributed throughout the mouse brain at postnatal day 12. There was a global blood vessel pattern of immunoreactive endocan that is exemplified by images from the cortex (a. CTX), hippocampus (b), and paraventricular nucleus of the hypothalamus (c. PVN). Scale bar = 100µm.

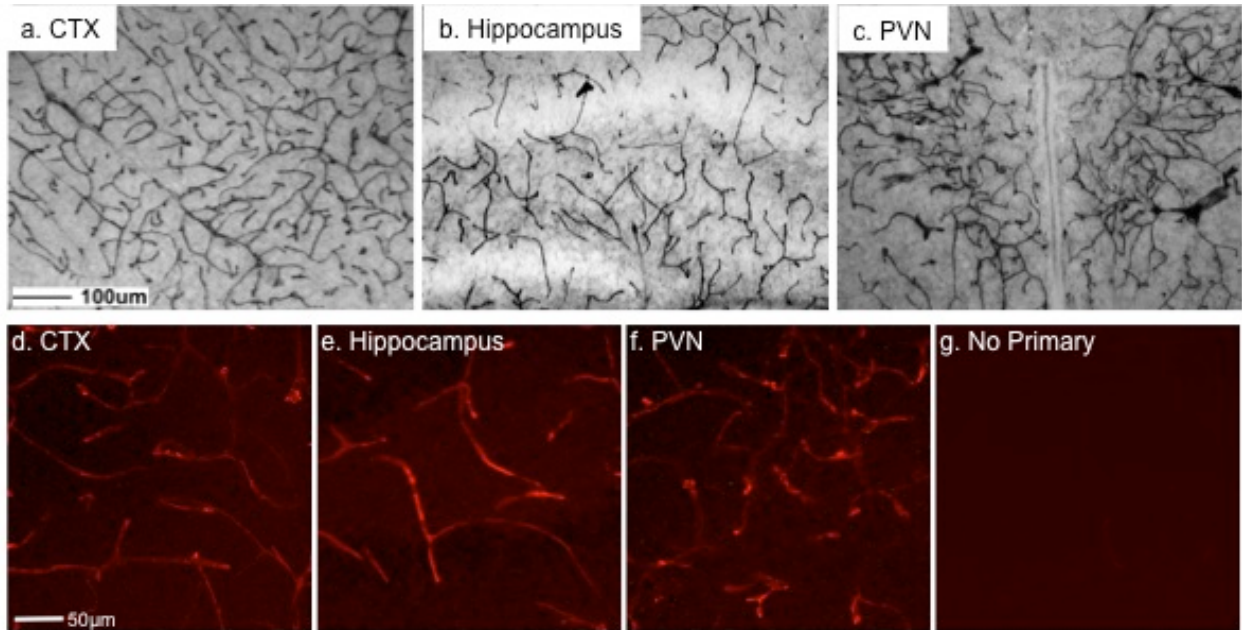


Figure 3.2. Immunoreactive endocan was distributed throughout the brain in C57BL/6J background mice on postnatal day 20. There was a global blood vessel pattern of immunoreactive endocan that is exemplified by images from the cortex (a, d; CTX), hippocampus (b, e), and paraventricular nucleus of the hypothalamus (c, f; PVN). Immunoreactivity was not detected in the absence of primary antibodies (g). Scale bar = 100µm for top images and 50µm for lower images.

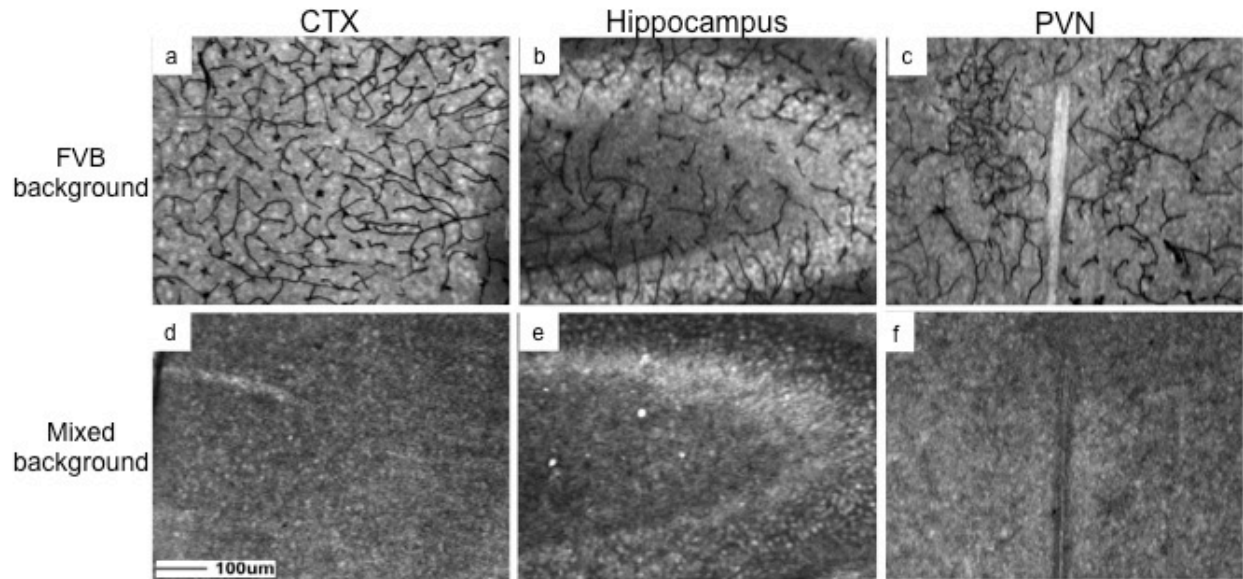


Figure 3.3. Immunoreactive endocan was distributed throughout the brain in FVB/N but not mixed C57BL/6J /S129/CBA background mice on postnatal day 20. There was a global blood vessel pattern of immunoreactive endocan in the cortex (a. CTX), hippocampus (b), and paraventricular nucleus of the hypothalamus (c. PVN) of FVB/N, but no immunoreactivity in C57BL/6J /S129/CBA background mice (d-f). Scale bar = 100µm

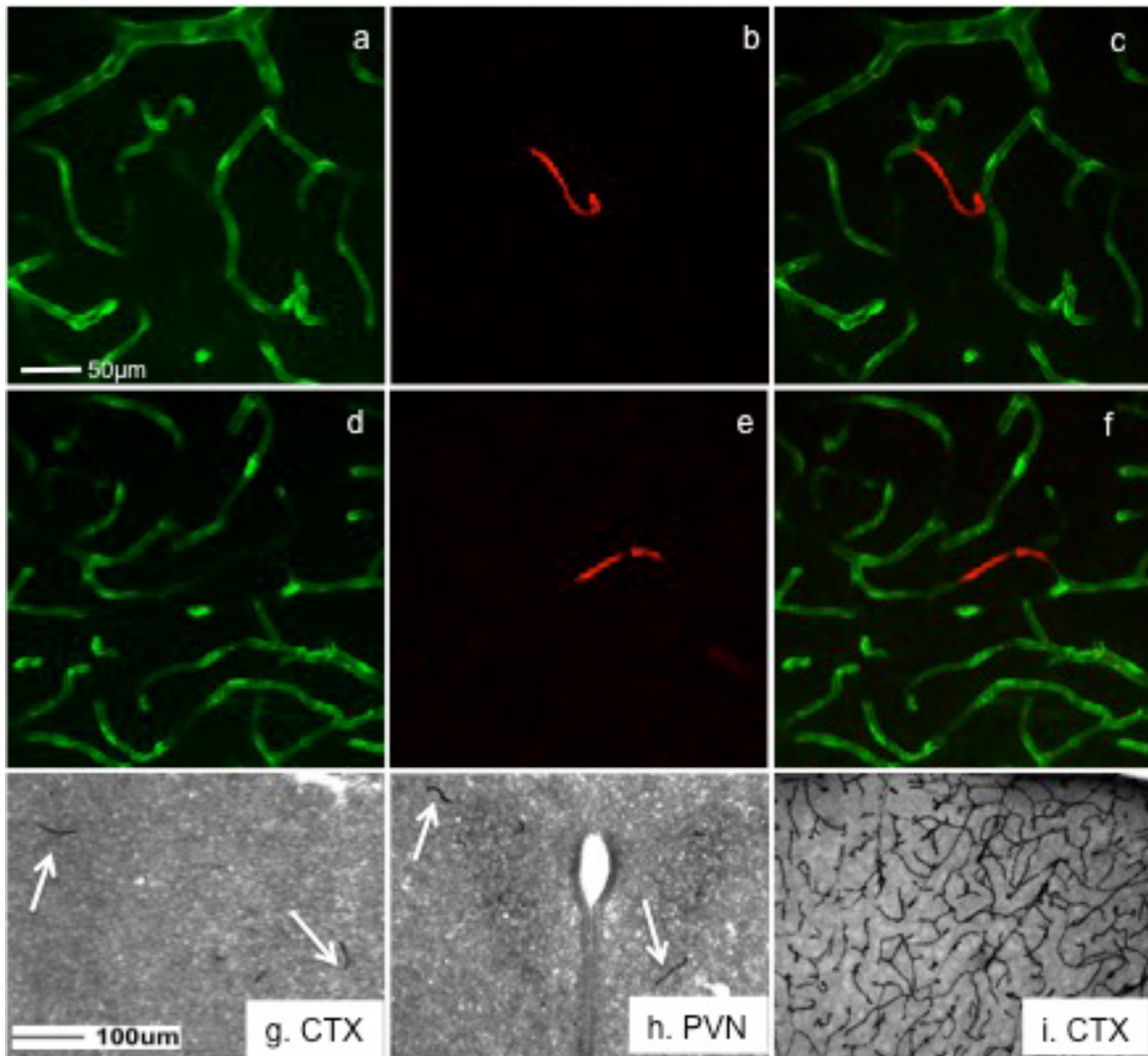


Figure 3.4. Vascular perfusion of FITC allowed identification of cerebral vasculature, but blocked detection of endocan immunoreactivity. Images of FITC labeled blood vessels (a,d) show lack of colocalization with endocan (c,f). Immunoreactive endocan was only found in blood vessels devoid of FITC (b,e). Vascular perfusion of FITC did not block detection of immunoreactive platelet endothelial cell adhesion molecule (i). This procedure may reveal prefunctional blood vessels in the brain (g, h). Scale bar = 50µm for top images and 100µm for lower images.

References

- Abid, M.R., Yi, X., Yano, K., Shih, S.C., Aird, W.C., 2006. Vascular endocan is preferentially expressed in tumor endothelium. *Microvasc Res.* 72:136-145.
- Chen, L.Y., Liu, X., Wang, S.L., Qin, C.Y., 2012. Over-expression of the Endocan Gene in Endothelial Cells from Hepatocellular Carcinoma is Associated with Angiogenesis and Tumour Invasion. *J Int Med Res.* 38, 498-510.
- Cornelius, A., Cortet-Rudelli, C., Assaker, R., Kerdraon, O., Gevaert, M.H., Prevot, V., Lassalle, P., Trouillas, J., Delehede, M., Mauragr, C.A., 2012. Endothelial expression of endocan is strongly associated with tumor progression in pituitary adenoma. *Brain Pathol.* 22, 757-764.
- Del Toro R., Prahst C., Mathivet T., Siegfried G., Kaminker J.S., Larrivee B., Breant C., Duarte A., Takakura N., Fukamizu A., Penninger J., Eichmann A., 2010. Identification and functional analysis of endothelial tip cell-enriched genes. *Blood.* 116, 4025-4033.
- Dellovade, T.L., Davis, A.M., Ferguson, C., Sieghart, W., Homanics, G.E., Tobet, S.A., 2001. GABA influences the development of the ventromedial nucleus of the hypothalamus. *J Neurobiol.* 49, 264-276.
- Depontieu, F., de Freitas Caires, N., Gourcerol, D., Giordano, J., Grigoriu, B., Delehede, M., Lassalle, P., 2012. Development of monoclonal antibodies and ELISA specific for the mouse vascular endocan. *J Immunol Methods.* 378, 88-94.
- Frahm, K.A., Schow, M.J., Tobet, S.A., 2012. The vasculature within the paraventricular nucleus of the hypothalamus in mice varies as a function of development, subnuclear location, and GABA signaling. *Horm Metab Res.* 44, 1-6.
- Lassalle, P., Molet, S., Janin, A., Heyden, J.V., Tavernier, J., Fiers, W., Devos, R., Tonnel, A.B., 1996. ESM-1 is a novel human endothelial cell-specific molecule expressed in lung and regulated by cytokines. *J Biol Chem.* 271, 20458-20464.
- Maurage, C.A., Adam, E., Mineo, J.F., Sarrazin, S., Debunne, M., Siminski, R.M., Baroncini, M., Blond, S., Delehede, M., 2009. Endocan expression and localization in human glioblastomas. *J Neuropathol Exp Neurol.* 68, 633-641.
- Miyata, S., Morita, S., 2011. A new method for visualization of endothelial cells and extravascular leakage in adult mouse brain using fluorescein isothiocyanate. *J Neurosci Methods.* 202, 9-16.
- Roudnicky, F., Poyet, C., Wild, P., Krampitz, S., Negrini, F., Huggenberger, R., Rogler, A., Strohr, A., Hartmann, A., Provenzano, M., Otto, V.I., Detmar, M., 2013. Endocan is upregulated on tumor vessels in invasive bladder cancer where it mediates VEGF-A-induced angiogenesis. *Cancer Res.* 73, 1097-1106.
- Scherpereel, A., Gentina, T., Grigoriu, B., Sénéchal, S., Janin, A., Tscopoulos, A., Plénat, F., Béchar, D., Tonnel, A.B., Lassalle, P., 2003. Overexpression of Endocan Induces Tumor Formation. *Cancer Res.* 63, 6064-6089.

Sarrazin, S., Adam, E., Lyon, M., Depontieu, F., Motte, V., Landolfi, C., Lortat-Jacob, H., Bechard, D., Lassalle, P., Delehedde, M., 2006. Endocan or endothelial cell specific molecule-1 (ESM-1): a potential novel endothelial cell marker and a new target for cancer therapy. *Biochim Biophys Acta*. 1765, 25-37.

Sarrazin, S., Lyon, M., Deakin, J.A., Guerrini, M., Lassalle, P., Delehedde, M., Lortat-Jacob, H., 2010. Characterization and binding activity of the chondroitin/dermatan sulfate chain from Endocan, a soluble endothelial proteoglycan. *Glycobiology*. 20, 1380-1388.

Solomon, M.B., Furay, A.R., Jones, K., Packard, A.E., Packard, B.A., Wulsin, A.C., Herman, J.P., 2012. Deletion of forebrain glucocorticoid receptors impairs neuroendocrine stress responses and induces depression-like behavior in males but not females. *Neuroscience*. 203, 135-43.

Zhang, S.M., Zuo, L., Zhou, Q., Gui, S.Y., Shi, R., Wu, Q., Wei, W., Wang., 2012. Expression and distribution of endocan in human tissue. *Biotech Histochem*. 87, 172-178.

CHAPTER 4. DEVELOPMENT OF THE BLOOD-BRAIN BARRIER WITHIN THE PARAVENTRICULAR NUCLEUS OF THE HYPOTHALAMIS: INFLUENCE OF FETAL GLUCOCORTICOID EXCESS

Overview

The blood-brain barrier (BBB) is a critical contributor to brain function. To understand its development and potential function in different brain regions, the postnatal (P) BBB was investigated in the mouse cortex (CTX), lateral hypothalamus (LH), and paraventricular nucleus of the hypothalamus (PVN). Brains were examined on postnatal days (P)12, P22 and P52 for BBB competency and for pericytes as key cellular components of the BBB demarcated by immunoreactive desmin. Glucocorticoid influences (excess dexamethasone; dex) during prenatal development were also assessed for their impact on the blood vessels within these regions postnatally. At P12 there was significantly more extravascular leakage of a low molecular weight dye (fluorescein isothiocyanate) in the CTX than within hypothalamic regions. For pericytes, there were low levels of desmin immunoreactivity at P12 that increased with age for all regions. There was more desmin immunoreactivity present in the PVN at each age examined. Fetal dex exposure resulted in decreased blood vessel density within the PVN at P20. In the CTX, dex exposure increased BBB competency, in contrast to the PVN where there was a decrease in BBB competency and increased pericyte presence. Overall, unique alterations in the functioning of the BBB within the PVN may provide a novel mechanism for fetal antecedent programming that may influence adult disorders.

Introduction

The vasculature of the brain differs from the periphery in several characteristics. A key difference is the blood-brain barrier (BBB), which restricts access to the brain parenchyma through a complex network of tight junction proteins, proteoglycans, endothelial cells, basal lamina, vascular smooth muscle cells, pericytes and glial cells (Norsted et al. 2008). As more research implicates the BBB in disease onset and progression (Gosselet et al. 2011; Daneman 2012; Abbott & Friedman 2012), its development and function becomes a more important area of focus.

Pericytes play a role in the development and integrity of the BBB. Immunoreactive desmin provides a reliable biochemical marker of pericytes (Hellstrom et al. 1999). When pericytes are deficient (e.g., PDGF KO mice; Armulik et al. 2010) there is an improper astrocyte end-feet distribution and an increase in injected tracers present in brain parenchyma. Neuronal degeneration resulting in memory impairment is preceded by pericyte loss (Bell et al. 2010). During disease states such as stroke, pericytes can migrate in to coordinate blood flow regulation, permeability of the BBB, and reestablishment of neurovascular unit (Liu et al. 2012).

Although much BBB research focuses on the cerebral cortex (CTX), there is no a priori reason to assume that all other brain regions maintain the BBB under the same rules. For example, circumventricular organs maintain a more permeable BBB within the brain but vary in their permeability (Morita & Miyata 2012). The current study focused on the paraventricular nucleus of the hypothalamus (PVN) that contains a 3-5 fold denser matrix of blood vessels than surrounding brain regions (Finley 1938; Ambach & Palkovits 1974; van den Pol 1982) and may play by different rules. The PVN houses neurons containing corticotropin-releasing hormone (CRH), arginine vasopressin and angiotensin that control physiological homeostasis, vasomotor

tone, and stress responses (Tobet et al. 2013). The vascular density arises postnatally and varies from rostral to caudal (Frahm et al. 2012). The greater density in the rostral and mid region corresponds with the general location of neuroendocrine neurons (Biag et al. 2012). Altering exposure of specific neurons to peripheral signals through a compromised BBB may contribute to various diseases and disorders (Quaegebeur et al. 2011). Within the PVN, decreases in BBB integrity might have effects amplified by the 3-fold greater vascular network (Goldstein et al. 2013).

Prenatal glucocorticoid excess leads to long-term functional consequences in adulthood (reviewed in Harris & Seckl 2011; Tobet et al. 2013). At a cellular level, prenatal glucocorticoids alter glucocorticoid receptor expression in the hippocampus in adulthood (Levitt et al. 1996) and increase CRH levels within the PVN (Welberg et al. 2001). Concerning the vasculature, prenatal glucocorticoid excess may decrease blood vessel density (Neigh et al. 2010; Vinukonda et al. 2010) and increase pericyte coverage (Vinukonda et al. 2010). A goal of the current study was to assess whether the dense blood vessel network in the PVN is impacted by fetal glucocorticoid excess.

The current study characterized the postnatal development of the BBB and desmin-immunoreactive pericytes in the CTX, lateral hypothalamus (LH) and PVN. Fetal exposure to dex resulted in enhanced BBB integrity in the CTX, while the same treatment resulted in decreased blood vessel density and BBB integrity within the PVN. The divergence of effect may be related to a selective increase in desmin-immunoreactive pericyte coverage in the PVN in offspring exposed to dex during pregnancy.

Materials and Methods

Animals

For experiments selectively examining BBB development, the mice used were from a mixed C57BL6/S129/CBA background (Solomon et al. 2012) and for experiments examining the influence of prenatal dex mice were from an FVB/N background. Males and females were combined by genotype after analysis (ANOVA sex x treatment x region at P20 $p > 0.50$) indicated no significant differences by sex. Mice were mated overnight and the day of a visible plug was designated as embryonic day 0 (E0). Pregnant dams were injected with either the synthetic glucocorticoid dexamethasone (0.1 mg/kg, Sigma, Inc.; Hadoke et al. 2006; O'Regan et al. 2004) or vehicle once daily from E11-17. The day of birth was designated P0. For tissue collection, mice were anesthetized using ketamine (80 mg/kg) and xylazine (8 mg/kg) and transcardially perfused with heparanized PBS (pH 7.4) containing fluorescein isothiocyanate (FITC, Thermoscientific, MW 389.4) followed by 4% paraformaldehyde in 0.1M phosphate buffer (pH 7.4; modified from Miyata & Morita 2011). To examine blood vessel density, a separate subset of mice was anesthetized by inhaling isoflurane (Vet One) and brains were removed and immersion fixed with 20 ml 4% paraformaldehyde in 0.1M phosphate buffer. For all mice, brains were removed, post fixed overnight, then changed into 0.1M phosphate buffer for storage at 4°C. Body weights were measured and sex determination was made through direct inspection of the gonads. There were at least 3 separate litters combined for analysis of each treatment.

Mice were maintained in plastic cages with aspen bedding (autoclaved Sani-chips, Harlan Teklad, Madison, WI, USA) in the Painter Building of Laboratory Animal Resources at Colorado State University. Food (#8640, Harlan Teklad, Madison, WI, USA) with filtered tap water and environmental enrichment provided ad libitum in a 14/10h light/dark cycle. Animal care and

handling was in accordance with the Colorado State University Animal Care and Use Committee guidelines.

Immunohistochemistry

Tissue was processed as previously described (Frahm et. al. 2012; 2013). Briefly, brains were embedded in 5% agarose and cut coronally into 50 μ m thick sections using a vibrating microtome (Leica VT1000S). Free-floating serial sections were collected in 0.05M phosphate-buffered saline (PBS, pH 7.4). Excess unreacted aldehydes were neutralized in 0.1M glycine for 30 minutes followed by 0.5% sodium borohydride for 15 minutes. Sections were washed in PBS then incubated in a blocking solution (5% normal goat serum (NGS), 0.5% Triton X-100 (Tx), and 1% hydrogen peroxide in PBS) for at least 30 minutes. Sections were then incubated in primary antiserum directed against platelet endothelial cell adhesion molecule (PECAM also known as CD31, 1:30; BD Biosciences, San Jose, CA) or Desmin (1:200; DAKO) in 1% BSA and 0.5% Tx. For desmin, sections were processed for antigen retrieval (Dellovade et al. 2001). In place of the standard processing steps prior to antisera application detailed above sections were washed in room temperature PBS for 15 min followed by a 1 h wash in sodium citrate (0.05 M, pH 8.6). The sections were then placed into sodium citrate buffer preheated to 80°C for 30 min. They were then allowed to slowly come back to room temperature (approximately 30–35 min) after which they were returned to PBS for an additional 15 min of washes. All sections were incubated for 2 nights at 4°C in primary antisera. Sections were then washed in room temperature with 1% NGS and 0.02% Tx in PBS. Sections were incubated with the appropriate secondary antibodies for 2h for either biotin conjugated donkey anti-rat antiserum (1:1000; Jackson ImmunoResearch, West Grove, PA), Cy3 conjugated anti-rabbit (1:200; Jackson ImmunoResearch) or Cy3 conjugated anti-mouse (1:200; Jackson ImmunoResearch) in PBS containing 1% NGS and 0.32% Tx. For PECAM, sections were incubated in a Vectastain

reagent (3 μ l/ml solutions A and B - Vectastain ABC Elite kit; Vector Laboratories, Burlingame, CA) at room temperature for 1 hr. After 1h of washing in Tris-buffered saline (pH 7.5), reaction product was developed over 5min in Tris-buffered saline containing 0.025% diaminobenzidine, 0.02% nickel, and 0.02% hydrogen peroxide.

Analysis

For blood vessel density, images were acquired for the PVN, LH and CTX using an Olympus BH2 microscope with an Insight QE digital camera in Spot Advanced Software. The section with the densest vascular network was selected by an investigator blind to treatment group for each PVN region (rostral, mid, caudal) for analysis (Frahm et al. 2012). Image representation for the regions selected for analysis (CTX, PVN, and LH) is provided in Figure 4.7.

Total number of blood vessel branches and length were used to characterize the density in each region of interest containing the PVN. For blood vessel length, images were light corrected (Image J, version 1.43u) then analyzed for length using Angiogenesis Tube Formation (Metamorph Software, version 7.7.0.0, Molecular Devices, Inc.). Branch points were manually identified and counted using Image J (cell counter). Blood vessel width was quantified by dividing total area by total length. For Desmin and FITC, images were acquired on a Zeiss 510-Meta laser-scanning confocal microscope. FITC was imaged using a 488/543 nm bandpass filter and emission detected using a 505/530 nm bandpass emission filter. Cy3 for Desmin was imaged using a 488/543 nm bandpass filter and emission detected using a 585/615 nm bandpass emission filter. Z-stacks were taken with 6 optical sections taken every 3 μ m obtained at 40x magnification using an oil immersion objective. FITC does not remain in blood vessels but rather accumulates in endothelial cell nuclei (Miyata & Morita 2011). Therefore, to view the vascular network within the brain we compiled Z-stacks for analysis. Extravascular leakage was analyzed using open-source CellProfiler (available from the Broad Institute at

www.cellprofiler.org). Blood vessels were identified and a 10-pixel expansion was mapped from each blood vessel to create a mask to quantify leakage. This intensity was divided by FITC intensity within blood vessels to account for differences in perfusions. A representation of the CellProfiler analysis is provided in Figure 4.8.

Because blood vessel density varies, final values were normalized to blood vessel area within the same section. For Desmin analysis, sections were measured for area of immunoreactive and additionally were normalized to blood vessel area using Metamorph software.

Representative images for figures were normalized for optimal contrast in Adobe Photoshop (version CS for Macintosh). Statistical significance was determined by 2-way ANOVAs: age x region for developmental studies and treatment x region for dex studies using SPSS software (version 21 for Macintosh, SPSS Inc., Chicago, IL). In all cases region was considered as a repeated measure. This was followed by post-hoc comparisons based on Bonferroni correction. Values of $p < 0.05$ were considered statistically significant and are reported as mean \pm SEM.

Results

Age- and region-dependent changes in BBB competency

The current study found changes in vasculature structure and extravascular leakage within the CTX, LH and PVN from P12 to P22 and P52. These time points were chosen based on the significant increase in PVN angiogenesis over these ages (Frahm et al. 2012). On P12 the BBB in the CTX was less competent compared to the LH and PVN. There was significant extravascular FITC leakage within the CTX at P12 compared to the LH and PVN (Figs. 4.1a, d, g, j; $p < 0.05$). This high level of extravascular FITC was not observed in the hypothalamic regions of LH and PVN at P12. At P22, there was significantly less extravascular FITC leakage

in the CTX compared to P12 (Figs. 4.1b, j; $p < 0.05$). There were no significant differences between brain regions concerning extravascular FITC leakage at P22 (Figs. 4.1b, e, h). At P52 the BBB appeared fully functional as extravascular FITC leakage did not change in CTX, LH, and PVN (Figs. 4.1c, f, i, j) compared to the same brain regions at P22 (Figs. 4.1b, e, h, j). These findings suggest that the BBB develops at different rates in the CTX compared to the hypothalamic brain regions examined.

Changes in Desmin immunoreactive pericytes by age and region

Concerning postnatal and region-specific pericyte development, results showed significantly greater desmin-immunoreactive pericyte coverage at P22 and P52 compared to P12 (Figs. 4.2a-i; $p < 0.01$). For different brain regions, there was significantly more desmin-immunoreactive pericyte coverage at P12 in the PVN (Figs. 4.2g-i) compared to the LH (Figs. 4.2d-f) and CTX (Figs. 4.2a-c). For the CTX, there was a significant increase in desmin-immunoreactive pericyte coverage between P12 and P22 (Figs. 4.2a, b, j, k). At all ages examined the PVN had significantly more desmin-immunoreactive pericyte coverage than the LH and the CTX (Fig. 4.2j; $p < 0.01$). When blood vessel density was taken into account, the PVN still had significantly more desmin-immunoreactive pericyte coverage than the CTX (Fig. 4.2k; $p < 0.05$). At P52, this increase in desmin-immunoreactive pericyte coverage was due to the morphology of the pericytes in the PVN (Fig. 4.3c) compared to the CTX (Fig. 4.3a). Desmin in the adult mouse labels processes running along small diameter and encircling larger diameter capillaries (Hellstrom et al. 1999). The pattern of desmin-immunoreactive pericyte coverage in the PVN showed a wrapping pattern around blood vessels while in the CTX more often it extended along the blood vessels. There were no differences in desmin-immunoreactive pericyte coverage in the LH (Fig. 4.3b) compared to the CTX or PVN after 50 days of age. To determine if the difference in pericyte coverage coincided with the size of blood vessels, blood vessel width was quantified (Fig. 4.3). Blood vessel widths were greater in the hypothalamus

(LH – Fig. 4.3b, PVN – Fig. 4.3c) compared to the CTX (Fig. 4.3a). Quantification showed a statistically significant greater blood vessel width in the PVN (but not the LH) compared to the CTX (Fig. 4.3d; $p < 0.05$) indicating that at P52, the greater desmin-immunoreactive pericyte coverage in the PVN (Figs. 4.2i-k) was associated with an increase in blood vessel width (Fig. 4.3d). To examine if this was due to the presence of larger arterioles, antibodies against smooth muscle actin (SMA), a marker for smooth muscle cells that surround cerebral arteries or arterioles (Ladecola 2004) was examined. SMA immunoreactivity was observed in the brain, however, not within the PVN (data not shown) suggesting the larger width of blood vessels within the PVN was not due to the presence of arterioles, although this did not rule out the presence of venules. In general, desmin-positive pericyte coverage increased postnatally, varied between brain regions, and was related to blood vessel width.

Fetal Dex exposure led to altered vascular characteristics at P20

Blood vessels that are potentially newly formed and not yet fully functional are not identified by vascular perfusion with FITC (Frahm et al. 2013). Therefore, Immunoreactive PECAM was utilized to visualize the more complete endothelial cell population. PECAM revealed an overall 13% decrease in blood vessel length in the PVN for dex-treated compared to vehicle-treated mice at P20 (Fig. 4.4a; $p < 0.01$). Offspring of dex-treated mothers had significantly less total blood vessel length across all regions of the PVN (Fig. 4.4b; $p < 0.01$), while decreased branch points was restricted to the rostral and mid regions compared to vehicle-treated (Fig. 4.4c; $p < 0.05$). Brains perfused with FITC were also examined and dex-exposed offspring had less blood vessel density compared to vehicle-treated (data not shown). There were no significant differences in blood vessel length or branch points in the LH or CTX due to dex-treatment (data not shown). This indicates that prenatal exposure to dex impacts blood vessels within the PVN of young offspring.

Fetal Dex exposure led to altered BBB competency at P20

Given that structural blood vessel characteristics were impacted in offspring of mothers treated with dex during gestation (Fig. 4.4), it was important to assess the state of the BBB (Fig. 4.5). Importantly, the impact of fetal dex exposure on later BBB competency was opposite in the CTX versus PVN. In the CTX, there was statistically significant 12% less extravascular FITC leakage in offspring from mothers treated with dex compared to those exposed to vehicle (Figs. 4.5a, d; $p < 0.05$). This suggests there was an increase in the competency of the BBB due to dex-treatment in the CTX. In stark contrast, the mid region of the PVN showed a statistically significant 17% increase in extravascular FITC leakage in dex-treated compared to vehicle-treated offspring (Figs. 4.5c, f, g; $p < 0.05$). There was a strong trend for prenatally dex-treated mice to have an increase in extravascular FITC in the rostral PVN compared to vehicle-treated (data not shown; $p < 0.09$) with no notable differences observed in the caudal PVN. For the LH, there was no change in extravascular FITC leakage in offspring from mothers either prenatally dex- or vehicle-treated (Fig. 4.5b, e). Due to the possibility of maternal injection providing a stressful stimulus that could increase endogenous glucocorticoid levels, a comparison was made between offspring of vehicle-injected mothers versus offspring from mothers that were not injected (Fig. 4.1). There were no differences in vascular characteristics or BBB competency when compared to non-injected mice. Together these findings suggest that fetal antecedent exposure to dex decreased the density and integrity of the blood vessels selectively within the PVN when examined in later life.

Fetal Dex exposure led to altered pericytes at P20

To complement and further expand on the extravascular FITC data, desmin-immunoreactive pericyte coverage was assessed. Prenatal dex-treatment led to a significant increase in immunoreactive desmin on a vascular network that was less dense at P20 (Fig. 4.6). When total desmin-immunoreactivity was examined in the PVN, LH or CTX, there were no dex-

dependent differences in any region (Figs. 4.6a-g). However, when blood vessel density was taken into account, there was a significant dex-dependent increase in desmin-immunoreactive pericyte coverage in the mid PVN (Fig. 4.6h; $p < 0.01$). There were no significant differences in the rostral or caudal PVN due to treatment. There were also no significant differences in the CTX or LH due to treatment although there was a trend of increased coverage due to dex-treatment for all brain regions examined. Overall, prenatal dex-treated mice increased immunoreactive desmin on blood vessels within the PVN at P20.

Discussion

Interest in the regulation of BBB function ranges from pharmaceutical perspectives for gaining or preventing drug access to the brain parenchyma (Abbott 2013), to questions of breakdown that might be antecedent to disorder (Gosset et al. 2011; Daneman 2012; Abbott & Friedman 2012). The current study was focused on the PVN as a unique site that gains several fold greater vascular density than surrounding regions over the course of postnatal development. The increased vasculature might make changes in BBB function in this site particularly important. As the PVN may be particularly important as a site susceptible to fetal antecedent actions of excess glucocorticoids (Tobet et al. 2013), the current study also determined whether excess fetal glucocorticoids could impact PVN vascular characteristics. The results highlighted several critical points. First, that the development of vascular and BBB characteristics differed in the PVN versus the CTX. Secondly, that maternal exposure to excess glucocorticoids during pregnancy impacted vascular and BBB characteristics in their offspring. Thirdly, fetal exposure to dex impacted the CTX differentially than the PVN. Finally, alterations in BBB competency were paralleled by changes in pericyte coverage as assessed by immunoreactive desmin in development and as a function of fetal dex-treatment.

The ability of compounds to “leak” from blood vessels clearly differs among brain regions and can be observed using several methods. Differences in leakage among circumventricular organs were shown using FITC even though all are fenestrated and lack a BBB (Morita & Miyata 2012). Many BBB studies predominantly focus on the cortex for changes (e.g., Sadowska et al. 2009; Daneman et al. 2010; Vorbrodt et al. 2001; Ezan et al. 2012; Armulik et al. 2010; Bell et al. 2010) and occasionally examine the cerebellum (Sadowska et al. 2009; Armulik et al. 2010). For BBB development, reports indicate cortical leakage of high molecular weight dyes until postnatal day 21 in rats (Utsumi et al. 2000), and postnatal day 14 in mice (Lossinsky et al. 1986; Volbrodt et al. 1986). The findings presented in this study also suggest that differences occur between brain regions such as the CTX and nuclear groups in the hypothalamus (i.e., LH and PVN). Not only were differences in BBB development observed, but fetal exposure to dex impacted the postnatal CTX differentially than the PVN and had little to no impact on the LH. This highlights the importance of studying cells in their anatomical context. For example, a number of studies have examined BBB competency by injecting Evans blue dye, perfusing saline to flush out circulating dye, and then homogenizing tissue to measure and analyze residual Evans blue in the tissue of interest (e.g., Bake & Sohrabji 2004). In the current study, this would have concealed differences between hypothalamic subregions. Overall, these findings suggests the need for further investigations to determine region-specific BBB development, how factors such as excess glucocorticoids during fetal development can impact BBB development, and what role this may play on an organism.

Prenatal glucocorticoid excess has been implicated in depression-like behaviors (Bale 2005), hypertension (Levitt et al. 1996), and hypothalamic-pituitary-adrenal axis dysregulation (Levy & Tasker 2012) in adulthood. Concerning the vasculature, previous work revealed decreased blood vessel density in the hippocampus (Neigh et al. 2010) and the germinal matrix at the level of the mid-septal nucleus (Vinukonda et al. 2010). In the current study, prenatal dex-treatment

resulted in offspring for which the entire PVN had a reduced vascular network, albeit predominantly in the rostral and mid regions. Rostral and mid regions of the mouse PVN have a greater density of blood vessels and neurons that correspond with the general location of neuroendocrine neurons. By contrast, the caudal PVN is less densely vascular than rostral regions and houses more preautonomic neuronal populations important for sympathetic and parasympathetic outflow (Biag et al. 2012). The findings in the current study indicated that the blood vessel density and BBB within the caudal PVN were less impacted by excess glucocorticoids during development than rostral and mid regions. There were no changes observed in the LH or CTX. Even though prenatal dex-treatment is “global” in access, and impacts can be broad (physiology and behavior), the influences in the current study were selective within brain compartments.

The hallmark of capillaries is the ability to pass red blood cells in single file through tissues of the body. If red blood cells are the same size throughout, it is curious that not all capillaries in the brain have the same width. Nonetheless, the current results confirm a previous study in rats showing that capillaries of the PVN have larger lumens when compared to a region ventrolateral to the PVN (Van den Pol 1982). Although this may be due to a higher presence of venules (Ambach & Palkovits 1974), we did not make this determination. The results of the current study extended observations to mice, a comparison to CTX, and further showed that capillary widths were not altered due to prenatal dex-treatment even when total capillary volumes changed.

The developmental time course for BBB proteins varies for detectability and relationship to BBB competency. In previous studies in mice BBB proteins did not reach adult levels in the CTX until around P14 (Vorbrodt et al. 2001). For the gap junction protein Connexin 30, immunoreactivity was detected in the mouse cortex beginning at postnatal P12 with the level of

protein comparable to adulthood identified around P15 (Ezan et al. 2012). Results in the current study showed higher levels of extravascular FITC leakage occurring in the CTX at P12 than at P22, in agreement with the proposal that the BBB is still developing postnatally. At P52, compared to P12 and P22, the results showed that the BBB prevented FITC from entering the brain parenchyma in all regions examined. Prenatal exposure to dex impacted the BBB at P20 with less detectable extravascular FITC leakage in the CTX. In sheep CTX, prenatal dex resulted in an increase in tight junction proteins, a component of a functional BBB (Sadowska et al. 2009) and in agreement with the current findings. By contrast for the PVN, fetal dex led to the opposite result, greater extravascular FITC leakage suggesting BBB compromise. Insults such as excess prenatal glucocorticoid exposure can alter permeability and integrity in a brain region dependent manner and for the PVN where the result is a less-dense vascular network that has a compromised BBB; the impact may alter physiology and behavior based on the neuronal population involved (Biag et al. 2012; Kádár et al. 2010; Tobet et al. 2013; Goldstein et al. 2013).

Prior studies examining pericytes found that fetal glucocorticoids increased cell coverage of NG2-positive pericytes in rabbits and humans (Vinukonda et al. 2010). While the prior report was in the germinal matrix for the cerebral cortex, the current study produced similar changes in the mid region of the PVN in mice. For pericytes, immunoreactive desmin suggests that changes have occurred, but not whether the number, distribution, or size of pericytes was impacted. One explanation for why there is the same level of desmin-immunoreactivity in the PVN on fewer blood vessels due to prenatal dex-treatment may be due to recruitment and migration. Pericytes migrate in response to new vessel formation, traumatic stress, or under hypoxic injury or state (Dore-Duffy et al. 2000). In dex-treated offspring that exhibited a decreased vascular network, this may be a sign of prior hypoxia with pericyte recruitment needed to promote recovery. Enhanced pericyte coverage may serve to help stabilize the

vasculature (Vinukoda et al. 2010). Since pericytes can regulate capillary diameter through constricting the vascular wall (Bell et al. 2010), differences due to prenatal glucocorticoid excess may impact blood flow within the PVN. Future studies are needed to determine how changes in desmin-positive pericyte coverage in dex-treated offspring impacts the ability of the BBB to function properly as observed here through extravascular FITC leakage and whether this impacts neuronal function.

In summary, the current study examined the postnatal development of the BBB and demonstrated that fetal dex exposure altered the integrity of the BBB in the PVN. There was an increase in BBB permeability at P20 in the highly vascularized middle region of the PVN. Decreases in blood vessel density and BBB integrity within the mid (and to some extent rostral) regions of the PVN may impact the ability of neuroendocrine neurons (Biag et al. 2012; Kádár et al. 2010) to function normally. Understanding changes in the crosstalk between neurons and blood vessels in the PVN may provide insight into the long-term behavioral and physiological consequences observed in human and animal studies when exposed to glucocorticoid excess during prenatal development.

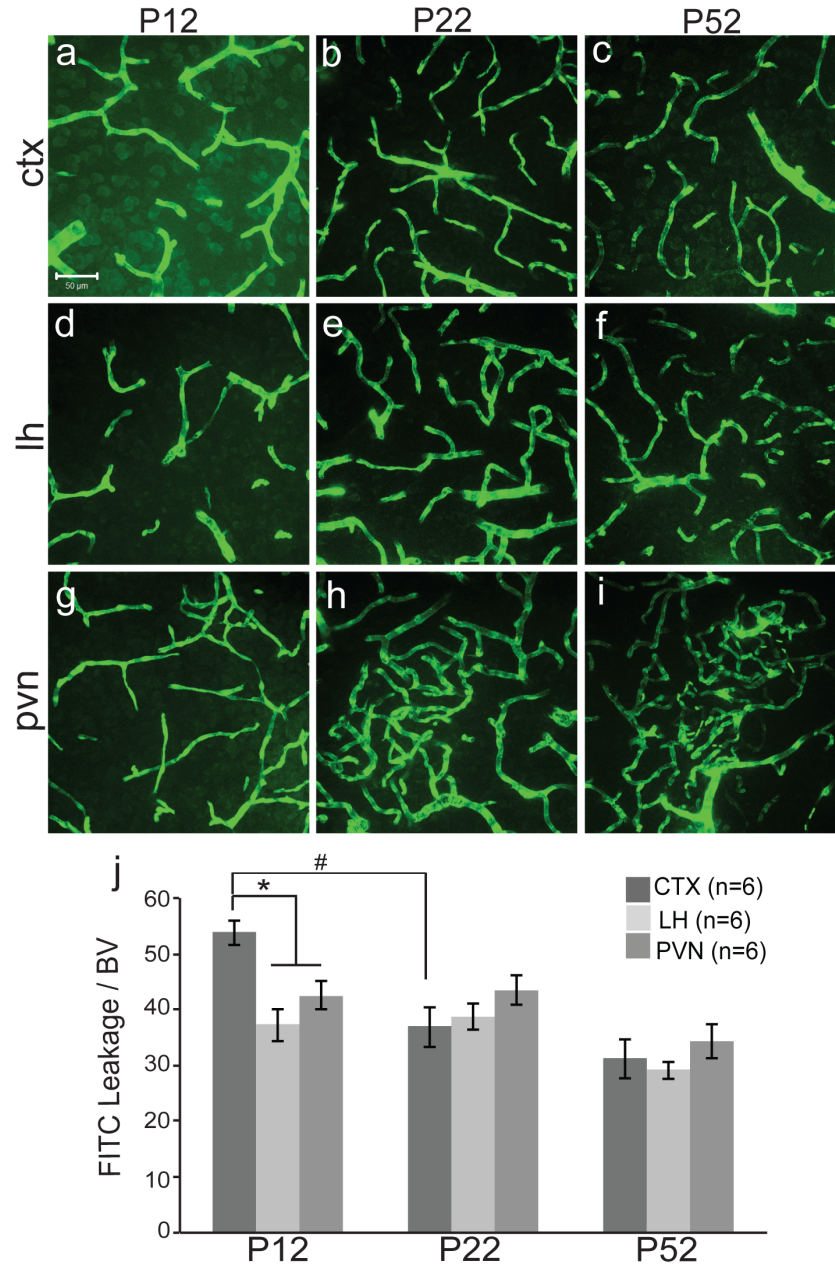


Figure 4.1 Postnatal blood-brain barrier development in the mouse cortex (CTX), lateral hypothalamus (LH) and paraventricular nucleus of the hypothalamus (PVN) at P12, P22 and P52. Example confocal images for each region are provided in panels a-i, and a quantitative summary by graph in j. There was a significant increase in extravascular FITC leakage in the CTX (a) compared to the LH (d) and PVN (g) at P12 (j; $p < 0.05$). Between P12 and P22 there was a significant decrease in extravascular FITC leakage specifically in the CTX (a, b; $p < 0.05$). At P22, there were no significant differences observed in extravascular FITC leakage between brain regions (b, e, h). At P52, there were no significant differences in extravascular FITC leakage (c, f, i) compared to P22 or between brain regions (j). Number of animals per group ($n=6$) is provided in the code for the bars panel j. Significant differences between regions indicated by * and for age as #. Scale bar = 50μm in panel a, which applies to all images.

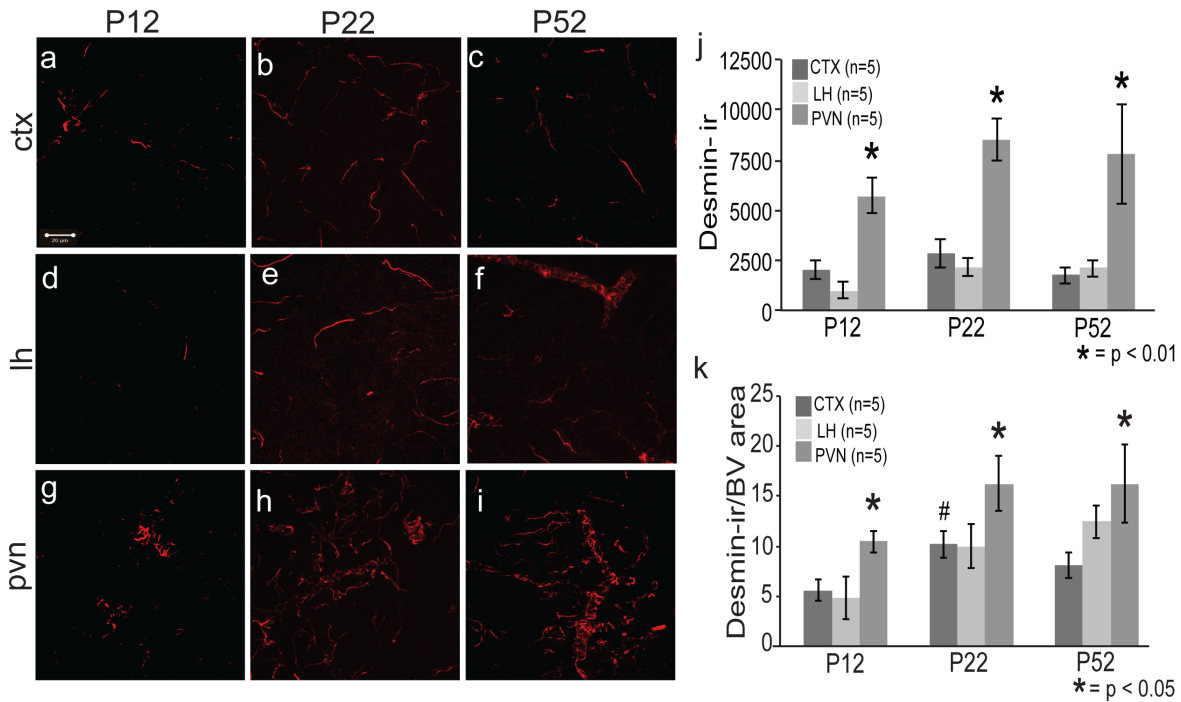


Figure 4.2 Postnatal desmin-immunopositive pericyte coverage in the mouse cortex (CTX), lateral hypothalamus (LH) and paraventricular nucleus of the hypothalamus (PVN) at P12, P22 and P52. Example confocal images for each region are provided in panels a-i, and a quantitative summary by graph in j and k. There was a significant increase in desmin-immunoreactive pericyte coverage in the PVN (g) compared to the CTX (a) and LH (d) at P12 (j, k; $p < 0.05$). At P22 there was a significant increase in desmin-immunoreactive pericyte coverage in the CTX (b) and PVN (h) compared to P12 (j, k; $p < 0.05$). There were no significant differences in any brain region between P22 and P52 for desmin-immunoreactive pericyte coverage (j, k). There was an overall significant increase in desmin-positive pericyte coverage for the PVN at all ages (g-i) compared to the LH (d-f) and CTX (a-c) for all ages (j, k; $p < 0.05$). Number of animals per group ($n=5$) is provided in the code for the bars panels j and k. Significant differences between regions indicated by * and for age as #. Scale bar = $50\mu\text{m}$ in panel a, which applies to all images.

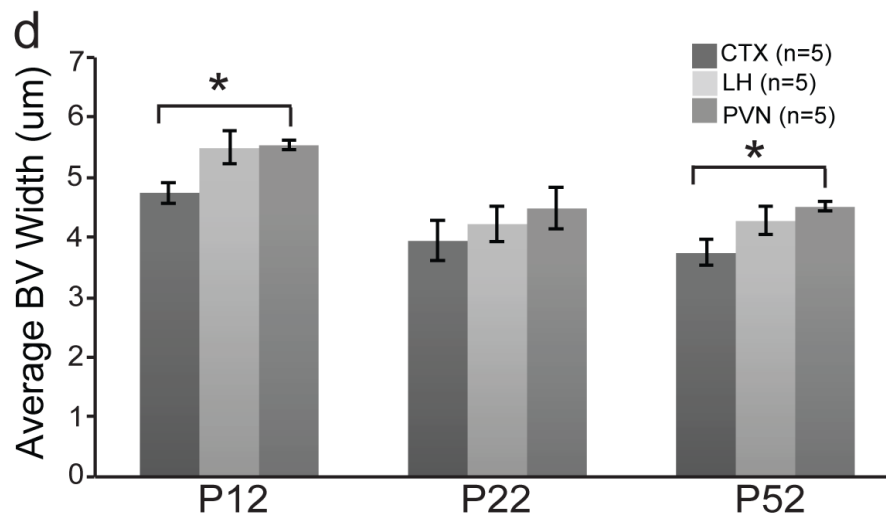
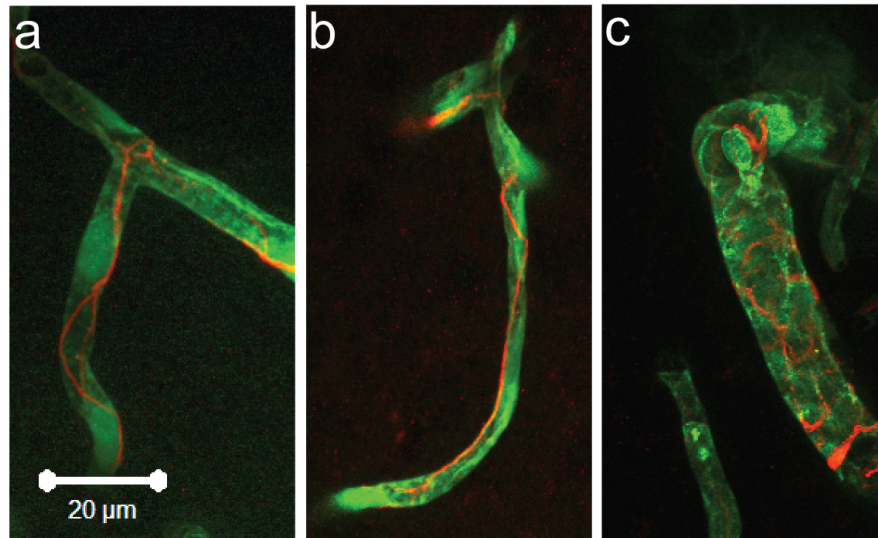


Figure 4.3 Blood vessels in the paraventricular nucleus of the hypothalamus (PVN) were wider than in the mouse cortex (CTX) at P12 and P52. Higher magnification of blood vessels at P52 visualized with fluorescein isothiocyanate perfusion in the CTX, lateral hypothalamus (LH) and PVN show that desmin morphology varied between brain regions with the PVN (c) having more of a wrapping pattern compared to the CTX (a) and LH (b). The wrapping may be related to a significantly greater blood vessel width in the PVN compared to the CTX at P12 and P22 (d, $p < 0.05$). There were no significant differences at P22 or in the LH when compared to the CTX or PVN at any age. Number of animals per group ($n=5$) is provided in the code for the bars panels j and k. Significant differences between regions indicated by *. Scale bar = $20\mu\text{m}$ in panel a, which applies to all images.

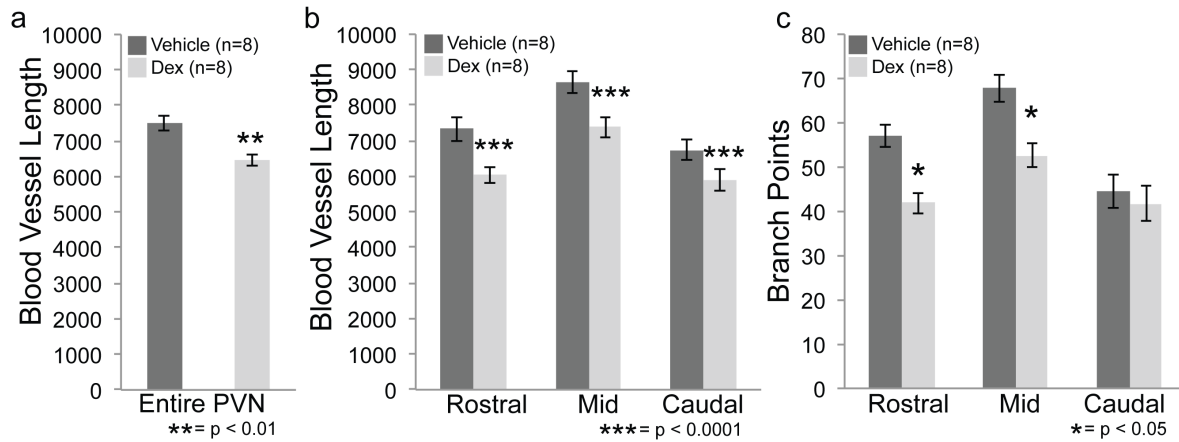


Figure 4.4 Prenatal exposure to dexamethasone (dex) impacted blood vessel density in the postnatal mouse paraventricular nucleus of the hypothalamus (PVN) at P20. There was a significant decrease in blood vessel length for the entire PVN for dex-treated compared to vehicle-treated mice (a, ** $p < 0.01$). There was also a region-specific significant decrease in blood vessel length in the rostral, mid and caudal regions of the PVN in dex-treated compared to vehicle-treated mice (b, *** $p < 0.0001$). For branch points, there was only a significant decrease in the rostral and mid PVN in dex-treated compared to vehicle-treated mice (c, * $p < 0.05$). Number of animals per group ($n=8$) is provided in the code for the bars in each panel.

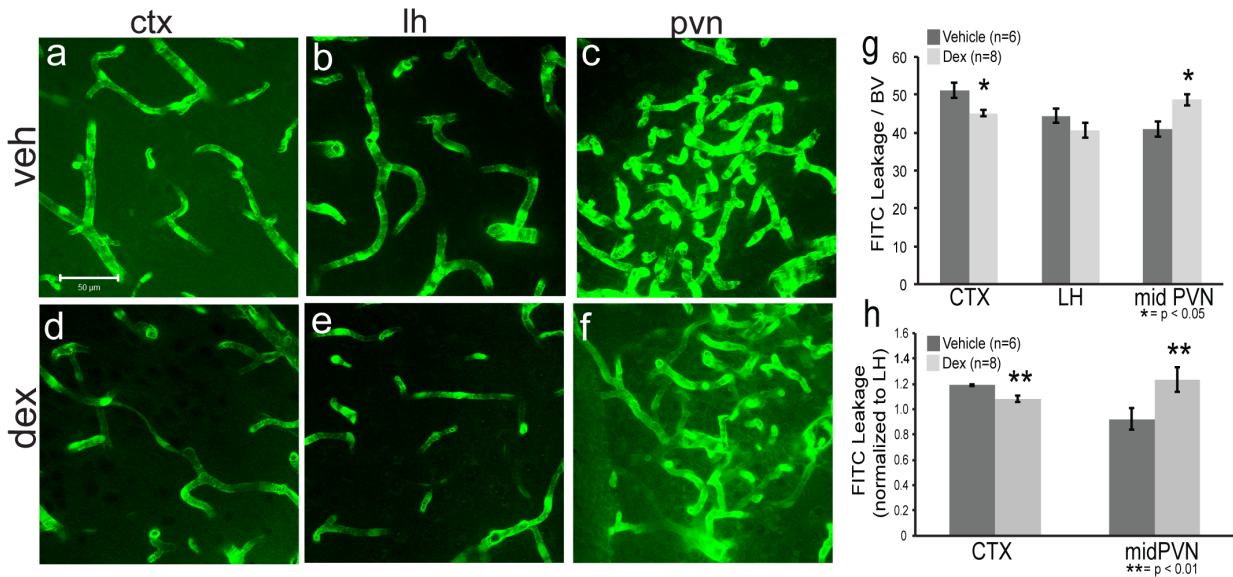


Figure 4.5 Prenatal exposure to dexamethasone (dex) impacted blood-brain barrier development in the mouse cortex (CTX) and paraventricular nucleus of the hypothalamus (PVN) at P20. Example confocal images for each region are provided in panels a-f, and a quantitative summary by graph in g and h. In the CTX, there was a significant decrease in extravascular FITC leakage in dex-treated compared to vehicle-treated mice (a, d, g; $p < 0.05$). For the PVN, there was a significant increase in extravascular FITC leakage in offspring of dex-treated compared to vehicle-treated mice in the mid region (c, f, g; $p < 0.05$). There was no impact of fetal dex observed in the lateral hypothalamus (LH; b, e, g). Number of animals per group is provided in the code for the bars in panels g and h. Significant differences for treatment indicated by * $p < 0.05$ and ** $p < 0.01$. Scale bar = $50\mu\text{m}$ in panel a, which applies to all images.

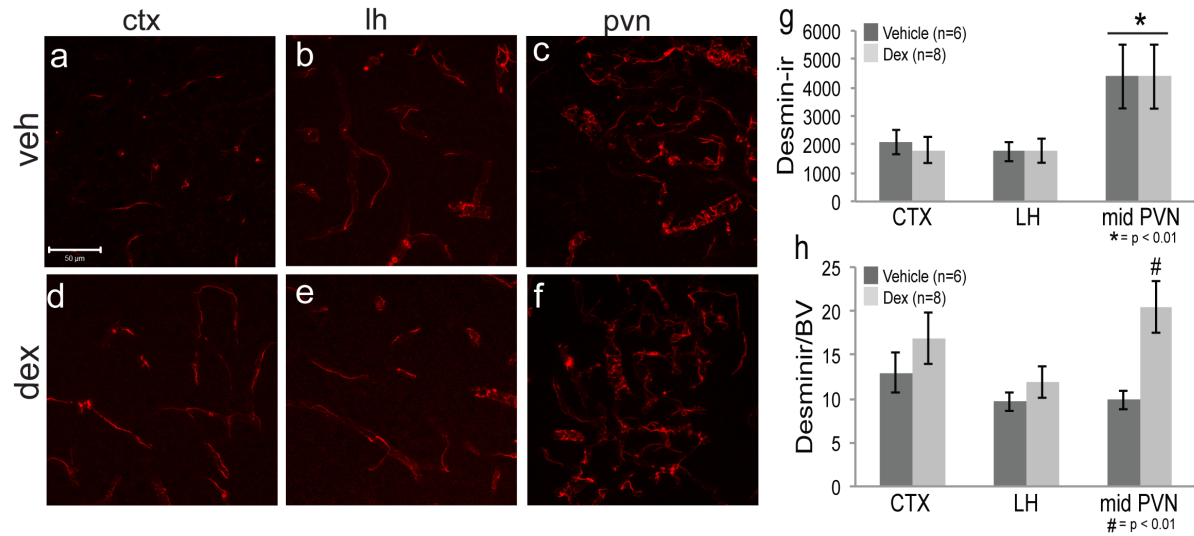


Figure 4.6 Prenatal exposure to dexamethasone (dex) impacted desmin-immunoreactive pericyte coverage in the mouse paraventricular nucleus of the hypothalamus (PVN) at P20. Example confocal images for each region are provided in panels a-f, and a quantitative summary by graph in g and h. In the PVN, there was a significant increase in desmin-immunoreactive pericyte coverage in dex-treated compared to vehicle-treated mice (c, f; * $p < 0.01$) when blood vessel density was taken into account (h; * $p < 0.01$). There were no significant differences observed in desmin-immunoreactive pericyte coverage in the cortex (CTX; a, d) or lateral hypothalamus (LH; b, e) between dex-treated or vehicle-treated mice. There was a significant increase in desmin-immunoreactive pericyte coverage in the PVN regardless of treatment compared to the CTX and LH (g). Number of animals per group is provided in the code for the bars in panels g and h. Significant differences between regions indicated by * and for treatment as #. Scale bar = 50 μ m in panel a, which applies to all images.

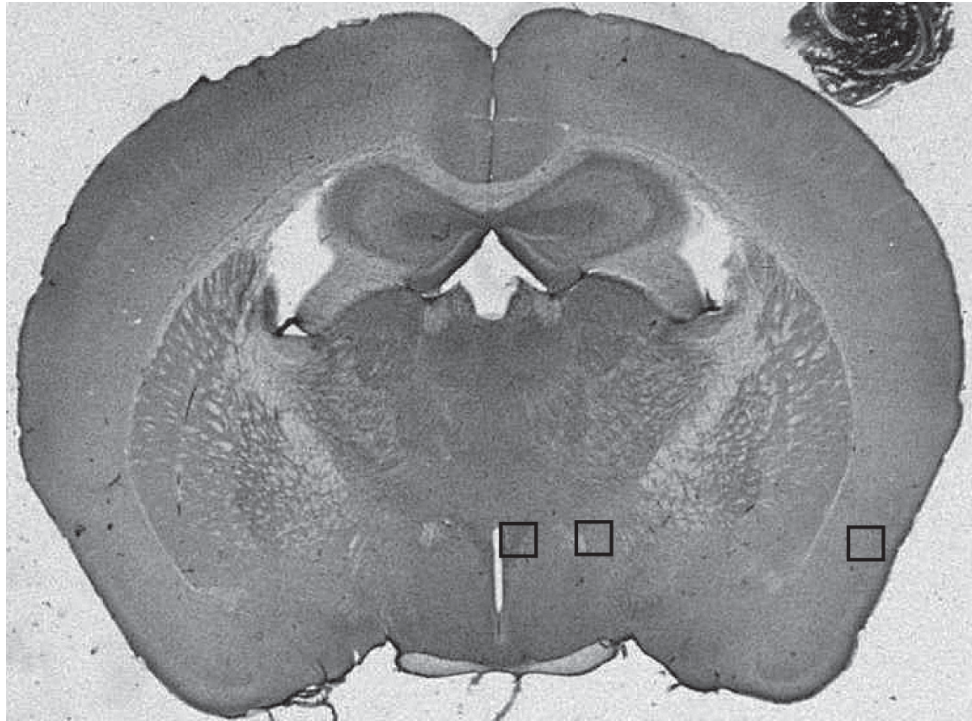


Figure 4.7 Regions selected for analysis. Brightfield image of a coronal section immunolabeled for Platelet Endothelial Cell Adhesion Molecule to visualize blood vessels. Boxes show representative regions of the Cortex (CTX), Lateral Hypothalamus (LH), and Paraventricular Nucleus of the Hypothalamus (PVN) that were selected for analysis.

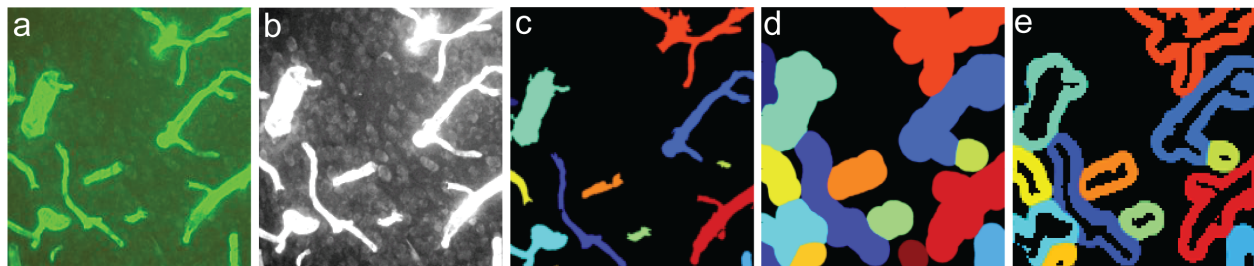


Figure 4.8. Analysis of vascular permeability. Fluorescence intensities were measured outside of blood vessels (i.e., leak) in the Cortex (CTX), Lateral Hypothalamus (LH) and Paraventricular Nucleus of the Hypothalamus (PVN). Semi-automated leakage calculations were made using CellProfiler software. Blood vessels were identified in panels a-c, a 10-pixel expansion was mapped from each blood vessel to create a mask and intensity was measured as shown in panel d, and blood vessel intensity was then subtracted as in panel e to generate blood-brain barrier permeability quantification.

References

- Abbott NJ (2013) Blood-brain barrier structure and function and the challenges for CNS drug delivery. *J Inherit Metab Dis* 36:437-449
- Abbott NJ, Friedman A (2012) Overview and introduction: The blood-brain barrier in health and disease. *Epilepsia* 53:1-6
- Ambach G, Palkovits M (1974) Blood supply of the rat hypothalamus. II. Nucleus paraventricularis. *Acta Morphol Acad Sci Hung* 22:311-320
- Armulik A, Genove G, Mae M, Nisancioglu MH, Wallgard W, Niaudet C, He L, Norlin J, Lindblom P, Strittmatter K, Johansson BR, Betsholtz C (2010) Pericytes regulate the blood-brain barrier. *Nature* 468:557-561
- Bake S, Sohrabji F (2004) 17beta-estradiol differentially regulates blood-brain barrier permeability in young and aging female rats. *Endocrinology* 145:5471-5475
- Bale TL (2005) Sensitivity to stress: dysregulation of CRF pathways and disease development. *Horm Behav* 48:1-10
- Bell RD, Winkler EA, Sagare AP, Singh I, LaRue B, Deane R, Zlokovic BV (2010) Pericytes control key neurovascular functions and neuronal phenotype in the adult brain and during brain aging. *Neuron* 68:409-427
- Biag J, Huang Y, Gou L, Askarinam A, Hahn JD, Toga AW, Hintiryan H, Dong HW (2012) Cyto- and chemoarchitecture of the hypothalamic paraventricular nucleus in the C57BL/6J male mouse: A study of immunostaining and multiple fluorescent tract tracing. *J Comp Neurol* 520:6-33
- Daneman R (2012) The blood-brain barrier in health and disease. *Ann Neurol* 72:648-672
- Daneman R, Zhou L, Kebede AA, Barres BA (2010) Pericytes are required for blood-brain integrity during embryogenesis. *Nature* 468:562-566
- Dellovade TL, Davis AM, Ferguson C, Sieghart W, Homanics GE, Tobet SA (2001) GABA influences the development of the ventromedial nucleus of the hypothalamus. *J Neurobiol* 49:264-276
- Dore-Duffy P, Owen C, Balabanov R, Murphy S, Beaumont T, Rafols JA (2000) Pericyte migration from the vascular wall in response to traumatic brain injury. *Microvascular Research* 60:55-69
- Ezan P, Andre P, Cisternino S, Saubamea B, Boulay A, Doutremer S, Thomas M, Quenech'du N, Giaume C, Cohen-Salmon M (2012) Deletion of astroglial connexins weakens the blood-brain barrier. *J Cereb Blood Flow Metab* 32:1457-1467
- Finley KH. The capillary bed of the paraventricular and supraoptic nuclei of the hypothalamus. *Res Publ Assoc Res Nerv Ment Dis* 1938, 18: 94-109

Frahm, KA, Schow, MJ, Tobet, SA (2012) The Vasculature within the Paraventricular Nucleus of the Hypothalamus in Mice Varies as a Function of Development, Sub-Nuclear Location, and GABA signaling. *Horm Metab Res* 44:1-6

Frahm KA, Nash CP, Tobet SA (2013) Endocan immunoreactivity in the mouse brain: Method for identifying nonfunctional blood vessels. *J Immunol Methods* 398: 27-32.

Goldstein JM, Handa RJ, Tobet SA (2013) Disruption of fetal hormone programming (prenatal stress) implicated shared risk for sex differences in depression and cardiovascular disease. *Front Neuroendocrinol*, epub ahead of print

Gosselet F, Candela P, Cecchelli R, Fenart L (2011) Role of the blood-brain barrier in Alzheimer's disease. *Med Sci* 27:987-92

Harris A, Seckl J (2011) Glucocorticoids, prenatal stress and the programming of disease. *Horm Behav* 59:279-289

Hadoke PW, Lindsay RS, Seckl JR, Walker BR, Kenyon CJ. Altered vascular contractility in adult female rats with hypertension programmed by prenatal glucocorticoid exposure. *J Endocrinol* 2006, 188: 435-442

Hellstrom M, Kalen M, Lindahl P, Abramsson A, Betscholtz C (1999) Role of PDGF-B and PDGFR-beta in recruitment of vascular smooth muscle cells and pericytes during embryonic blood vessel formation in the mouse. *Development* 126:3047-3055

Kádár A, Sánchez E, Wittmann G, Singru PS, Füzesi T, Marsili A, Larsen PR, Liposits Z, Lechan RM, Fekete C (2010) Distribution of hypophysiotropic thyrotropin-releasing hormone (TRH)-synthesizing neurons in the hypothalamic paraventricular nucleus of the mouse. *J Comp Neurol* 518:3948-3961

Ladecola C (2004) Neurovascular regulation in the normal brain and in Alzheimer's disease. *Nat Rev Neurosci* 5:347-360

Levitt NS, Lindsay RS, Holmes MC, Seckl JR (1996) Dexamethasone in the last week of pregnancy attenuated hippocampal glucocorticoid receptor gene expression and elevates blood pressure in the adult offspring in the rat. *Neuroendocrinology* 64:412-418

Levy BH, Tasker JG (2012) Synaptic regulation of the hypothalamic-pituitary-adrenal axis and its modulation by glucocorticoids and stress. *Front Cell Neurosci* 6:24

Liu S, Agalliu D, Yu C, Fisher M (2012) The role of pericytes in the blood-brain barrier function and stroke. *Curr Pharm Des* 18:3653-3662

Lossinsky AS, Vorbodt AW, Wisniewski HM (1986) Characterization of endothelial cell transport in the developing mouse blood-brain barrier. *Dev Neurosci* 8: 61-75

Miyata S, Morita S (2011) A new method for visualization of endothelial cells and extravascular leakage in adult mouse brain using fluorescein isothiocyanate. *J Neurosci Methods* 202:9-16

Morita S & Miyata S (2012) Difference vascular permeability between the sensory and secretory circumventricular organs of adult mouse brains. *Cell Tissue Res* 349:589-603

- Neigh GN, Ownes MJ, Taylor WR, Nemeroff CB (2010) Changes in the vascular area fraction of the hippocampus and amygdala are induced by prenatal dexamethasone and/or adult stress. *J Cereb Blood Flow Metab* 30:1100-1104
- Norsted E, Gomuc B, Meiserter B (2008) Protein components of the blood-brain barrier (BBB) in the mediobasal hypothalamus. *J Chem Neuroanat* 36:107-21
- O'Regan D, Kenyon CJ, Seckl JR, Holmes MC. Glucocorticoid exposure in late gestation in the rat permanently programs gender-specific differences in adult cardiovascular and metabolic physiology. *Am J Physiol Endocrinol Metab* 2004, 287: 863-870
- Quaegebeur A, Lange C, Carmeliet P (2011) The neurovascular link in health and disease: molecular mechanisms and therapeutic implications. *Neuron* 71:406-424
- Sadowska GB, Malaeb SN, Stonestreet BS (2009) Maternal glucocorticoid exposure alters tight junction protein expression in the brain of fetal sheep. *Am J Physiol Heart Circ Physiol* 298:179-188
- Solomon MB, Furay AR, Jones K, Packard AE, Packard BA, Wulsin AC, Herman JP (2012) Deletion of forebrain glucocorticoid receptors impairs neuroendocrine stress responses and induces depression-like behavior in males but not females. *Neuroscience* 203:135-43
- Tobet SA, Handa RJ, Goldstein JM (2013) Sex-dependent pathophysiology as predictors of comorbidity of major depressive disorder and cardiovascular disease. *Pflugers Arch* 465:585-594
- Utsumi H, Chiba H, Kamimura Y, Osanai M, Igarashi Y, Tobioka H, Mori M, Sawada N (2000) Expression of GFRalpha-1, receptor for GDNF, in rat brain capillary during postnatal development of the BBB. *Am J Physiol Cell Physiol* 279: C361-368
- Van den Pol AN (1982) The magnocellular and parvocellular paraventricular nucleus of the rat: intrinsic organization. *J Comp Neurol* 206:317-345
- Vinukonda G, Dummula K, Malik S, Hu F, Thompson C, Csiszar A, Ungvari Z, Ballabh P (2010) Effect of Prenatal Glucocorticoids on Cerebral Vasculature of the Developing Brain. *Stroke* 41:1766-1773
- Vorbrodt AM, Lossinsky AS, Dobrogowska DH, Wisiewski HM (1986) Distribution of anionic sites and glycoconjugates on the endothelial surfaces of the developing blood-brain barrier. *Brain Res* 394: 69-79
- Vorbrodt AW, Dobrogowska DH, Tarnawski M (2001) Immunogold study of interendothelial junction-associated and glucose transporter proteins during postnatal maturation of the mouse blood-brain barrier. *J Neurocytol* 30:705-716
- Welberg LA, Seckl JR, Holmes MC (2001) Prenatal glucocorticoid programming of brain corticosteroid receptors and corticotrophin-releasing hormone: possible implications for behavior. *Neuroscience* 104:71-79

CHAPTER 5. PRENATAL DEXAMETHASONE ALTERS THE COMPOSITION OF THE BLOOD-BRAIN BARRIER WITHIN THE PARAVENTRICULAR NUCLEUS OF THE HYPOTHALAMUS OF ADULT MICE

Overview

Neurons within the paraventricular nucleus of the hypothalamus (PVN) integrate peripheral signals and coordinate responses that are important for maintaining homeostasis, vasomotor tone, energy balance, stress responses and behavioral functions. In addition to the density of its cytoarchitecture, the PVN also contains 3-fold more blood vessels than surrounding brain regions. Previously, exposure to excess glucocorticoids during fetal development resulted at postnatal day (P)20 in an increased area of desmin immunoreactive (ir) pericytes on a significantly smaller blood vessel network within the PVN coincident with increased blood-brain barrier (BBB) permeability (Frahm & Tobet, 2013abs). To further define the temporal parameters of these effects, pregnant mice were exposed to vehicle (veh) or the synthetic glucocorticoid dexamethasone (dex; 0.1mg/kg) during embryonic days 11-17. To determine if changes observed at molecular and cellular levels impacts behavior, offspring were tested for depressive-like behavior using a tail-suspension test (TST) after P50. After behavior testing, males and females were perfused with the low molecular weight dye fluorescein isothiocyanate (FITC) and fixed using paraformaldehyde. Brain sections containing the PVN were examined for ir-GFAP+ astrocytes and ir-desmin+ pericytes. Veh-treated females had significantly more total ir-GFAP than dex-treated females in the PVN. Astrocyte associations with blood vessels were estimated by examining GFAP-ir fluorescent overlap with FITC labeled vasculature. There was a similar pattern of significantly decreased ir-GFAP covering blood vessels in dex-treated females compared to veh-treated females. For ir-desmin+ pericytes in the PVN, there was a

significant increase in α -desmin normalized to blood vessel density in dex-treated compared to veh-treated males. There were no significant differences observed for dex treatment or sex in extravascular FITC leakage as a proxy for BBB function, or blood vessel density. For the TST, male and female offspring from pregnant mice treated with dex had significantly shorter latencies to first bout of immobility compared to vehicles demonstrating that there are long-term behavioral consequences of prenatal dex exposure. We hypothesize that these alterations in BBB components in combination with environmental or physiological challenges may result in sex-related susceptibility to changes in BBB competency.

Introduction

Cardiovascular disease (CVD) is the number one cause of death worldwide (Thayer et al., 2010). Individuals suffering from CVD are more likely to have major depressive disorder (MDD; The World Health Report, 2001). This co-morbidity constitutes an approximate 20% population prevalence (Reviewed in Goldstein et al., 2014), and by 2020 is postulated to be the number one cause of disability worldwide (The World Health Report, 2001). To understand the etiology with hopes of reducing the incidence of MDD and CVD, independently and collectively, studies are needed to identify potential mechanisms.

A key brain region involved in the comorbidity of CVD and MDD is the paraventricular nucleus of the hypothalamus (PVN; Baune et al., 2012; Goldstein et al., 2014). The PVN is comprised of numerous neuronal phenotypes that integrate peripheral signals to regulate many important functions that range from initiating flight or fight responses, maintaining homeostasis, vasomotor tone, and energy balance (Ferguson et al., 2008; Handa & Weiser, 2013; Hill, 2012; Swanson & Sawchenko, 1983). PVN neurons contain the neuropeptides corticotropin releasing hormone,

arginine vasopressin, oxytocin, thyrotropin-releasing hormone, somatostatin, and angiotensin (Armstrong et al., 1980; Biag et al., 2012; Ford-Holevinski et al., 1991; Handa & Weiser, 2013; Simmons & Swanson, 2009; Swanson and Sawchenko, 1983). Receptors for gamma-aminobutyric acid (GABA), estrogens, androgens, glucocorticoids, and angiotensin II type 1 are also present (Bingham et al., 2006; Fan et al., 2012; Lund et al., 2004; McClellan et al., 2010; Mitra et al., 2003). Glucocorticoid signaling within the PVN has been shown to change the neural circuitry within the PVN resulting in dysregulation of the hypothalamic-pituitary-adrenal (HPA) axis, similar to the effects observed in patients with depression (Levy & Tasker, 2012). Interestingly, the PVN also contains neurons that attenuate hypertension (Biancardi et al., 2013; Braga et al., 2011; Ferguson et al., 2008; Sriramula et al., 2011). Therefore, the PVN may provide a site for cell-based mechanisms that underlie the co-morbidity of CVD and MDD.

In addition to its dense neuronal population, the PVN also has a high blood vessel density (Ambach & Palkovits, 1974; Basir 1931; Craigie, 1940; Finley, 1938; Menendez & Alvarez-Uria, 1987; Poppi, 1928) that in the mouse develops postnatally (Frahm et al., 2012). The highest density is also localized to the rostral two-thirds of the PVN (Frahm et al., 2012), which coincides with the sites of the majority of neuroendocrine neurons (Biag et al., 2012). The role(s) of this dense vascular bed is unknown; however, it has been shown to decrease at postnatal day (P)20 due to either a loss of functional GABA_B receptors (Frahm et al., 2012) or exposure to excess glucocorticoids during prenatal development (Frahm & Tobet, 2013abs). The ability to regulate the vascular network within the PVN suggests that changes may impact physiology and behavior.

What sets brain blood vessels apart from their peripheral counterparts is a restrictive barrier referred to as the blood-brain barrier (BBB). The BBB regulates a microenvironment necessary for reliable neuronal signaling by protecting the brain from potentially harmful items such as

toxins. The BBB consists of a continuous layer of endothelial cells, which form the walls of blood vessels, connected to one another through tight junctions (Reviewed in Abbott et al., 2006; Hawkins & Davis, 2005; Iadecola, 2004; Saunders et al., 2013). Other components include pericytes and astrocytic endfeet that surround endothelial cells (Hawkins & Davis, 2005). Changes to any of these components that together form the BBB could compromise its functional integrity.

Recently, there has been a focus to understand the BBB in the context of communication with neurons. There are coordinated interactions between neurons, astrocytes, and pericytes that are essential for the health and function of the central nervous system. This collection of anatomical partners is often referred to as neurovascular units (NVU; Hawkins & Davis, 2005). In adulthood, the NVU is formed by astrocytic endfeet and pericytes in close proximity to blood vessels (Saunders et al., 2013). Changes in the NVU within the PVN could potentially result in a wide range of diseases and disorders (Quaegebeur et al., 2011). For example, spontaneously hypertensive rats exhibited increased BBB permeability allowing circulating angiotensin II to leak into the PVN and directly alter blood pressure regulation (Biancardi et al., 2013).

Increased fetal exposure to glucocorticoids can also contribute to CVD (Maccari et al., 2003; Baum et al., 2003; Hadoke et al., 2006) and depression-like behavior (Bale, 2005; Roque et al., 2011). At the cellular level, exposure to excess glucocorticoid during prenatal development impacts the neuronal (Levitt et al., 1996; Welberg et al., 2001) and vascular network (Frahm & Tobet, 2013abs) within the PVN. Also, mice exposed to excess glucocorticoids during prenatal development displayed an increase in extravascular leakage of the low molecular weight dye FITC along with an increase in desmin-ir pericytes coverage at postnatal day (P) 20 (Frahm & Tobet, 2013abs). This demonstrates changes in BBB components accompanied by a partial breakdown of BBB function following in response to change in glucocorticoid exposure.

The current study was conducted to determine the long-term impact of fetal dex exposure on changes in PVN NVU. Mice were exposed to excess glucocorticoids during prenatal development and examined at P50. Assessment of blood vessel density, BBB competency, desmin-ir pericyte coverage and GFAP-ir astrocytes within the PVN at indicated that there is partial recovery of BBB function after puberty, but sex-dependent differences in BBB components during adulthood. Both males and females displayed an increase in depression-like behavior, indicating long-term functional consequences of fetal glucocorticoid excess.

Materials and Methods

Mice from an inbred FVB/N background were maintained in plastic cages with aspen bedding (autoclaved Sani-chips, Harlan Teklad, Madison, WI, USA) in the Painter Building of Laboratory Animal Resources at Colorado State University. Food (#8640, Harlan Teklad, Madison, WI, USA) with filtered tap water and environmental enrichment provided ad libitum in a 14/10h light/dark cycle. Animal care and handling was in accordance with the Colorado State University Animal Care and Use Committee guidelines.

Mice were mated overnight and the day of a visible plug was designated as embryonic day 0 (E0). Pregnant dams were injected with the synthetic glucocorticoid dexamethasone (dex, 0.1 mg/kg, Sigma, Inc.; Frahm & Tobet, 2013abs; Hadoke et al. 2006; O'Regan et al. 2004) or vehicle (veh) once daily from E11-17. The day of birth was designated P0. Mice were weaned and ear punched for identification on P19 and then left relatively undisturbed until P50 when they were subjected to behavior tests followed by tissue collection. Animals were handled for at least two days before each behavior test and were tested using the tail suspension test (TST) and Sucrose Preference Test (SPT). For females, cycle stage was determined by analysis of

vaginal cytology (Becker et al., 2005) and testing only occurred during estrus. Behavior tests occurred between 11:00 am – 3:00 pm in the light phase, was video recorded using a Sony HD Handicam, and analyzed by an individual blinded to treatment and sex using the Stopwatch+ program (Center for behavioral Neuroscience; Atlanta, GA).

At least four days after the last behavior test, mice were anesthetized using ketamine (80 mg/kg) and xylazine (8 mg/kg) and transcardially perfused with heparanized PBS (pH 7.4) containing fluorescein isothiocyanate (FITC, Thermochemical, MW 389.4) followed by 4% paraformaldehyde in 0.1M phosphate buffer (pH 7.4; modified from Miyata & Morita, 2011). Brains were removed, post fixed overnight, and changed into 0.1M phosphate buffer for storage at 4°C.

Behavior Testing

After P50, mice were tested using the tail suspension test as previously described (Stratton, 2012). The TST is widely used to identify changes in depression- and helpless-like behaviors (Cryan et al., 2005). Briefly, mice were suspended by their tail, to a horizontal rod with adhesive tape at a height of 40 cm for 6 min and behavior was recorded via camcorder. Females were tested only during estrus. At least 4 days after the TST, SPT was initiated. SPT consisted of fluid intake measurement of 0.1% sucrose concentration with 2 days acclimation followed by 4 days with a two-bottle- choice paradigm (Mueller & Bale, 2008). Specially, mice were allowed to acclimate to individual housing and two bottles that were filled with water for two consecutive days. The following two days bottles were changed to contain sucrose. Days 5 – 9 mice were given the choice of either water or sucrose. Bottle weights were collected during the same time period during the 4 testing days and switch daily. The SPT was omitted because it was conducted using a subphysiological 0.1% (Alsio et al., 2011) and results would not be an adequate measurement of anhedonia.

Immunohistochemistry

Tissue was processed as previously described (Frahm et al. 2012; 2013). Brains were embedded in 5% agarose and cut coronally into 50 μ m thick sections using a vibrating microtome (Leica VT1000S). Free-floating serial sections were collected in 0.05M phosphate-buffered saline (PBS, pH 7.4). Excess unreacted aldehydes were neutralized in 0.1M glycine for 30 minutes followed by 0.5% sodium borohydride for 15 minutes. Sections were washed in PBS and incubated in a blocking solution (5% normal goat serum (NGS), 0.5% Triton X-100 (Tx), and 1% hydrogen peroxide in PBS) for at least 30 minutes. Sections were then incubated in primary antisera directed against Desmin (1:200; DAKO M0760) or GFAP (1:250; DAKO Z0334) in 1% BSA and 0.5% Tx. For desmin, sections were processed for antigen retrieval (Dellovade et al. 2001; Frahm et al., 2013). In place of the standard processing steps prior to antisera application detailed above, sections were washed in room temperature PBS for 15 min followed by a 1 h wash in sodium citrate (0.05 M, pH 8.6), then placed into sodium citrate buffer preheated to 80°C for 30 min. They were then allowed to slowly come back to room temperature (approximately 30–35 min) after which they were returned to PBS for an additional 15 min of washes. All sections were incubated for 2 nights at 4°C in primary antisera. Sections were then washed in room temperature with 1% NGS and 0.02% Tx in PBS followed by incubation with the appropriate secondary antibodies for 2h for using either Cy3 conjugated anti-rabbit (1:200; Jackson ImmunoResearch 711-166-152) or Cy3 conjugated anti-mouse (1:200; Jackson ImmunoResearch 711-165-150) in PBS containing 1% NGS and 0.32% Tx.

Analysis

Desmin, GFAP and FITC images were acquired for the PVN, LH and CTX on a Zeiss 510-Meta laser-scanning confocal microscope. FITC was imaged using a 488/543 nm bandpass filter and emission detected using a 505/530 nm bandpass emission filter. Cy3 for Desmin and GFAP

were imaged using a 488/543 nm bandpass filter and emission detected using a 585/615 nm bandpass emission filter. Z-stacks were acquired with 6 optical sections taken every 3 μ m obtained at 40x magnification using an oil immersion objective. The section with the densest vascular network was selected by an investigator blind to treatment group for each PVN region (rostral, mid, caudal) for analysis (Frahm et al. 2012). To view the vascular network within the brain Z-stacks were compiled.

Blood vessel density, width and extravascular leakage were determined as previously described (Frahm & Tobet, 2013abs). Images were inverted (Photoshop), light corrected (ImageJ, version 1.43u) then analyzed for length, as a measure of density, using Angiogenesis Tube Formation (Metamorph Software, version 7.7.0.0, Molecular Devices, Inc.). Extravascular leakage was analyzed using open-source CellProfiler (available from the Broad Institute at www.cellprofiler.org). Blood vessels were identified and a 10-pixel expansion was mapped from each blood vessel to create a mask to quantify leakage. This value was divided by FITC measured within blood vessels to account for differences in perfusions. Total Desmin-ir and GFAP-ir was measured for area of immunoreactivity and normalized to blood vessel area using Metamorph software. For GFAP-ir astrocytes in proximity to FITC labeled blood vessels, confocal stacks were merged and FITC-labeled blood vessels and GFAP-ir astrocytes were independently threshold, converted to binary, multiplied together, and areas that overlapped were quantified (ImageJ). Statistical significance was determined by ANOVA as sex X treatment (veh vs. dex) X region as a repeated measure using SPSS software (SPSS Inc., Chicago, IL). Values are reported as mean \pm SEM and $p < 0.05$ was considered significant. Representative images for figures were normalized for optimal contrast in Adobe Photoshop (version CS for Macintosh).

For the TST, times spent struggling or immobile were quantified. Time to first bout of immobility was determined as an indication of depression-like and helpless-like despair behavior (Francis et al., 2012). Animals that climbed their tail were removed from the analysis.

Results

Blood vessel density was analyzed after P50 in both males and females exposed to excess glucocorticoids during prenatal development. There was a significant increase in the rostral (figure 1a) and mid (figure 1b) PVN compared to CTX or LH ($p < 0.05$), consistent with previous studies (Frahm et al., 2012; Frahm & Tobet, 2013abs). Within the PVN, however, there were no differences in offspring of dex-treated mothers when examined after P50 for blood vessel area (Figure 5.1). Looking in the subregions of the PVN, there were no differences observed in the rostral (figure 5.1a), mid (figure 5.1b) or caudal (figure 5.1c) regions, or in the cortex or lateral hypothalamus due to sex or fetal treatment. These findings show that excess glucocorticoids during fetal development did not impact blood vessel density within the PVN in adulthood.

The current study found long-term changes in desmin-ir pericytes due to prenatal dex-treatment. To determine if fetal exposure to excess glucocorticoids impacts post-pubertal BBB components, desmin-ir pericytes were examined in relation to blood vessel density. After P50, there was a significant increase within the entire PVN for desmin-ir pericyte coverage in the male offspring of dex-treated mothers (figures 5.2d & 5.2e) compared to the males of veh-treated mothers (figures 5.2b & 5.2e; $p < 0.05$). For females at P50, there was a strong trend for offspring of dex-treated mothers (figures 5.2c & 5.2e) to have less desmin-ir pericyte coverage compared to veh-treated (figures 5.2a & 5.2e). The results suggest that long-term

changes in BBB components due to prenatal excess glucocorticoid exposure are dependent upon sex.

Astrocytes are another component of the BBB that were examined for long-term changes due to prenatal excess glucocorticoid exposure after P50. Total GFAP-ir was examined as a marker for astrocytes. There was a significant decrease in GFAP-ir within the entire PVN in the female offspring of dex-treated mothers (figures 5.3c & 5.3e) compared to female offspring of veh-treated mothers (figure 5.3a & 5.3e; $p < 0.05$). In addition, there was a trend for male offspring of veh-treated mothers (figures 5.3b & 5.3e) to have significantly less GFAP-ir than female offspring of veh-treated mothers (figures 5.3d & 5.3e). These results suggest that excess glucocorticoids during prenatal development may lead to decreased GFAP-ir astrocytes in young adult females.

Astrocytes serve many roles within the brain including their end-feet attachment to blood vessels as part of the BBB. GFAP-ir was quantified when there was optical overlap with blood vessels as a measure of astrocytes in proximity to blood vessels. There was a significant difference in GFAP-ir covering blood vessels within female offspring of dex-treated mothers (figures 5.4c, 5.4g, 5.4m) when compared to female offspring of veh-treated mothers within the mid region of the PVN (figure 5.4a, 5.4e, 5.4m; $p < 0.05$). There was also a significant decrease in GFAP-ir covering blood vessels in male offspring of veh-treated mothers (figure 5.4b, 5.4f, 5.4m) compared to female offspring of veh-treated mothers in the mid region of the PVN (figures 5.4a, 5.4e, 5.4m; $p < 0.05$). Differences observed in GFAP-ir overlapping blood vessels are also present with higher magnification (figures 5.4i-l). Results demonstrate that sex and excess prenatal glucocorticoid exposure impacted astrocytic end-feet coverage of blood vessels within the mid, most dense vascular region of the PVN (Frahm et al., 2012).

BBB competency was investigated by quantifying extravascular FITC dye leakage to determine if there are long-term changes to BBB competency within the PVN. Despite the alterations in BBB components, there were no differences in dye leakage observed due to sex or treatment in the CTX (figure 5.5a), LH (figure 5.5b) or PVN (figure 5.5c) at P50.

To test for long-term behavioral consequences of excess glucocorticoids during prenatal development, male and female offspring were assessed using the TST. There was a significant decrease in the time until the first bout of immobility in male and female offspring from dex-treated mothers compared to veh-treated (figure 5.6; $p < 0.05$). Thus excess glucocorticoids during fetal development resulted in an increase in helplessness- and depression-like behaviors compared to veh-treated mice in adulthood.

Discussion

The PVN has been known for some time to have a dense vascular network (Ambach & Palkovits, 1974; Basir 1931; Craigie, 1940; Finley, 1938; Frahm et al., 2012; Menendez & Alvarez-Uria, 1987; Poppi, 1928), but only recently have regulated changes been studied and observed (Biancardi et al., 2013; Cortes-Sol et al. 2013; Frahm & Tobet, 2013abs). The current study expands on alterations within the PVN vasculature by examining long-term consequences in adult offspring of dex-treated mothers. Results demonstrated an increase in desmin-ir pericyte coverage in male offspring of mice exposed to excess glucocorticoids. Female offspring of dex-treated mothers had a decrease in GFAP-ir astrocytes and a decrease in GFAP-ir astrocytes in proximity to blood vessels selectively within the PVN. In addition, both male and female offspring of dex-treated mothers had increased depressive-like behavior. This study provides another example of a long-lasting consequence of fetal dex-treatments on

behavior of offspring, and a novel view of simultaneous impact on components of the BBB within the PVN in a sex dependent manner.

There are a limited number of studies that examine changes in brain vasculature due to fetal exposure to excess glucocorticoids (Frahm & Tobet, 2012abs; Neigh et al., 2010). Prenatal dex administration reduced the vasculature within the Ca3 region of the hippocampus in adult males, which was further attenuated by restraint stress (Neigh et al., 2010). Interestingly within the basolateral amygdala, dex-treatment initially did not alter the vascular density, but after chronic stress there was a significant reduction (Neigh et al., 2010). Within the PVN, a decrease in the blood vessel density was observed in prepubertal males and females following fetal exposure to dex (Frahm & Tobet, 2012abs). In the current study, mice were examined after P50 (after puberty and in early adulthood) and blood vessel densities in the PVN were similar in offspring from veh- and dex-exposed mothers. These findings show changes in blood vessel density within the brain can be age, region, and activity-dependent. Further studies are needed to determine the direct impact of this diverse regulation on physiology and behavior.

Much work on blood vessels or the BBB focus on the cerebral cortex (Sadowska et al. 2009; Vorbrodt et al. 2001; Ezan et al. 2012; Armulik et al. 2010; Bell et al. 2010). Given the 3-fold greater density of vasculature in the PVN, there is significant need to determine the impact of stress responses and homeostasis in this region. For example, spontaneously hypertensive rats have a breakdown of the BBB within the PVN causing a feed forward loop increasing blood pressure (Biancardi et al., 2013). In the current study, the increase in desmin-ir pericytes in males and decreased GFAP-ir astrocytes in females observed in offspring of dex-treated mothers leads us to hypothesize that the BBB may be more susceptible to breakdown in the PVN during a disease state such as hypertension.

Pericytes stabilize vasculature (Vinukoda et al. 2010) and regulate capillary diameter through constricting vascular walls (Bell et al. 2010; Hall et al., 2014). In the current study, adult male offspring of dex-treated mothers had increased desmin-ir pericytes within the PVN. Previously, prepubertal males and females had an increase in pericytes coverage due to excess fetal glucocorticoids within the PVN (Frahm & Tobet, 2012abs). Differences due to prenatal glucocorticoid excess may impact blood flow within the PVN in males in adulthood, which has been shown to modulate metabolic exchange between capillaries and the parenchyma (Villringer & Dimagi, 1995). Within the PVN, changes in capillary diameter have been proposed to change blood flow (Cortes-Sol et al., 2013), although real measurements are really needed.

Astrocytic endfeet are an important component for a functional BBB. Astrocytes covering endothelial cells regulate water influx and efflux through aquaporin 4 (AQP4) that is distributed throughout the brain (Alvarez et al., 2013; Haj-Yasein et al., 2011; Nico & Ribatti, 2012). The observation that female offspring from dex-treated mothers had decreased GFAP-ir astrocytes in proximity to blood vessels may reduce AQP4 and alter water balance within the PVN. In addition, certain endothelial transporters such as P-glycoprotein (P-gp) or the glucose transporter GLUT-1 are present in perivascular glial end-feet and alterations could change BBB regulation of glucose and other metabolites (reviewed in Nico & Ribatti, 2012). Studies have directly shown glucocorticoids impact levels of PgP during late but not early gestation in the entire brain (Petropoulos et al., 2010), but whether these changes occur specifically within the PVN or last into adulthood are still unknown.

Changes in BBB components can impact its function. Loss of the gap junction proteins (i.e., connexins) specifically in astrocytes weaken the BBB, allowing circulating factors to gain access during increased hydrostatic vascular pressure and shear stress (Ezan et al., 2012). Under normal conditions, there is a lack of extravascular FITC leakage (e.g., figure 2), but mice

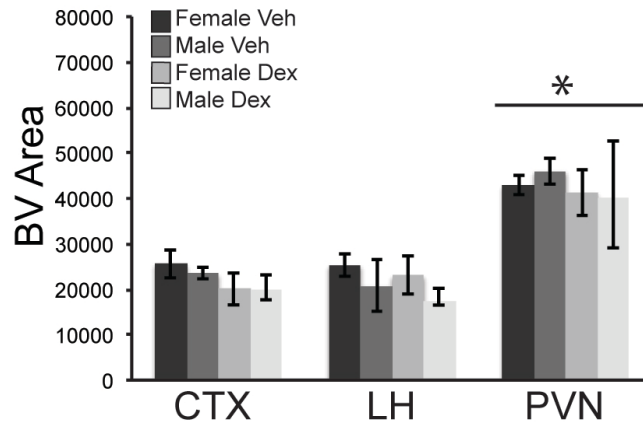
exposed to excess glucocorticoids during prenatal development may have an opening of the PVN BBB during an increase in blood pressure or flow. The loss of GFAP-ir astrocytes in proximity to blood vessels in male offspring or the increase in desmin-ir pericyte coverage in female offspring of dex-treated mothers may indicate loci of disorder susceptibility under certain conditions that decrease BBB function and integrity within the PVN.

In agreement with a number of prior studies (Roque et al., 2011; Bale, 2005) these results provide further evidence of long-lasting behavioral consequences due to excess glucocorticoids during prenatal development. A decrease in first bout to immobility demonstrates excess glucocorticoids during embryonic days 11-17 increased depression-like behavior in adulthood. Previously, prenatal dex has been shown to increase anxiolytic-like (Hossain et al., 2008) and depressive-like behaviors in adulthood (Roque et al., 2011). The results presented in this study show a similar increase in depression-like behaviors as well as changes in BBB components within the PVN. Whether other brain regions were impacted by global dex administration and may play a role in the observed increase in depression-like behavior is unknown. In addition, what role dex treatment has on pregnant females that may directly or indirectly impact offspring in utero or during postnatal maternal care is unknown.

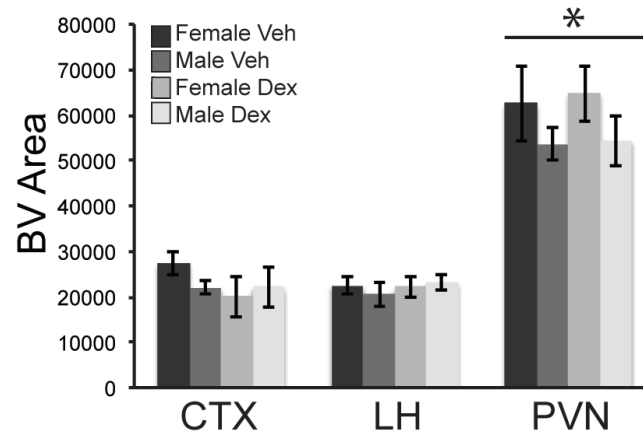
The current study was conducted to test the hypothesis that exposure to excess glucocorticoids during prenatal development has long term impact on the vasculature within the PVN and also has behavioral consequences that are commensurate with alterations in the HPA axis. The results indicate that maternal treatment with excess glucocorticoids (dex) lead to site selective (i.e., within the PVN) changes in components of the BBB in a sex-dependent manner in adulthood. An increase in displayed depression-like behavior was also observed. Therefore, there are long-lasting consequences on the BBB within the PVN and behavior in offspring of dex-treated mothers and potentially of all fetuses exposed to excess glucocorticoid stimulation

whether by exogenous (e.g., dex injection as per this study) or endogenous (e.g., maternal stress) means.

a. Rostral



b. Mid



c. Caudal

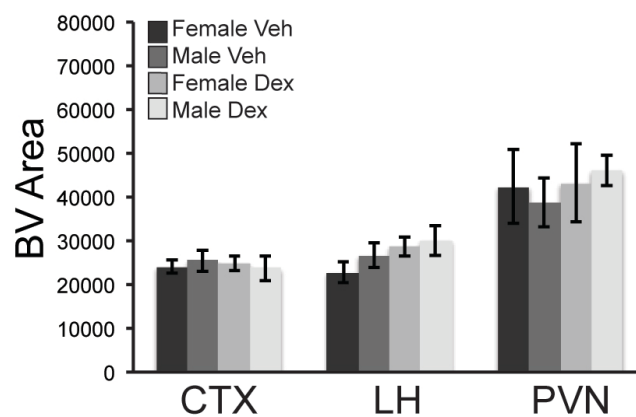


Figure 5.1. Prenatal exposure to dexamethasone (dex) does not impact blood vessel density within mouse paraventricular nucleus of the hypothalamus (PVN) at P50. The Rostral and Mid PVN has significantly more BV area that the CTX or LH. There were no differences due to dex treatment or for sex observed in either the rostral, mid, or caudal area of the PVN.

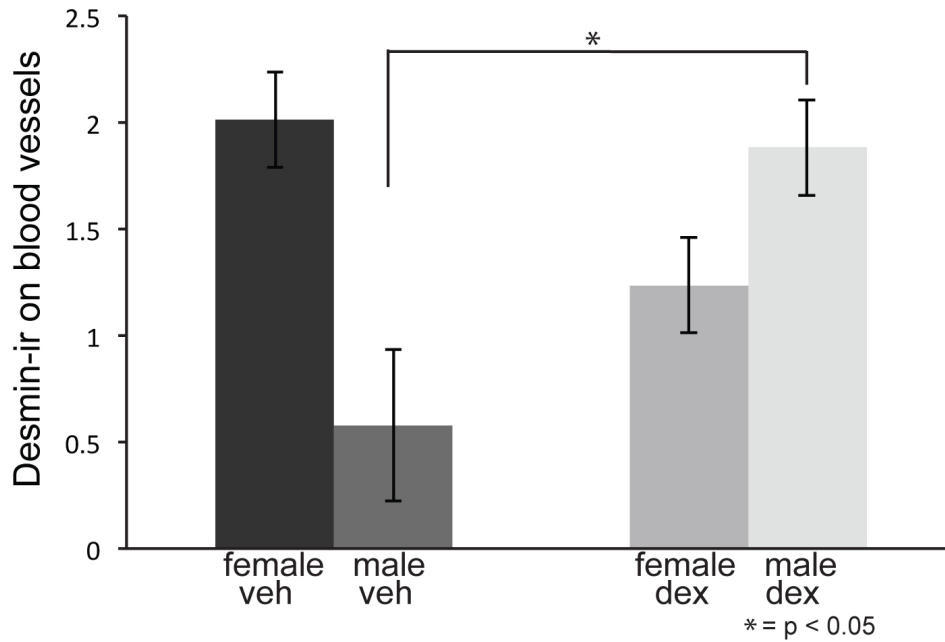
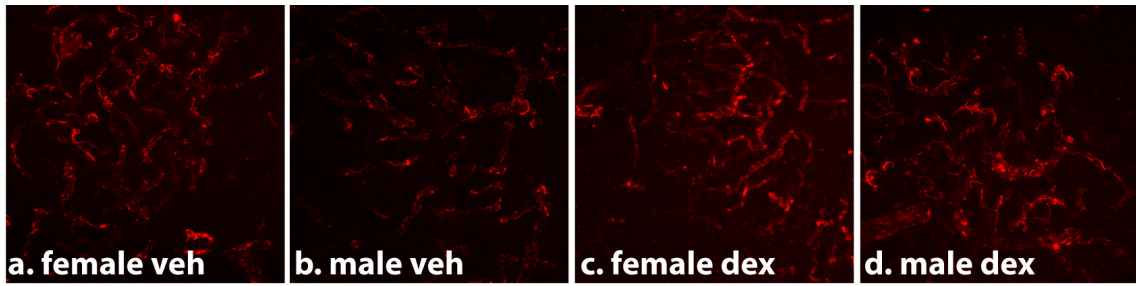


Figure 5.2. Prenatal exposure to dexamethasone (dex) impacted desmin-immunoreactive pericyte coverage in the male mouse paraventricular nucleus of the hypothalamus (PVN) at P50. There was a significant increase in total desmin-ir in dex-treated males (d) compared to veh-treated males (b; $p < 0.05$). There were differences observed for veh-treated (a) or dex-treated (c) females.

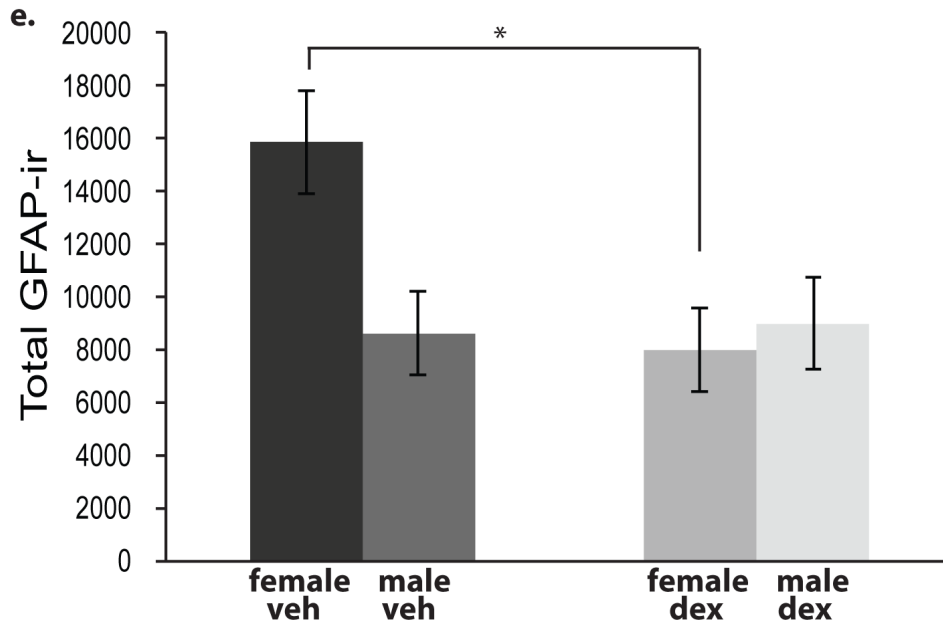
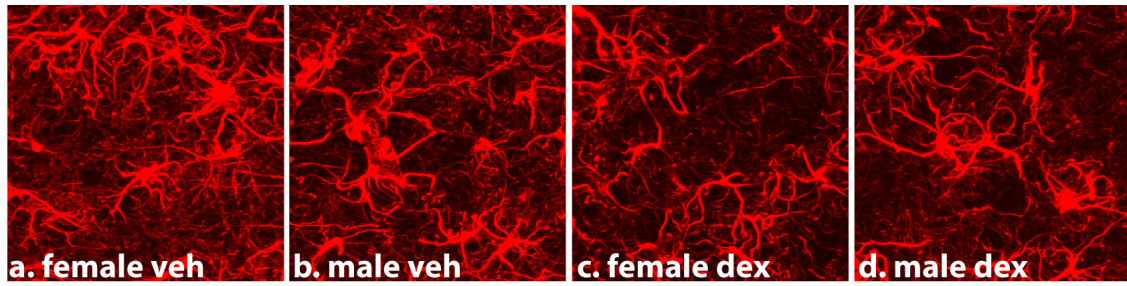


Figure 5.3. Prenatal exposure to dexamethasone (dex) impacted total GFAP-immunoreactive astrocytes in the female mouse paraventricular nucleus of the hypothalamus (PVN) at P50. There was a significant decrease on total GFAP-ir in the mid region of the PVN in dex-treated females (c, e) compared to veh-treated females (a, e; $p < 0.05$).

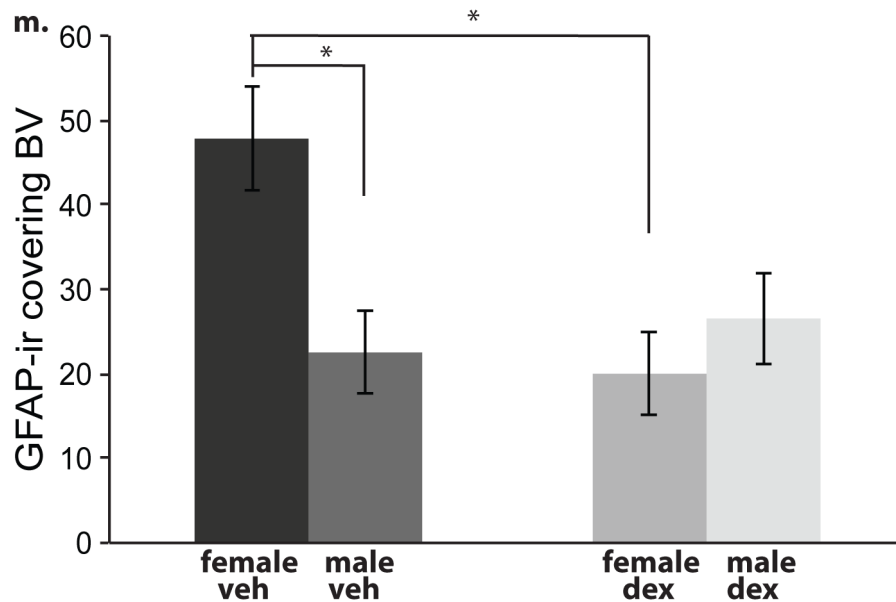
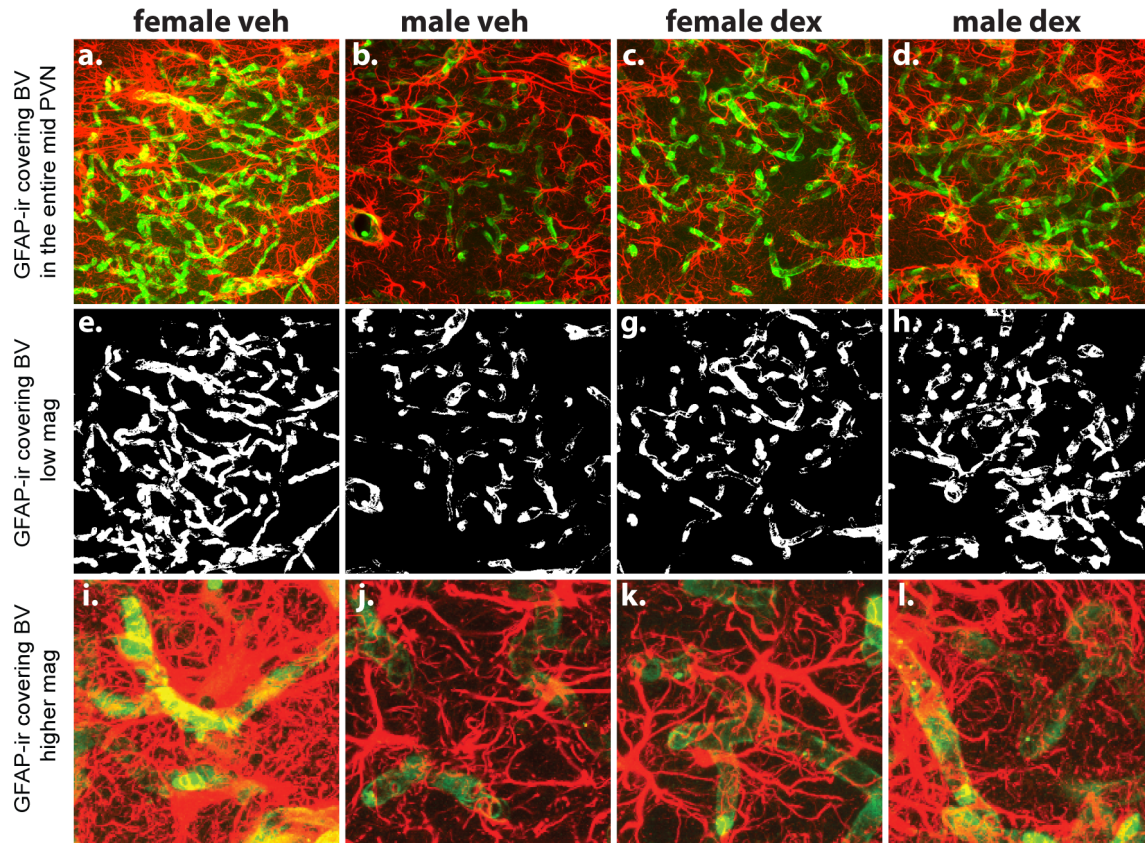
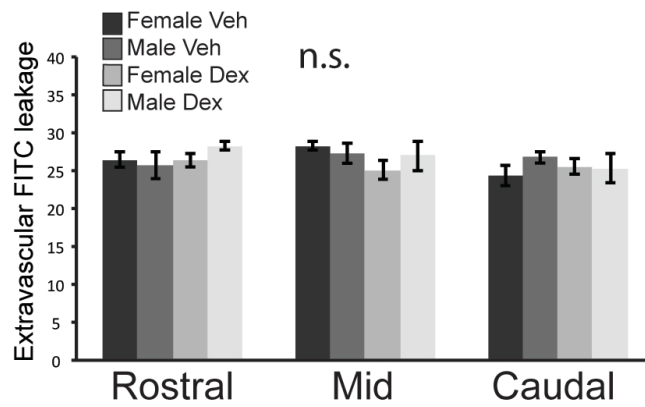
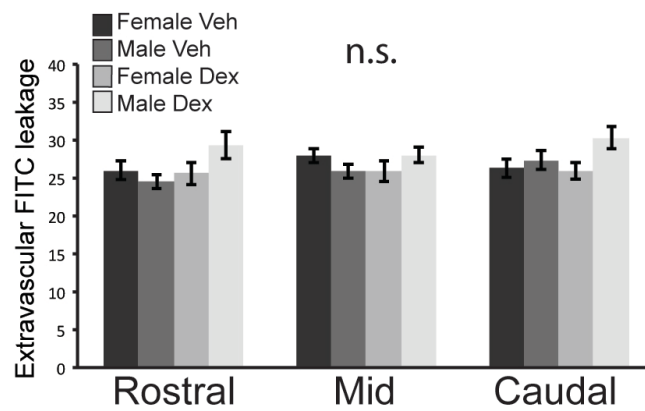


Figure 5.4. Prenatal exposure to dexamethasone (dex) impacted ir-GFAP surrounding blood vessels in the female mouse paraventricular nucleus of the hypothalamus (PVN) at P50. There was significantly more ir-GFAP in proximity to blood vessels in veh-treated females (a, e, i, m) compared to veh-treated males (b, f, j, m; $p < 0.05$) and dex-treated females (c, g, k, m; $p < 0.05$).

a. Cortex



b. Lateral Hypothalamus



c. Paraventricular Nucleus of the Hypothalamus

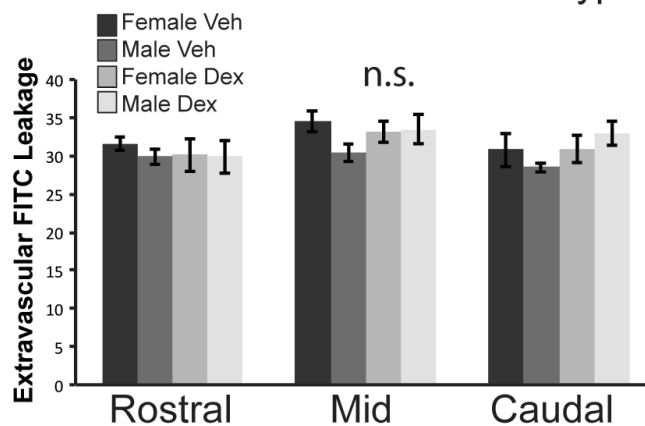


Figure 5.5. Prenatal exposure to dexamethasone (dex) does not impact the blood-brain barrier development in the mouse paraventricular nucleus (PVN) at P50. There were no differences observed in the rostral, mid or caudal regions of the PVN or in the lateral hypothalamus or cortex due to sex or treatment.

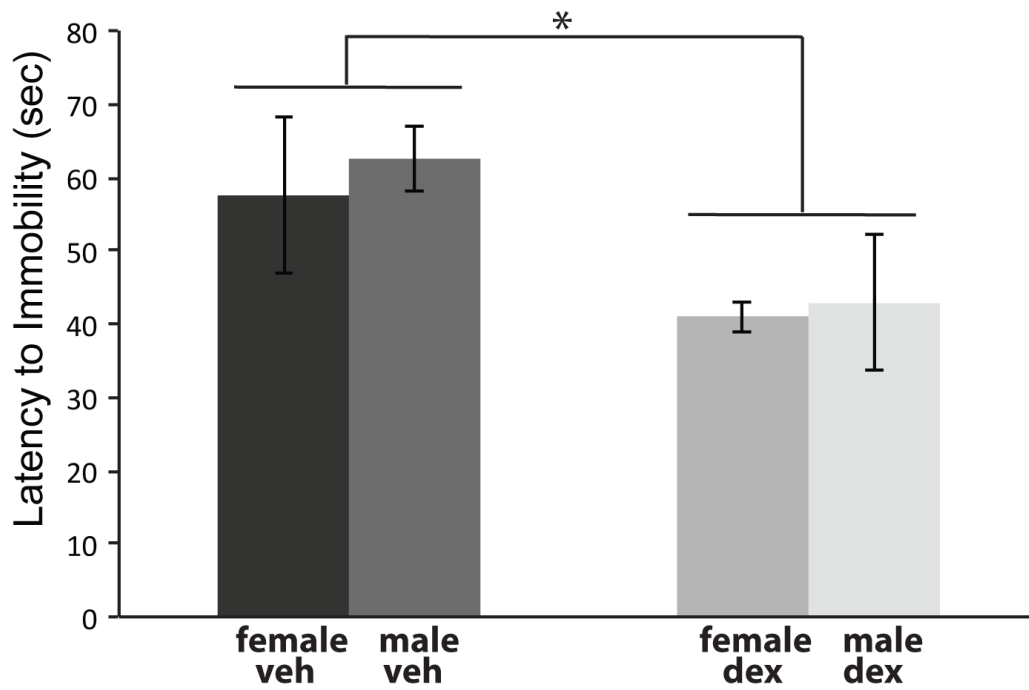


Figure 5.6. Testing for depression-like behavior using the tail suspension test (TST). Results showed dex-treated males had a significantly decrease latency until their first display of immobility ($p < 0.05$). This was true for both males and females treated with dex.

References

Abbott NJ, Ronnback L, Hansson E. Astrocyte-endothelial interactions at the blood-brain barrier. *Nat Rev Neurosci* 2006, 7: 41-53.

Alsio J, Nordenankar K, Arvidsson E, Birgner C, Mahmoudi S, Halbout B, Smith C, Fortin GM, Olson L, Descarries L, Trudeau LE, Kullander K, Levesque D, Wallen-Mackenzie A. Enhanced sucrose and cocaine self-administration and cue-inducing drug seeking after loss of VGLUT2 in midbrain dopamine neurons in mice. *J Neurosci* 2011, 31: 12593-12603.

Alvarez JI, Katayama T, Prat A. Glial influence on the blood brain barrier. *Glia* 2013, 61: 1939-1958.

Ambach G, Palkovits M. Blood supply of the rat hypothalamus. II. Nucleus paraventricularis. *Acta Morphol Acad Sci Hung* 1974, 22: 311-320.

Armulik A, Genove G, Mae M, Nisancioglu MH, Wallgard W, Niaudet C, He L, Norlin J, Lindblom P, Strittmatter K, Johansson BR, Betsholtz C (2010) Pericytes regulate the blood-brain barrier. *Nature* 468:557-561

Armstrong WE, Warach S, Hatton G I, McNeill TH. Subnuclei in the rat hypothalamic paraventricular nucleus: a cytoarchitectural, horseradish peroxidase and immunocytochemical analysis. *Neuroscience* 1980, 5: 1931-1958.

Basir MA. Vascular supply of pituitary in the dog. *Jour Anal* 1931, 66: 387.

Baum M, Ortiz L, Quan A. Fetal origins of cardiovascular disease. *Curr Opin Pediatr* 2003, 15: 166-70.

Baune BT, Stuart M, Gilmour A, Wersching H, Heindel W, Arolt V, Berger K. The relationship between subtypes of depression and cardiovascular disease: a systematic review of biological models. *Transl Psychiatry* 2012, 2: 92.

Becker JB, Arnold AP, Berkley KJ, Blaustein JD, Eckel LA, Hampson E, Herman JP, Marts S, Sadee W, Steiner M, Taylor J, Young E. Strategies and methods for research on sex differences in brain and behaviors. *Endocrinology* 2005, 146: 1650-1673.

Bell RD, Winkler EA, Sagare AP, Singh I, LaRue B, Deane R, Zlokovic BV (2010) Pericytes control key neurovascular functions and neuronal phenotype in the adult brain and during brain aging. *Neuron* 68:409-427

Biag J, Huang Y, Gou L, Askarinam A, Hahn JD, Toga AW, Hintiryan H, Dong HW. Cyto- and chemoarchitecture of the hypothalamic paraventricular nucleus in the C57BL/6J male mouse: A study of immunostaining and multiple fluorescent tract tracing. *J Comp Neurol* 2012, 520: 6-33.

Biancardi, VC, Son SJ, Ahmadi A, Filosa JA, Stern JE. Circulating angiotension II gains access to the hypothalamus and brain stem during hypertension via breakdown of the blood-brain barrier. *Hypertension* 2013, epub ahead of print.

Bingham B, Williamson M, Viau V. Androgen and estrogen receptor-beta distribution within spinal-projecting and neurosecretory neurons in the paraventricular nucleus of the male rat. *J Comp Neurol* 2006, 499: 911-923.

Braga VA, Medeiros IA, Ribeiro TP, Franca-Silva MS, Botelho-Ono MS, Guimaraes DD. Angiotension-II- induced reactive oxygen species along the SFO-PVN-RVLM pathway: implications in neurogenic hypertension. *Braz J Med Biol Res* 2011, 44: 871-6.

Cortes-Sol A, Lara-Garcia M, Alvarado M, Hudson R, Berbel P, Pacheco P. Inner capillary diameter of hypothalamic paraventricular nucleus of female rat increases during lactation. *BMC Neurosci* 2013, 14: 7.

Craigie EH. On the relative vascularity of various parts of the central nervous system of the albino rat. *J Comp Neurol* 1920, 20: 310-319.

Cryan JF, Mombereau C., Vassout A. The tail suspension test as a model for assessing antidepressant activity: review of pharmacological and genetic studies in mice. *Neurosci Biobehav Rev* 2005, 29: 571-625.

Dellovade TL, Davis AM, Ferguson C, Sieghart W, Homanics GE, Tobet SA. GABA influences the development of the ventromedial nucleus of the hypothalamus. *J Neurobiol* 2001, 49: 264-276.

Fan ZD, Zhang L, Shi Z, Gan ZB, Gao XY, Zhu GQ. Artificial microRNA interference targeting AT(1a) receptors in the paraventricular nucleus attenuated hypertension in rats. *Gene Ther* 2012, 1-8.

Ferguson AV, Latchford, KJ, Samson WK. The paraventricular nucleus of the hypothalamus – a potential target for integrative treatment of autonomic dysfunction. *Expert Opin Ther Targets* 2008, 12: 717-721.

Finley KH. The capillary bed of the paraventricular and supraoptic nuclei of the hypothalamus. *Res Publ Assoc Res Nerv Ment Dis* 1938, 18: 94-109.

Ford-Holevinski TS, Castle MR, Herman JP, Watson SJ. Microcomputer-based three-dimensional reconstruction of in situ hybridization autoradiographs. *J Chem Neuroanat* 1991, 4: 373-385.

Frahm, KA, Schow, MJ, Tobet, SA. The Vasculature within the Paraventricular Nucleus of the Hypothalamus in Mice Varies as a Function of Development, Sub-Nuclear Location, and GABA signaling. *Horm Metab Res* 2012, 44: 1-6.

Frahm KA, Nash CP, Tobet SA. Endocan immunoreactivity in the mouse brain: Method for identifying nonfunctional blood vessels. *J Immunol Methods* 2013, 398: 27-32.

Frahm, K. A., Tobet, S. A. Development of the blood-brain barrier within the paraventricular nucleus of the hypothalamus: influence of fetal glucocorticoid excess. Presented at Society for Endocrinology 2013, San Francisco CA. *Endocrine Abstracts* FP03-4/SAT-5.

Francis BM, Yang J, Hajderi E, Brown ME, Michalski B, McLaurin J, Fahnestock M, Mount HT. Reduced tissue levels of noradrenaline are associated with behavioral phenotypes of the

TgCRND8 mouse model of alzheimer's disease. *Neuropsychopharmacology* 2012, 37: 1934-1944.

Goldstein JM, Handa RJ, Tobet SA. Disruption of fetal hormone programming (prenatal stress) implicated shared risk for sex differences in depression and cardiovascular disease. *Front Neuroendocrinol* 2014, 35: 140-158.

Hadoke PW, Lindsay RS, Seckl JR, Walker BR, Kenyon CJ. Altered vascular contractility in adult female rats with hypertension programmed by prenatal glucocorticoid exposure. *J Endocrinol* 2006, 188: 435-442.

Haj-Yasein NN, Vindedal GF, Eilert-Olsen M, Gundersen GA, Skare O, Laake P, Klungland A, Thoren AE, Burkhardt JM, Ottersen OP, Nagelhus EA. Glial-conditional deletion of aquaporin-4 (Aqp4) reduces blood-brain water uptake and confers barrier function on perivascular astrocyte endfeet. *Proc Natl Acad Sci* 2011, 108: 17815-17820.

Handa RJ, Weiser MJ. Gonadal steroid hormones and the hypothalamo-pituitary-adrenal axis. *Front Neuroendocrinol* 2013, epub ahead of print.

Hawkins BT, Davis TP. The blood-brain barrier/neurovascular unit in health and disease. *Pharmacol Rev* 2005, 57: 173-185.

Hill JW. PVN pathways controlling energy homeostasis. *Indian J Endocrinol Metab* 2012, 16: S627-636.

Hossain A, Haiman K, Charitidi K, Erhardt S, Zimmermann U, Knipper M, Canlon B. Prenatal dexamethasone impairs behavior and the activation of the BDNF exon IV promoter in the paraventricular nucleus in adult offspring. *J Endocrinol* 2008, 149: 6356-6365.

Iadecola C. Neurovascular regulation in the normal brain and in alzheimer's disease. *Nat Rev Neurosci* 2004, 5: 347-360.

Levitt NS, Lindsay RS, Holmes MC, Seckl JR. Dexamethasone in the last week of pregnancy attenuated hippocampal glucocorticoid receptor gene expression and elevates blood pressure in the adult offspring in the rat. *Neuroendocrinology* 1996, 64:412-418.

Levy BH, Tasker JG. Synaptic regulation of the hypothalamic-pituitary-adrenal axis and its modulation by glucocorticoids and stress. *Front Cell Neurosci* 2012, 6: 24.

Lund TD, Munson DJ, Haldy ME, Handa RJ. Androgen inhibits, while oestrogen enhances, restraint-induced activation of neuropeptide neurones in the paraventricular nucleus of the hypothalamus. *J Neuroendocrinol* 2004, 16: 272-278.

Maccari S, Darnaudery M, Morley-Fletcher S, Zuena AR, Cinque C, Van Reeth O. Prenatal stress and long-term consequences: implications of glucocorticoid hormones. *Neurosci Biobehav Rev* 2003, 27: 119-127.

McClellan KM, Stratton MS, Tobet SA. Roles for gamma-aminobutyric acid in the development of the paraventricular nucleus of the hypothalamus. *J Comp Neurol* 2010; 518: 2710-2728.

- Menendez A, Alvarez-Uria M. The development of vascularization in the postnatal rat paraventricular nucleus: a morphometric analysis. *J Hirnforsch* 1987, 28: 325-329.
- Mitra SW, Hoskin E, Yudkovitz J, Pear L, Wilkinson HA, Hayashi S, Pfaff DW, Ogawa S, Rohrer SP, Schaeffer JM, McEwen BS, Alves SE. Immunolocalization of estrogen receptor beta in the mouse brain: comparison with estrogen receptor alpha. *Endocrinology* 2003, 144: 2055-2067.
- Miyata S, Morita S. A new method for visualization of endothelial cells and extravascular leakage in adult mouse brain using fluorescein isothiocyanate. *J Neurosci Methods* 2011, 202: 9-16.
- Mueller BR, Bale TL. Sex-specific programming of offspring emotionality after stress early in pregnancy. *J Neurosci* 2008, 28: 9055-9065.
- Neigh GN, Owens MJ, Taylor WR, Nemeroff CB. Changes in the vascular area fraction of the hippocampus and amygdala are induced by prenatal dexamethasone and/or adult stress. *J Cereb Blood Flow Metab* 2010, 30: 1100-1104.
- Nico B, Ribatti D. Morphofunctional aspects of the blood-brain barrier. *Curr Drug Metab* 2012, 13: 50-60.
- O'Regan D, Kenyon CJ, Seckl JR, Holmes MC. Glucocorticoid exposure in late gestation in the rat permanently programs gender-specific differences in adult cardiovascular and metabolic physiology. *Am J Physiol Endocrinol Metab* 2004, 287: 863-870.
- Petropoulos S, Gibb W, Matthews SG. Developmental expression of multidrug resistance phosphoglycoprotein (p-gp) in the mouse fetal brain and glucocorticoid regulation. *Brain Res* 2010, 1357, 9-18.
- Poppi U. La syndrome anatome-clinica conseguente a lesione dell'art coroidea anteriore. *Rev Di neurol* 1928.
- Quaegebeur A, Lange C, Carmeliet P. The neurovascular link in health and disease: molecular mechanisms and therapeutic implications. *Neuron* 2011, 71: 406-424.
- Roque S, Oliveira TG, Nobrega C, Barreira-Silva P, Nunes-Alves C, Sousa N, Palha JA, Correia-Neves M. Interplay between depressive-like behavior and the immune system in an animal model of prenatal dexamethasone administration. *Front Behav Neurosci* 2011, 5: 1-8.
- Sadowska GB, Malaeb SN, Stonestreet BS (2009) Maternal glucocorticoid exposure alters tight junction protein expression in the brain of fetal sheep. *Am J Physiol Heart Circ Physiol* 298:179-188
- Saunders NR, Daneman R, Dziegielewska MK, Liddelow SA. Transporters of the blood-brain and blood-CSF interfaces in development and in the adult. *Molecular Aspects of Medicine* 2013, 34: 742-752.
- Simmons DM, Swanson LW. Comparison of the spatial distribution of seven types of neuroendocrine neurons in the rat paraventricular nucleus: toward a global 3D model. *J Comp Neurol* 2009; 516: 423-441.

Sriramula S, Cardinale JP, Lazartigues E, Francis J. ACE2 overexpression in the paraventricular nucleus attenuates angiotension II-induced hypertension. *Cardiovasc Res* 2011, 92: 401-408.

Stratton MS. Gamma-aminobutyric acid (GABA) in the development of the paraventricular nucleus of the hypothalamus (PVN): implications for adult disease. PhD dissertation, Colorado State University, Fort Collins, 2012, <http://hdl.handle.net/10217/71591>.

Swanson LW, Sawchenko PE. Hypothalamic integration: organization of the paraventricular and supraoptic nuclei. *Annu Rev Neurosci* 1983; 6: 269-324.

Thayer JF, Yamamoto SS, Brosschot JF. The relationship of autonomic imbalance, heart rate variability and cardiovascular disease risk factors. *Int J Cardiol* 2010, 141: 122-131.

The World Health Report 2001 - Mental Health: New Understanding, New Hope. <http://www.who.int/whr/2001/en/>.

Villringer A, Dirnagl U. Coupling of brain activity and cerebral blood flow: basis of functional neuroimaging. *Cerebrovasc Brain Metab Rev* 1995, 7: 240-276.

Vinukonda G, Dummula K, Malik S, Hu F, Thompson C, Csiszar A, Ungvari Z, Ballabh P (2010) Effect of Prenatal Glucocorticoids on Cerebral Vasculature of the Developing Brain. *Stroke* 41:1766-1773

Welberg LA, Seckl JR, Holmes MC. Prenatal glucocorticoid programming of brain corticosteroid receptors and corticotrophin-releasing hormone: possible implications for behavior. *Neuroscience* 2001, 104: 71-79.

CHAPTER 6: DISCUSSION

The current set of studies establishes that the dense vascular network within the PVN develops postnatally in mice. Within the PVN, the blood vessels were selectively densest in the rostral and mid regions of the nucleus. Capillaries of the PVN were of larger diameters compared to other brain regions. The vascular network of the PVN can be regulated by both endogenous and exogenous factors. In mice lacking a functional GABA_B receptor blood vessel density was decreased in the mid region at P20. Maternal treatment with exogenous glucocorticoids resulted in offspring that at P20 had decreased blood vessel density, and increased extravascular FITC leakage and desmin-ir pericyte coverage. In an independent replication of the fetal glucocorticoid treatment that examined offspring PVN vasculature after puberty there were sex-dependent alterations of blood brain barrier components, but no steady state differences in vascular density or extravascular FITC leakage. Overall, these findings demonstrate that GABAergic stimulation and glucocorticoid receptor activation during fetal development provide examples of regulatory targets for the development of the uniquely dense vasculature of the PVN.

There is a growing body of evidence showing that nonneuronal cells are critical for brain development and degeneration. Astrocytes were previously thought to be “brain glue” or simply support cells (Reviewed in Freeman & Rowitch, 2013; Ransom et al., 2003). Now, it is apparent that they enhance neuronal function and play important roles in neurological diseases.

Progress has been made in advancing the role astrocytes play on neuron development and function (Clark & Barres, 2013; del Puerto et al., 2013; Freeman & Rowitch, 2013; Ransom et al., 2003), but there is still work to be done on their role in NVUs and the BBB. Data from clinical studies show a reduction in the total number of GFAP-ir astrocytes and astrocytic endfeet coverage of blood vessels in patients diagnosed with MDD (Rajkowska et al., 2013). In

female offspring of dex-treated mothers I observed a decrease in total ir-GFAP and in ir-GFAP proximal to blood vessels within the PVN. This suggests a mechanism for how excess glucocorticoids during prenatal development could predispose an individual to developing a disorder such as MDD in adulthood (Wyrwoll & Holmes, 2012). The potential role a decrease in PVN astrocyte coverage specifically may exert on the physiology and behavior of an organism is still unknown.

Vascular coverage by pericytes increased due to excess glucocorticoids during fetal development in the germinal matrix of rabbits and humans (Vinukonda et al. 2010). I found an increase at P20 in both dex-treated males and females, but at P50 this increase was limited to dex-treated males. It is possible that at P20 pericytes migrated into the PVN in response to new vessel formation, traumatic stress, or other hypoxic injury or state (Dore-Duffy et al. 2000) indicated by excess FITC leakage within the PVN. At P50, enhanced pericyte coverage may stabilize the vasculature (Vinukonda et al. 2010). Since pericytes can regulate capillary diameter through constricting the vascular wall (Bell et al. 2010), increases at both P20 and P50 due to prenatal glucocorticoid excess may impact blood flow within the PVN and subsequently the health of the neuronal population.

The physiological role for the postnatal increase in blood vessel density remains elusive. Many studies have characterized the dramatic blood vessel density within the adult PVN (e.g. Ambach & Palkovits, 1974; Basir 1931; Craigie, 1940; Poppi, 1928; van den Pol, 1997). In rats, this increase occurs on the day of birth and decrease by P2, and then increases again over the next few weeks (Menendez & Alvarez-Uria, 1987). Notably I observed at birth the blood vessel network is similar to surrounding brain regions. By P8 there is a significant increase in blood vessel density. This suggests the factors responsible for the postnatal angiogenic period in mice may be delayed or different than rats. It has been hypothesized that the vast blood vessel

network of the PVN may be used to detect plasma osmotic pressure by magnocellular neurons (Badaut et al., 2000) that are abundant in the mid PVN region in mice (Biag et al., 2012). A decrease in PVN vasculature may reduce accessibility to oxygen and nutrients, which could impact a neuron's ability to effectively relay its metabolic needs (Quaegebeur et al., 2011) or receive proper feedback resulting in dysfunction. Since the mid region of the mouse PVN houses the majority of CRH, OT, AVP, TRH and somatostatin neurons as compared to the rostral or caudal regions (Biag et al., 2012), changes in vascular characteristics may alter their ability to respond properly to signals from the periphery. Future studies should attempt to identify the factor(s) involved in the postnatal angiogenic period and if inhibition disrupts physiology and behavior.

GABA_BR1 deficient mice were used to show disruptions of development for neuronal populations within the PVN (McClellan et al., 2010; Stratton et al., 2011). I observed these mice also displayed reduced vasculature at P20 (Frahm et al., 2012). The mechanisms responsible for this decrease in blood vessel development remain unclear. These findings are consistent with the hypothesis that the disruption of cell placement has a direct impact on the postnatal angiogenic period. Whether the phenotypes previously characterized in these mice can be directly tied to changes in blood vessel density remain to be determined. Examining the development of the PVN from neuronal to vascular will provide insight into function as well as help delineate the loci of dysfunction.

As the blood vessel density increases during postnatal development, so do the components of the BBB, maintaining its integrity. Desmin-ir pericytes significantly increased within the PVN between P12 and P22. For BBB competency, perfusion with FITC at P12 and P22 did not result in extravascular dye leakage. Future studies should delineate developmental timing for BBB components (e.g. pericytes and astrocytes as well as particular proteins components). The

timing of BBB component development can then be related to BBB functional development. This can be examined through FITC perfusion followed by ir-endocan. Chapter 3 indicates that prior perfusion with FITC blocks endocan immunoreactivity and can be used to identify non-functional, developing blood vessels during the postnatal angiogenic period (Frahm et al, 2013).

In response to a global treatment, most observed changes were restricted to the PVN. This suggests the BBB varies at the individual endothelial cell level (Saubamea et al., 2012). In fact, endothelial cells in the heart respond differently in the myocardium than the brain when exposed to glucocorticoids (Forster et al., 2006). Differences in responsiveness to glucocorticoids in cultured brain endothelial cells have been observed depending on the days of embryonic collection (Iqbal et al., 2011). In addition, it has been shown that excess glucocorticoids during prenatal development in female rats resulted in changes in vascular responsiveness in different blood vessels in adulthood. Specifically, dex-treated females were less responsive to angiotensin II in the aorta while the mesenteric arteries when exposed to norepinephrine, vasopressin and potassium were more responsive (Hadoke et al., 2006). In my studies within the PVN there was a loss of blood vessel density that did not occur in the LH or CTX. Therefore, future studies should focus on looking at specific brain regions for changes due to excess glucocorticoids.

In seeking to identify potential angiogenic markers to further characterize the postnatal angiogenic period within the PVN we observed that ir-endocan was present uniformly throughout the brain in certain mouse strains. This suggests that unlike the periphery, endocan is not a suitable marker for angiogenesis within the brain. Endocan in the periphery and elevated levels in serum have been proposed to be a biomarker for cancer and sepsis (Lee et al., 2014; Sarrazin et al., 2006). Recently, it was suggested that administering neutralizing endocan antibodies to reduce serum endocan levels may provide a therapeutic treatment for

sepsis *in vivo* (Lee et al., 2014). Therefore, it may be useful to determine the role that endocan plays in brain vasculature brain before inhibiting it globally.

The presence of extravascular FITC leakage and decrease in blood vessel density in offspring exposed to excess glucocorticoids during prenatal development only at P20 and not in a separate cohort at P50 indicates a potential delay in the postnatal angiogenic period within the PVN. In addition, the increased presence of pericytes may indicate they were recruited to aid in the postnatal development of the BBB within the PVN. Further support is shown by a functional BBB and normal blood vessel density within dex-treated mice during adulthood. The exact cause of BBB disruption in dex-treated mice at P20 is currently unknown. Other BBB components, such as tight junction proteins, do play a role and should be examined. Prenatal dex increases certain tight junction proteins in the sheep cortex when looking during gestation at the cerebral cortex (Malaeb et al., 2007; Sadowska et al., 2009) or *in vitro* (Burek & Forster, 2009; Forster et al., 2005; Romero et al., 2003). It is possible there is a decrease at P20 in tight junctional proteins, consequently reducing the integrity of the BBB and permitting FITC to leak into the PVN in dex-treated mice. Preliminary studies to examine tight junction proteins ZO1 and claudin 5 by immunohistochemistry were not successful due to reagent failures. In situ hybridization experiments localized claudin 5 mRNA densely within the postnatal PVN (Zhang & Tobet, unpublished findings), but this was not examined relative to fetal dex exposure.

BBB breakdown can be problematic due to disruption of the highly regulated microenvironment and the protection from circulating toxins (Erickson et al., 2012). During hypertension, circulating angiotensin II gains access to the PVN and its receptor AT1 due to BBB breakdown (Biancardi et al., 2013). Therefore, circulating factors may gain access with physiological consequences. In the case of angiotensin II, binding to AT1 contributes to sympathetic outflow and increased blood pressure during hypertension (Biancardi et al., 2013). In addition, during BBB breakdown

it is possible for other circulating factors, which are normally regulated by transport across the BBB into the PVN, to have free access to their receptors. It has been shown that increases in transmission of vasopressin from the PVN can increase blood pressure and heart rate (Kc et al., 2010). Therefore, loss of BBB competency can allow circulating factors to penetrate the PVN and have negative consequences.

In vitro models may provide important venues for future studies. Organotypic brain slices may be used to determine whether excess glucocorticoids or GABA_B receptor antagonists such as CGP 55845 impact angiogenesis and components of the BBB and neurovascular unit within the PVN in real time. The neuronal population may be initially impacted, then when the postnatal angiogenic period initiates it varies due to differences in the placement of neurons. Since differences in desmin-ir pericytes varied at P20 and P50 in dex-treated mice, and blood vessel density was decreased in both GABA_B KO and dex-treated mice, it suggests that the blood vessels and BBB respond to disruptions in the neuronal population. BBB components and blood vessels may respond simultaneously and the use of organotypic slices may delineate this. The benefit of *in vitro* studies is the ability to control variables. While *in vitro* studies have potential drawbacks such as the absence of blood flow and consequent shear stresses that affect the properties of endothelial cells (Warboys et al., 2010), studies have shown that blood vessels and neurons can persist in these conditions (Moser et al., 2003). I was able to maintain blood vessels up to 3 days *in vitro* and capture video sequences using Tie2-GFP mice of increased GFP-positive endothelial cells (figure 6.1). Unfortunately, the paradigm was unreliable and improvements are still needed. The benefits of an *in vitro* system to study blood vessel and BBB development within the PVN encourage future efforts.

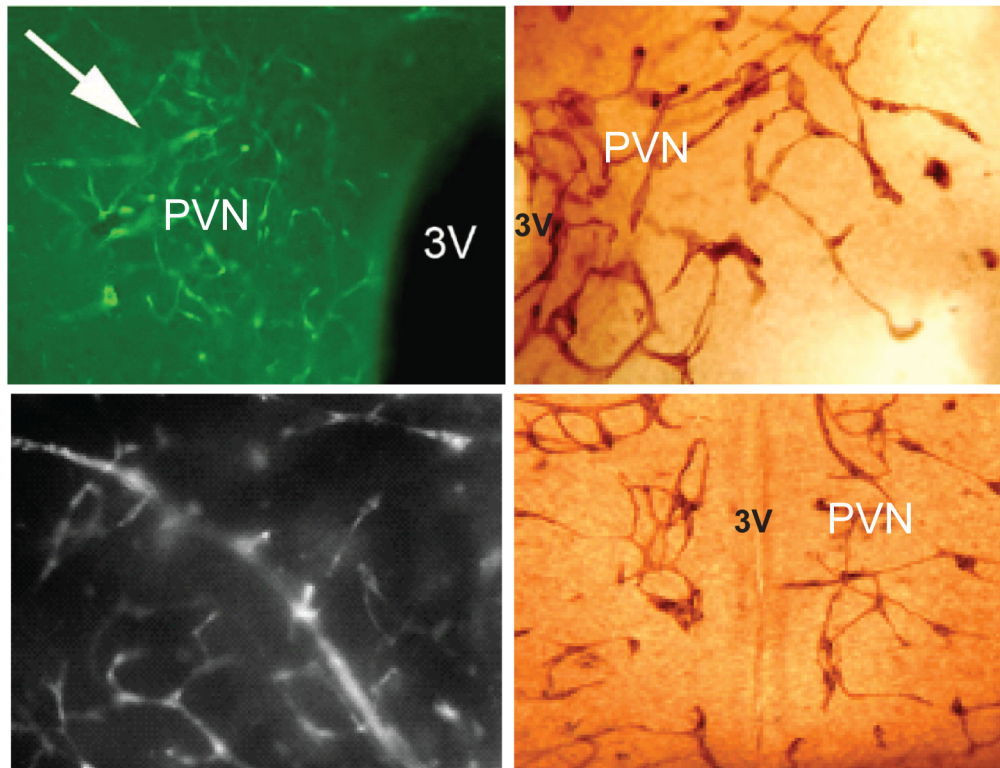


Fig 6.1. Blood vessels maintained in vitro. Top left: Fluorescent vessels in the PVN in an adult fixed Tie2-GFP mouse. Provided by MJ Schow. Top right: 20x image of BVs in a P12 slice after 2 days *in vitro*. Bottom left: image was taken live from a slice from Tie-2-GFP mouse in vitro for 48h treated with 30ng VEGF. Bottom right: BVs within the PVN in a P2 slice after 5 days *in vitro*.

There is mounting evidence that BBB disruption is associated with neurological disorders.

Initially it was assumed that BBB disruption was secondary to neuronal loss. A prime example

is the amyloid cascade hypothesis, which states that amyloid- peptide deposits in the brain

initiate Alzheimer's disease (Erickson & Banks, 2013). Much research today focuses on this

hypothesis; however, evidence supports looking at the BBB at its role upstream of amyloid.

This shift in focus has extended beyond Alzheimer's disease to other neurological disorders,

suggesting BBB disruption proceeds and can accelerate degeneration in adulthood and aging

(Zlokovic, 2008). For PVN development, these studies show excess glucocorticoids or a loss of

GABA_B receptors directly or indirectly change the vascular network. Whether there is a

propensity for BBB breakdown to occur during aging is an area for future study.

In summary, this work shows a postnatal angiogenic period with the greatest increase in blood vessel density occurring in the rostral and mid regions of the mouse PVN. This was disrupted at P20 in mice either deficient in GABA_B signaling or exposed to excess glucocorticoids during fetal development. Excess fetal glucocorticoids also decreased BBB competency at P20 and increased desmin-ir pericyte coverage. Into adulthood, there were long lasting impacts in BBB components in a sex-dependent manner. These changes observed within the neurovascular unit, specifically within the PVN in GABA_BR1 KO or dex-treated mice, may be an important locus for understanding disorders of the HPA axis with potential impact for mood disorders and other comorbid disorders with ties to PVN functions such as CVD (figure 6.2).

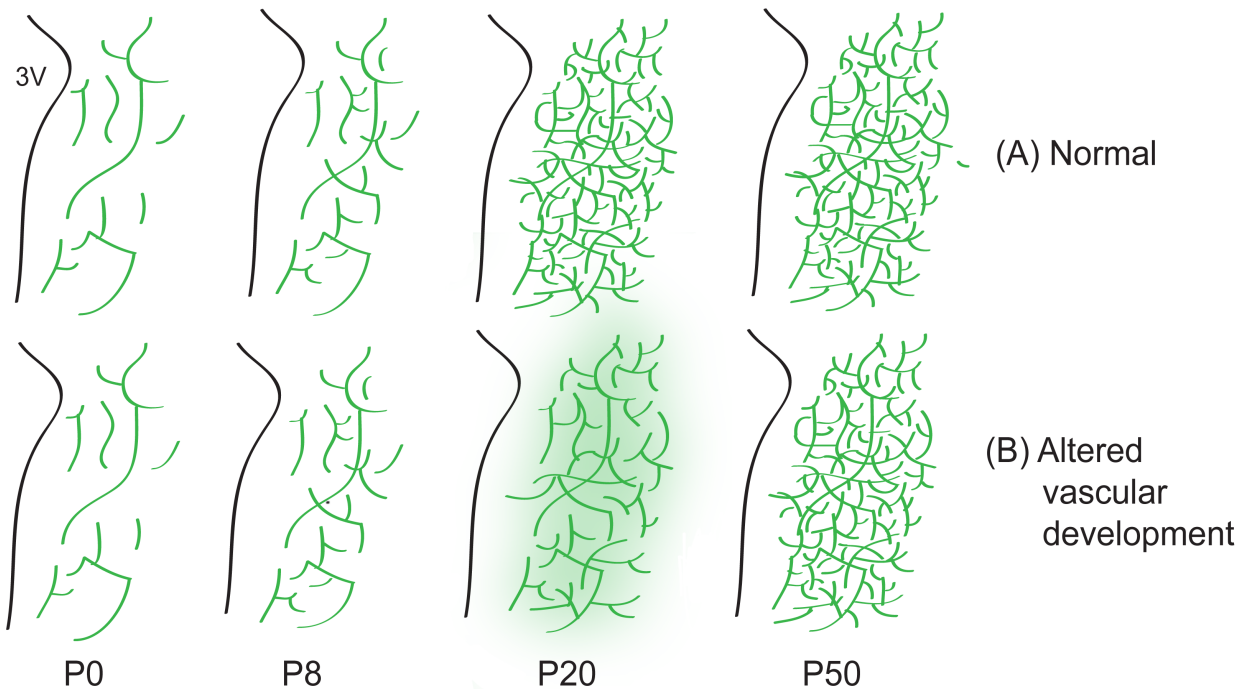


Figure 6.2. Current model of postnatal blood vessel development in the paraventricular nucleus of the hypothalamus (PVN) along with alterations due to excess glucocorticoids during embryonic development. In the mouse PVN, there is a 40% increase in blood vessel density between postnatal (P) days 12 and 20 and is maintained out into adulthood (A). Excess glucocorticoid during prenatal development does not disturb the initial vascular network in the PVN but at P20 there is a decreased vascular network that has a compromised blood-brain barrier (BBB), while at P50 there are no differences observed in the density or BBB (B).

REFERENCES

Abbott NJ, Ronnback L, Hansson E. Astrocyte-endothelial interactions at the blood-brain barrier. *Nat Rev Neurosci* 2006, 7: 41-53.

Abbott NJ. Blood-brain barrier structure and function and the challenges for CNS drug delivery. *J Inher Metab Dis* 2013, 36: 437-449.

Abbott NJ, Friedman A. Overview and introduction: The blood-brain barrier in health and disease. *Epilepsia* 2012, 53: 1-6.

Abid MR, Yi X, Yano K, Shih SC, Aird WC. Vascular endocan is preferentially expressed in tumor endothelium. *Microvasc Res* 2006, 72: 136-145.

Alsio J, Nordenankar K, Arvidsson E, Birgner C, Mahmoudi S, Halbout B, Smith C, Fortin GM, Olson L, Descarries L, Trudeau LE, Kullander K, Levesque D, Wallen-Mackenzie A. Enhanced sucrose and cocaine self-administration and cue-inducing drug seeking after loss of VGLUT2 in midbrain dopamine neurons in mice. *J Neurosci* 2011, 31: 12593-12603.

Alvarez JI, Katayama T, Prat A. Glial influence on the blood brain barrier. *Glia* 2013, 61: 1939-1958.

Ambach G, Palkovits M. Blood supply of the rat hypothalamus. II. Nucleus paraventricularis. *Acta Morphol Acad Sci Hung* 1974, 22: 311-320.

Armulik A, Genove G, Mae M, Nisancioglu MH, Wallgard W, Niaudet C, He L, Norlin J, Lindblom P, Strittmatter K, Johansson BR, Betsholtz C. Pericytes regulate the blood-brain barrier. *Nature* 2010, 468: 557-561.

Armstrong WE, Warach S, Hatton G I, McNeill TH. Subnuclei in the rat hypothalamic paraventricular nucleus: a cytoarchitectural, horseradish peroxidase and immunocytochemical analysis. *Neuroscience* 1980, 5: 1931-1958.

Badaut J, Nehlig A, Verbavatz J, Stoeckel M, Freund-Mercier M, Lasbennes F. Hypervascularization in the Magnocellular Nuclei of the Rat Hypothalamus: Relationship with the Distribution of Aquaporin-4 and Markers of Energy Metabolism. *J Neuroendocrinol* 2000, 12: 960-969.

Bake S, Sohrabji F. 17beta-estradiol differentially regulates blood-brain barrier permeability in young and aging female rats. *Endocrinology* 2004, 145: 5471-5475.

Bale TL. Sensitivity to stress: dysregulation of CRF pathways and disease development. *Horm Behav* 2005, 48: 1-10.

Basir MA. Vascular supply of pituitary in the dog. *Jour Anal* 1931, 66: 387.

Baum M, Ortiz L, Quan A. Fetal origins of cardiovascular disease. *Curr Opin Pediatr* 2003, 15: 166-70.

Baune BT, Stuart M, Gilmour A, Wersching H, Heindel W, Arolt V, Berger K. The relationship between subtypes of depression and cardiovascular disease: a systematic review of biological models. *Transl Psychiatry* 2012, 2: 92.

Becker JB, Arnold AP, Berkley KJ, Blaustein JD, Eckel LA, Hampson E, Herman JP, Marts S, Sadee W, Steiner M, Taylor J, Young E. Strategies and methods for research on sex differences in brain and behaviors. *Endocrinology* 2005, 146: 1650-1673.

Bell RD, Winkler EA, Sagare AP, Singh I, LaRue B, Deane R, Zlokovic BV. Pericytes control key neurovascular functions and neuronal phenotype in the adult brain and during brain aging. *Neuron* 2010, 68: 409-427.

Bertram CE, Hanson MA. Prenatal programming of postnatal endocrine responses by glucocorticoids. *Reproduction* 2002, 124: 459-67.

Biag J, Huang Y, Gou L, Askarinam A, Hahn JD, Toga AW, Hintiryan H, Dong HW. Cyto- and chemoarchitecture of the hypothalamic paraventricular nucleus in the C57BL/6J male mouse: A study of immunostaining and multiple fluorescent tract tracing. *J Comp Neurol* 2012, 520: 6-33.

Biancardi, VC, Son SJ, Ahmadi A, Filosa JA, Stern JE. Circulating angiotension II gains access to the hypothalamus and brain stem during hypertension via breakdown of the blood-brain barrier. *Hypertension* 2013, epub ahead of print.

Bingham B, Williamson M, Viau V. Androgen and estrogen receptor-beta distribution within spinal-projecting and neurosecretory neurons in the paraventricular nucleus of the male rat. *J Comp Neurol* 2006, 499: 911-923.

Bonaventura MM, Catalano PN, Chamson-Reig A, Arany E, Hill D, Bettler B, Saravia F, Libertun C, Lux-Lantos VA. GABAB receptors and glucose homeostasis: evaluation in GABAB receptor knockout mice. *Am J Physiol Endocrinol Metab* 2008, 294: 157-167.

Bonkowski D, Katyshev V, Balabanov RD, Borisov A, Dore-Duffy P. The CNS microvascular pericyte: pericyte-astrocyte crosstalk in the regulation of tissue survival. *Fluids and Barriers of the CNS* 2011, 8: 8.

Bonthuis PJ, Cox KH, Searcy BT, Kumar P, Tobet S, Rissman EF. Of mice and rats: key species variations in the sexual differentiation of brain and behavior. *Front Neuroendocrinol* 2010, 31: 341-358.

Bozoyan L, Khightyan J, Saghatelian A. Astrocytes control the development of the migration-promoting vascular scaffold in the postnatal brain via VEGF signaling. *J Neurosci* 2012, 32: 1687-1704.

Braga VA, Medeiros IA, Ribeiro TP, Franca-Silva MS, Botelho-Ono MS, Guimaraes DD. Angiotension-II- induced reactive oxygen species along the SFO-PVN-RVLM pathway: implications in neurogenic hypertension. *Braz J Med Biol Res* 2011, 44: 871-6.

Brunton PJ. Resetting the dynamic range of hypothalamic-pituitary-adrenal axis stress responses through pregnancy. *J Neuroendocrinol* 2010, 22: 1198-1213.

- Burek M, Forster CY. Cloning and characterization of the murine claudin-5 promoter. *Mol Cell Endocrinol* 2009, 298: 19-24.
- Callahan MF, Kirby RF, Cunningham JT, Eskridge-Sloop SL, Johnson AK, McCarty R, Gruber KA. Central oxytocin systems may mediate a cardiovascular response to acute stress in rats. *Am J Physiology* 1989, 256: 1369-77.
- Catalano PN, Bonaventura MM, Silveyra P, Bettler B, Libertun C, Lux-Lantos VA. GABA(B1) knockout mice reveal alterations in prolactin levels, gonadotropic axis, and reproductive function. *Neuroendocrinology* 2005, 82: 294-305.
- Chen LY, Liu X, Wang SL, Qin CY. Over-expression of the Endocan Gene in Endothelial Cells from Hepatocellular Carcinoma is Associated with Angiogenesis and Tumour Invasion. *J Int Med Res* 2012, 38: 498-510.
- Chip S, Nitsch C, Wellmann S, Kapfhammer JP. Subfield-specific neurovascular remodeling in the entorhino-hippocampal-organotypic slice culture as a response to oxygen-glucose deprivation and excitotoxic cell death. *J Cereb Blood Flow Metab* 2013, 33: 508-518.
- Clarke LE, Barres BA. Emerging roles of astrocytes in neural circuit development. *Nat Rev Neurosci* 2013, 14: 311-321.
- Cornelius A, Cortet-Rudelli C, Assaker R, Kerdraon O, Gevaert MH, Prevot V, Lassalle P, Trouillas J, Delhedde M, Mauragr CA. Endothelial expression of endocan is strongly associated with tumor progression in pituitary adenoma. *Brain Pathol* 2012, 22: 757-764.
- Cortes-Sol A, Lara-Garcia M, Alvarado M, Hudson R, Berbel P, Pacheco P. Inner capillary diameter of hypothalamic paraventricular nucleus of female rat increases during lactation. *BMC Neurosci* 2013, 14: 7.
- Craigie EH. On the relative vascularity of various parts of the central nervous system of the albino rat. *J Comp Neurol* 1920, 20: 310-319.
- Dalkara T, Gursoy-Ozdemir Y, Yemisci M. Brain microvascular pericytes in health and disease. *Acta Neuropathol* 2011, 122: 1-9.
- Damsted SK, Born AP, Paulson OB, Uldall P. Exogenous glucocorticoids and adverse cerebral effects in children. *European journal of pediatric neurology. Eur Pediatric Neurol Soc*, 15: 465-477.
- Daneman R. The blood-brain barrier in health and disease. *Ann Neurol* 2012, 72: 648-672.
- Daneman R, Zhou L, Kebede AA, Barres BA. Pericytes are required for blood-brain integrity during embryogenesis. *Nature* 2010, 468: 562-566.
- Davis AM, Henion TR, Tobet SA. Gamma-aminobutyric acidB receptors and the development of the retromedial nucleus of the hypothalamus. *J Comp Neurol* 2002, 449: 270-280.
- DeFranco DB. Subnuclear trafficking of steroid receptors. *Biochem Soc Trans* 1997, 25: 592-597.

- Del Puerto A, Wandosell F, Garrido JJ. Neuronal and glial purinergic receptors in neuron development and brain disease. *Front Cell Neurosci* 2013, 7: 197.
- Del Toro R, Prahst C, Mathivet T, Siegfried G, Kaminker JS, Larrivee B, Breant C, Duarte A, Takakura N, Fukamizu A, Penninger J, Eichmann A. Identification and functional analysis of endothelial tip cell-enriched genes. *Blood* 2010, 116: 4025-4033.
- Dellovade TL, Davis AM, Ferguson C, Sieghart W, Homanics GE, Tobet SA. GABA influences the development of the ventromedial nucleus of the hypothalamus. *J Neurobiol* 2001, 49: 264-276
- Depontieu F, de Freitas Caires N, Gourcerol D, Giordano J, Grigoriu B, Delehedde M, Lassalle P. Development of monoclonal antibodies and ELISA specific for the mouse vascular endocan. *J Immunol Methods* 2012, 378: 88-94.
- Dore-Duffy P, Cleary K. Morphology and properties of pericytes. *Methods Mol Biol* 2011, 686: 49-68.
- Dore-Duffy P, Owen C, Balabanov R, Murphy S, Beaumont T, Rafols JA. Pericyte migration from the vascular wall in response to traumatic brain injury. *Microvascular Research* 2000, 60: 55-69.
- Erickson MA & Banks WA. Blood-brain barrier dysfunction as a cause and consequences of Alzheimer's disease. *J Cereb Flow Metab* 2013, 33: 1500-1513.
- Erickson MA, Dohi K, Banks WA. Neuroinflammation: A common pathway in CNS diseases as mediated at the blood-brain barrier. *Neuroimmunomodulation* 2012, 19: 121-130.
- Ezan P, Andre P, Cisternino S, Saubamea B, Boulay A, Doutremer S, Thomas M, Quenech'du N, Giaume C, Cohen-Salmon M. Deletion of astroglial connexins weakens the blood-brain barrier. *J Cereb Blood Flow Metab* 2012, 32: 1457-1467.
- Fan ZD, Zhang L, Shi Z, Gan ZB, Gao XY, Zhu GQ. Artificial microRNA interference targeting AT(1a) receptors in the paraventricular nucleus attenuated hypertension in rats. *Gene Ther* 2012, 1-8.
- Feng G, Mellor RH, Bernstein M, Keller-Peck C, Nguyen QT, Wallace M, Nerbonne JM, Lichtman JW, Sanes JR. Imaging neuronal subsets in transgenic mice expressing multiple spectral variants of GFP. *Neuron* 2000, 28:41-51.
- Ferguson AV, Latchford, KJ, Samson WK. The paraventricular nucleus of the hypothalamus – a potential target for integrative treatment of autonomic dysfunction. *Expert Opin Ther Targets* 2008, 12: 717-721.
- Finley KH. The capillary bed of the paraventricular and supraoptic nuclei of the hypothalamus. *Res Publ Assoc Res Nerv Ment Dis* 1938, 18: 94-109.
- Ford-Holevinski TS, Castle MR, Herman JP, Watson SJ. Microcomputer-based three-dimensional reconstruction of in situ hybridization autoradiographs. *J Chem Neuroanat* 1991, 4: 373-385.

Forster C, Silwedel C, Golenhofen N, Burek M, Kietz S, Mankertz J, Drenckhahn D. Occludin as direct target for glucocorticoid-induced improvement of blood-brain barrier properties in a murine *in vitro* system. *J Physiology* 2005, 565: 475-86.

Forster C, Waschke J, Burek M, Leers J, Drenckhahn. Glucocorticoid effects on mouse microvascular endothelial barrier permeability are brain specific. *J Physiol* 2006, 573: 413-425.

Frahm, KA, Schow, MJ, Tobet, SA. The Vasculature within the Paraventricular Nucleus of the Hypothalamus in Mice Varies as a Function of Development, Sub-Nuclear Location, and GABA signaling. *Horm Metab Res* 2012, 44: 1-6.

Frahm KA, Nash CP, Tobet SA. Endocan immunoreactivity in the mouse brain: Method for identifying nonfunctional blood vessels. *J Immunol Methods* 2013, 398: 27-32.

Frahm, K. A., Tobet, S. A. Development of the blood-brain barrier within the paraventricular nucleus of the hypothalamus: influence of fetal glucocorticoid excess. Presented at Society for Endocrinology 2013, San Francisco CA. *Endocrine Abstracts* FP03-4/SAT-5.

Francis BM, Yang J, Hajderi E, Brown ME, Michalski B, McLaurin J, Fahnstock M, Mount HT. Reduced tissue levels of noradrenaline are associated with behavioral phenotypes of the TgCRND8 mouse model of alzheimer's disease. *Neuropsychopharmacology* 2012, 37: 1934-1944.

Freeman MR, Rowitch DH. Evolving concepts of gliogenesis: a look way back and ahead to the next 25 years. *Neuron* 2013, 80: 613-623.

Goldman JM, Murr AS, Cooper RL. The rodent estrous cycle: characterization of vaginal cytology and its utility in toxicological studies. *Birth Defects Res B Dev Reprod Toxicol* 2007, 80: 84-97.

Goldstein JM, Handa RJ, Tobet SA. Disruption of fetal hormone programming (prenatal stress) implicated shared risk for sex differences in depression and cardiovascular disease. *Front Neuroendocrinol* 2014, 35: 140-158.

Gosselet F, Candela P, Cecchelli R, Fenart L. Role of the blood-brain barrier in Alzheimer's disease. *Med Sci* 2011, 27: 987-92.

Gu Y, Qin L, Qin X, Xu F. The molecular mechanism of dexamethasone-mediated effect on the blood-brain barrier permeability in a rat brain tumor model. *Neuroscience Letters* 2009, 452: 114-118.

Gyurko R, Leupen S, Huang PL. Deletion of exon 6 of the neuronal nitric oxide synthase gene in mice results in hypogonadism and infertility. *Endocrinology* 2002; 143: 2767-2774.

Harris A, Seckl J. Glucocorticoids, prenatal stress and the programming of disease. *Horm Behav* 2011, 59: 279-289.

Hadoke PW, Lindsay RS, Seckl JR, Walker BR, Kenyon CJ. Altered vascular contractility in adult female rats with hypertension programmed by prenatal glucocorticoid exposure. *J Endocrinol* 2006, 188: 435-442.

Haj-Yasein NN, Vindedal GF, Eilert-Olsen M, Gundersen GA, Skare O, Laake P, Klungland A, Thoren AE, Burkhardt JM, Ottersen OP, Nagelhus EA. Glial-conditional deletion of aquaporin-4 (Aqp4) reduces blood-brain water uptake and confers barrier function on perivascular astrocyte endfeet. *Proc Natl Acad Sci* 2011, 108: 17815-17820.

Handa RJ, Weiser MJ. Gonadal steroid hormones and the hypothalamo-pituitary-adrenal axis. *Front Neuroendocrinol* 2013, epub ahead of print.

Hawkins BT, Davis TP. The blood-brain barrier/neurovascular unit in health and disease. *Pharmacol Rev* 2005, 57: 173-185.

Hedley-Whyte ET, Hsu DW. Effect of dexamethasone on blood-brain barrier in the normal mouse. *Ann Neurol* 1986, 19: 373-377.

Heitzer MD, Wolf IM, Sanchez ER, Witchel SF, DeFranco DB. Glucocorticoid receptor physiology. *Rev Endocr Disord* 2007, 8: 321-330.

Hellstrom M, Kalen M, Lindahl P, Abramsson A, Betscholtz C. Role of PDGF-B and PDGFR-beta in recruitment of vascular smooth muscle cells and pericytes during embryonic blood vessel formation in the mouse. *Development* 1999, 126: 3047-3055.

Herman JP, Ostrander MM, Mueller NK, Figueiredo H. Limbic system mechanisms of stress regulation: hypothalamo-pituitary-adrenocortical axis. *Prog Neuropsychopharmacol Biol Psychiatry* 2005, 29:1201-1213.

Hill JW. PVN pathways controlling energy homeostasis. *Indian J Endocrinol Metab* 2012, 16: S627-636.

Holmes MC, Abrahamsen CT, French KL, Paterson JM, Mullins JJ, Seckl JR. The mother or the fetus? 11beta-hydroxysteroid dehydrogenase type 2 null mice provide evidence for direct fetal programming of behavior by endogenous glucocorticoids. *J Neurosci* 2006, 26: 3840-3844.

Hossain A, Haiman K, Charitidi K, Erhardt S, Zimmermann U, Knipper M, Canlon B. Prenatal dexamethasone impairs behavior and the activation of the BDNF exon IV promoter in the paraventricular nucleus in adult offspring. *J Endocrinol* 2008, 149: 6356-6365.

Iadecola C. Neurovascular regulation in the normal brain and in alzheimer's disease. *Nat Rev Neurosci* 2004, 5: 347-360.

Iqbal M, Gibb W, Mathews SG. Corticosteroid regulation of P-glycoprotein in the developing blood-brain barrier. *Endocrinology* 2011, 152: 1067-1079.

Jacobson LH, Bettler B, Kaupmann K, Cryan JF. Behavioral evaluation of mice deficient in GABA(B(1)) receptor isoforms in tests of unconditioned anxiety. *Psychopharmacology* 2007, 190: 541-553.

Kádár A, Sánchez E, Wittmann G, Singru PS, Füzesi T, Marsili A, Larsen PR, Liposits Z, Lechan RM, Fekete C. Distribution of hypophysiotropic thyrotropin-releasing hormone (TRH)-synthesizing neurons in the hypothalamic paraventricular nucleus of the mouse. *J Comp Neurol* 2010, 518: 3948-3961.

Karemaker R, Kavelaars A, ter Wolbeek M, Tersteeg-Kamperman M, Baerts W, Veen S, Samsom JF, Visser G. H., van Bel F, Heljnen CJ. Neonatal dexamethasone treatment for chronic lung disease of prematurity alters the hypothalamus-pituitary-adrenal axis and immune system activity at school age. *Pediatrics* 2008, 121: e870-878.

Kc P, Balan KV, Tjoe SS, Martin RJ, Lamanna JC, Haxhiu MA, Dick TE. Increased vasopressin transmission from the paraventricular nucleus to the rostral medulla augments cardiorespiratory outflow in chronic intermittent hypoxia-conditioned rats. *J Physiol* 2010, 588: 725-740.

Kim H, Lee JM, Park JS, Jo SA, Kim Y, Kim C, Jo I. Dexamethasone coordinately regulates angiopoietin-1 and VEGF: A mechanism of glucocorticoid-induced stabilization of the blood-brain barrier. *Biochemical and Biophysical Research Communications* 2008, 372: 243-248.

Ladecola C. Neurovascular regulation in the normal brain and in Alzheimer's disease. *Nat Rev Neurosci* 2004, 5: 347-360.

Langlet F, Levin BE, Luquet S, Mazzone M, Messina A, Dunn-Meynell AA, Balland E, Lacombe A, Mazur D, Carmeliet P, Bouret SG, Prevot V, Dehouck B. Tanycytic VEGF-A boosts blood-hypothalamus barrier plasticity and access of metabolic signals to the arcuate nucleus in response to fasting. *Cell Metab* 2013, 17: 607-617.

Lassalle P, Molet S, Janin A, Heyden JV, Tavernier J, Fiers W, Devos R, Tonnel AB. ESM-1 is a novel human endothelial cell-specific molecule expressed in lung and regulated by cytokines. *J Biol Chem* 1996, 271: 20458-20464.

Lee BJ, McDonald SA, Higgins RD. Neurodevelopmental outcomes of extremely low birth weight infants exposed prenatally to dexamethasone versus betamethasone. *Pediatrics* 2008, 121: 289-296.

Lee W, Ku SK, Kim SW, Bae JS. Endocan elicits severe vascular inflammatory responses in vitro and in vivo. *J Cell Physiol* 2014, 229: 620-630.

Levitt NS, Lindsay RS, Holmes MC, Seckl JR. Dexamethasone in the last week of pregnancy attenuated hippocampal glucocorticoid receptor gene expression and elevates blood pressure in the adult offspring in the rat. *Neuroendocrinology* 1996, 64:412-418.

Levy BH, Tasker JG. Synaptic regulation of the hypothalamic-pituitary-adrenal axis and its modulation by glucocorticoids and stress. *Front Cell Neurosci* 2012, 6: 24.

Li S, Haigh K, Haigh JJ, Vasudevan A. Endothelial VEGF sculpts cortical cytoarchitecture. *J Neurosci* 2013, 33: 14809-14815.

Li DP, Pan HL. Role of GABAA and GABAB receptors in the paraventricular nucleus in control of sympathetic vasomotor tone in hypertension. *J Pharmacol Exp Ther* 2007, 320: 615-626.

Li K, Xu E. The role and mechanism of gamma-aminobutyric acid during central nervous system development. *Neurosci Bull* 2008, 24: 195-200.

Liggins GC, Howie RN. A controlled trial of antepartum glucocorticoid treatment for prevention of the respiratory distress syndrome in premature infants. *Pediatrics* 1972, 50: 515-525.

Liu S, Agalliu D, Yu C, Fisher M. The role of pericytes in the blood-brain barrier function and stroke. *Curr Pharm Des* 2012, 18: 3653-3662.

Lossinsky AS, Vorbodt AW, Wisniewski HM. Characteriation of endothelial cell transport in the developming mouse blood-brain barrier. *Dev Neurosci* 1986, 8: 61-75.

Lund TD, Munson DJ, Haldy ME, Handa RJ. Androgen inhibits, while oestrogen enhances, restraint-induced activation of neuropeptide neurones in the paraventricular nucleus of the hypothalamus. *J Neuroendocrinol* 2004, 16: 272-278.

Ma S, Kwon HJ, Huang Z. A functional requirement for astroglia in promoting blood vessel development in the early postnatal brain. *Plos one* 2012, 7: e48001.

Maccari S, Darnaudery M, Morley-Fletcher S, Zuena AR, Cinque C, Van Reeth O. Prenatal stress and long- term consequences: implications of glucocorticoid hormones. *Neurosci Biobehav Rev* 2003, 27: 119-127.

Malaeb SN, Sadowska GB, Stonestreet BS. Effects of maternal treatment with corticosteroids on tight junction protein expression in the cerebral cortex of the ovine fetus with and without exposure to in utero brain ischemia. *Brain Res* 2007, 1160: 11-19.

Maurage CA, Adam E, Mineo JF, Sarrazin S, Debunne M, Siminski RM, Baroncini M, Blond S, Delehedde M. Endocan expression and localization in human glioblastomas. *J Neuropathol Exp Neurol* 2009, 68: 633-641.

McClellan KM, Calver AR, Tobet SA. GABAB receptors role in cell migration and positioning within the ventromedial nucleus of the hypothalamus. *Neuroscience* 2008, 151: 1119-1131.

McClellan KM, Parker KL, Tobet SA. Development of the ventromedial nucleus of the hypothalamus. *Front Neuroendocrinol* 2006; 27: 193-209.

McClellan KM, Stratton MS, Tobet SA. Roles for gamma-aminobutyric acid in the development of the paraventricular nucleus of the hypothalamus. *J Comp Neurol* 2010; 518: 2710-2728.

Menendez A, Alvarez-Uria M. The development of vascularization in the postnatal rat paraventricular nucleus: a morphometric analysis. *J Hirnforsch* 1987, 28: 325-329.

Mitra SW, Hoskin E, Yudkovitz J, Pear L, Wilkinson HA, Hayashi S, Pfaff DW, Ogawa S, Rohrer SP, Schaeffer JM, McEwen BS, Alves SE. Immunolocalization of estrogen receptor beta in the mouse brain: comparison with estrogen receptor alpha. *Endocrinology* 2003, 144: 2055-2067.

Miyata S, Morita S. A new method for visualization of endothelial cells and extravascular leakage in adult mouse brain using fluorescein isothiocyanate. *J Neurosci Methods* 2011, 202: 9-16.

Mombereau C, Kaupmann K, Gassmann M, Bettler B, van der Putten H, Cryan JF. Altered anxiety and depression-related behaviour in mice lacking GABAB(2) receptor subunits. *Neuroreport* 2005, 16: 307-310.

Morita S & Miyata S. Difference vascular permeability between the sensory and secretory circumventricular organs of adult mouse brains. *Cell Tissue Res* 2012, 349: 589-603.

Mueller BR, Bale TL. Sex-specific programming of offspring emotionality after stress early in pregnancy. *J Neurosci* 2008, 28: 9055-9065.

Nakamura O, Ueki K, Hibi T, Shitara N, Matsutani M, Takakura K, Oikawa T. Inhibition of neovascularization and tumor growth by dexamethasone. *No To Shinkei* 1992, 44: 37-41.

Neigh GN, Ownes MJ, Taylor WR, Nemeroff CB. Changes in the vascular area fraction of the hippocampus and amygdala are induced by prenatal dexamethasone and/or adult stress. *J Cereb Blood Flow Metab* 2010, 30: 1100-1104.

Nico B, Ribatti D. Morphofunctional aspects of the blood-brain barrier. *Curr Drug Metab* 2012, 13: 50-60.

Norsted E, Gomuc B, Meiserter B. Protein components of the blood-brain barrier (BBB) in the mediobasal hypothalamus. *J Chem Neuroanat* 2008, 36: 107-21.

O'Regan D, Kenyon CJ, Seckl JR, Holmes MC. Glucocorticoid exposure in late gestation in the rat permanently programs gender-specific differences in adult cardiovascular and metabolic physiology. *Am J Physiol Endocrinol Metab* 2004, 287: 863-870.

Pariante CM. Risk factors for development of depression and psychosis. Glucocorticoid receptors and pituitary implications for treatment with antidepressant and glucocorticoids. *Ann N Y Acad Sci* 2009, 1179: 144-152.

Peixoto EB, Collares-Buzato CB. Modulation of the epithelial barrier by dexamethasone and prolactin in cultured Madin-Darby canine kidney (MDCK) cells. *Cell Biol Int* 2006, 30: 101-113.

Petropoulos S, Gibb W, Matthews SG. Developmental expression of multidrug resistance phosphoglycoprotein (p-gp) in the mouse fetal brain and glucocorticoid regulation. *Brain Res* 2010, 1357, 9-18.

Poppi U. La syndrome anatome-clinica conseguente a lasione dell'art coroidea anteriore. *Rev Di neurol* 1928.

Prosser HM, Gill CH, Hirst WD, Grau E, Robbins M., Calver A, Soffin EM, Farmer CE, Lanneau C, Gray J, Schenck E, Warmerdam BS, Clapham C, Reavill C, Rogers DC, Stean T, Upton N, Humphreys K, Randall A, Geppert M, Davies CH, Pangalos MN. Epileptogenesis and enhances prepulse inhibition in GABA(B1)-deficient mice. *Mol Cell Neurosci* 2001, 17: 1059-1070.

Quaegebeur A, Lange C, Carmeliet P. The neurovascular link in health and disease: molecular mechanisms and therapeutic implications. *Neuron* 2011, 71: 406-424.

Rajowska G, Hughes J, Stockmeier CA, Miguel-Hidalgo J, Maciag D. Coverage of blood vessels by astrocytic endfeet is reduced in major depressive disorder. *Biol Psychiatry* 2013, 73: 613-621.

Romero IA, Radewicz K, Jubin E, Michel CC, Greenwood J, Couraud PO, Adamson P. Changes in cytoskeletal and tight junctional proteins correlate with decreased permeability induced by dexamethasone in cultured rat brain endothelial cells. *Neurosci Lett* 2003, 344: 112-116.

- Ransom B, Behar T, Nedergaard M. New roles for astrocytes (stars at last). *Trends Neurosci* 2003, 26: 520-522.
- Roque S, Oliveira TG, Nobrega C, Barreira-Silva P, Nunes-Alves C, Sousa N, Palha JA, Correia-Neves M. Interplay between depressive-like behavior and the immune system in an animal model of prenatal dexamethasone administration. *Front Behav Neurosci* 2011, 5: 1-8.
- Roudnicky F, Poyet C, Wild P, Krampitz S, Negrini F, Huggenberger R, Rogler A, Strohr A, Hartmann A, Provenzano M, Otto VI, Detmar M. Endocan is upregulated on tumor vessels in invasive bladder cancer where it mediates VEGF-A-induced angiogenesis. *Cancer Res* 2013, 73: 1097-1106.
- Sadowska GB, Malaeb SN, Stonestreet BS. Maternal glucocorticoid exposure alters tight junction protein expression in the brain of fetal sheep. *Am J Physiol Heart Circ Physiol* 2009, 298: 179-188.
- Sarrazin S, Adam E, Lyon M, Depontieu F, Motte V, Landolfi C, Lortat-Jacob H, Bechard D, Lassalle P, Delehedde M. Endocan or endothelial cell specific molecule-1 (ESM-1): a potential novel endothelial cell marker and a new target for cancer therapy. *Biochim Biophys Acta* 2006, 1765: 25-37.
- Sarrazin S, Lyon M, Deakin JA, Guerrini M, Lassalle P, Delehedde M, Lortat-Jacob H. Characterization and binding activity of the chondroitin/dermatan sulfate chain from Endocan, a soluble endothelial proteoglycan. *Glycobiology* 2010, 20: 1380-1388.
- Saubamea B, Cochois-Guegan V, Cisternino S, Scherrmann J. Heterogeneity in the rat brain vasculature revealed by quantitative confocal analysis of endothelial barrier antigen and P-glycoprotein expression. *J Cereb Blood Flow Metab* 2012, 32: 81-92.
- Saunders NR, Daneman R, Dziegielewska MK, Liddelow SA. Transporters of the blood-brain and blood-CSF interfaces in development and in the adult. *Molecular Aspects of Medicine* 2013, 34: 742-752.
- Scherpereel A, Gentina T, Grigoriu B, Sénéchal S, Janin A, Tsicopoulos A, Plénat F, Béchard D, Tonnel AB, Lassalle P. Overexpression of Endocan Induces Tumor Formation. *Cancer Res* 2003, 63: 6064-6089.
- Schuler V, Luscher C, Blanchet C, Klix N, Sansig G, Klebs K, Schmutz M, Heid J, Gentry C, Urban L, Fox A, Spooren W, Jatou AL, Vigouret J, Pozza M, Kelly PH, Mosbacher J, Froestl W, Kaslin E, Korn R, Bischoff S, Kaupmann K, van der Putten H, Bettler B. Epilepsy, hyperalgesia, impaired memory, and loss of pre- and postsynaptic GABA(B) responses in mice lacking GABA(B(1)). *Neuron* 2001, 31: 47-58.
- Shim SH, Hah JH, Hwang SY, Heo DS, Sung MW. Dexamethasone treatment inhibits VEGF production via suppression of STAT3 in head and neck cancer cell line. *Oncol Rep* 2010, 23: 1139-1143.
- Simmons DM, Swanson LW. Comparison of the spatial distribution of seven types of neuroendocrine neurons in the rat paraventricular nucleus: toward a global 3D model. *J Comp Neurol* 2009; 516: 423-441.

Solomon MB, Furay AR, Jones K, Packard AE, Packard BA, Wulsin AC, Herman JP. Deletion of forebrain glucocorticoid receptors impairs neuroendocrine stress responses and induces depression-like behavior in males but not females. *Neuroscience* 2012, 203: 135-43.

Sriramula S, Cardinale JP, Lazartigues E, Francis J. ACE2 overexpression in the paraventricular nucleus attenuates angiotension II-induced hypertension. *Cardiovasc Res* 2011, 92: 401-408.

Stratton MS. Gamma-aminobutyric acid (GABA) in the development of the paraventricular nucleus of the hypothalamus (PVN): implications for adult disease. PhD dissertation, Colorado State University, Fort Collins, 2012, <http://hdl.handle.net/10217/71591>.

Stratton MS, Searcy BT, Tobet SA. GABA regulated corticotropin releasing hormone levels in the paraventricular nucleus of the hypothalamus in newborn mice. *Physiol Behav* 2011, 104: 327-33.

Strekalova T, Couch Y, Kholod N, Boyks M, Marlin D, Leprince P, Steinbusch HM. Update in the methodology of the chronic stress paradigm: internal control matters. *Behav Brain Funct* 2011, 27: 7-9.

Swanson LW, Sawchenko PE. Hypothalamic integration: organization of the paraventricular and supraoptic nuclei. *Annu Rev Neurosci* 1983; 6: 269-324.

Thayer JF, Yamamoto SS, Brosschot JF. The relationship of autonomic imbalance, heart rate variability and cardiovascular disease risk factors. *Int J Cardiol* 2010, 141: 122-131.

Tobet SA, Bless EP, Schwarting GA. Developmental aspects of the GnRH neuronal system. *Mol Cell Endocrinol* 2001, 185: 173-184.

Tobet SA, Chickering TW, King JC, Stopa EG, Kim K, Kuo-Leblank V, Schwarting GA. Expression of gamma-aminobutyric acid and gonadotropin-releasing hormone during neuronal migration through the olfactory system. *Endocrinology* 1996, 137: 5415-5420.

Tobet SA, Handa RJ, Goldstein JM. Sex-dependent pathophysiology as predictors of comorbidity of major depressive disorder and cardiovascular disease. *Pflugers Arch* 2013, 465: 585-594.

Tobet SA, Walker HJ, Seney ML, Yu KW. Viewing cell movement in the developing neuroendocrine brain. *Integr Comp Biol* 2003, 43: 794-801.

Utsumi H, Chiba H, Kamimura Y, Osanai M, Igarashi Y, Tobioka H, Mori M, Sawada N. Expression of GFRalpha-1, receptor for GDNF, in rat brain capillary during postnatal development of the BBB. *Am J Physiol Cell Physiol* 2000, 279: C361-368.

Van den Pol AN. The magnocellular and parvocellular paraventricular nucleus of the rat: intrinsic organization. *J Comp Neurol* 1982, 206: 317-345.

van den Pol AN. GABA immunoreactivity in hypothalamic neurons and growth cones in early development *in vitro* before synapse formation. *J Comp Neurol* 1997, 383: 178-188.

- Van Sorge NM, Doran KS. Defense at the border: the blood-brain barrier versus bacterial foreigners. *Future Microbiol* 2011, 7: 383-394.
- Villringer A, Dimagi U. Coupling of brain activity and cerebral blood flow: basis of functional neuroimaging. *Cerebrovasc Brain Metab Rev* 1995, 7: 240-276.
- Vinukonda G, Dummula K, Malik S, Hu F, Thompson C, Csiszar A, Ungvari Z, Ballabh P. Effect of Prenatal Glucocorticoids on Cerebral Vasculature of the Developing Brain. *Stroke* 2010, 41: 1766-1773.
- Vorbrodt AM, Lossinsky AS, Dobrogowska DH, Wisiewski HM. Distribution of anionic sites and glycoconjugates on the endothelial surfaces of the developing blood-brain barrier. *Brain Res* 1986, 394: 69-79.
- Vorbrodt AW, Dobrogowska DH, Tarnawski M. Immunogold study of interendothelial junction-associated and glucose transporter proteins during postnatal maturation of the mouse blood-brain barrier. *J Neurocytol* 2001, 30: 705-716.
- Vos AA, Bruinse HW. Congenital adrenal hyperplasia: do the benefits of prenatal treatment defeat the risks? *Obstet & Gynecol Surv* 2010, 65: 196-205.
- Warboys CM, Berson RE, Mann GE, Pearson JD, Weinberg PD. Acute and chronic exposure to shear stress have opposite effects on endothelial permeability to macromolecules. *Am J Physiol Heart Circ Physiol* 2010, 298: 1850-1856.
- Waubant E. Biomarkers indicative of blood-brain barrier disruption in multiple sclerosis. *Dis Markers* 2006, 22: 235-244.
- Welberg LA, Seckl JR, Holmes MC. Prenatal glucocorticoid programming of brain corticosteroid receptors and corticotrophin-releasing hormone: possible implications for behavior. *Neuroscience* 2001, 104: 71-79.
- Winkler EA, Bell RD, Zlokovic BV. Central nervous system pericytes in health and disease. *Nat Neurosci* 2011, 14: 1398-1405.
- The World Health Report 2001 - Mental Health: New Understanding, New Hope. <http://www.who.int/whr/2001/en/>.
- Wyrwoll CS, Homes MC. Prenatal excess glucocorticoids exposure and adult affective disorders: A role for serotonergic and catecholamine pathways. *Neuroendocrinology* 2012, 95: 47-55.
- Ye ZY, Li DP, Byan HS, Li L, Pan HL. NKCC1 upregulation disrupts chloride homeostasis in the hypothalamus and increases neuronal activity-sympathetic drive in hypertension 2012, 32: 8560-8568.
- Zandi-Nejad K, Luyckx VA, Brenner BM. Adult hypertension and kidney disease: the role of fetal programming. *Hypertension* 2006, 47: 502-508.
- Zhang SM, Zuo L, Zhou Q, Gui SY, Shi R, Wu Q, Wei W, Wang Y. Expression and distribution of endocan in human tissue. *Biotech Histochem* 2012, 87: 172-178.

Zlokovic BV. The Blood-brain barrier in health and chronic neurodegenerative disorders. *Neuron* 2008, 57: 178-201.

Zuberi Z, Birnbaumer L, Tinker A. The role of inhibitory heterotrimeric G proteins in the control of in vivo heart rate dynamics. *Am J Physiol Regul Integr Comp Physiol* 2008, 295: 1822-1830.

APPENDIX

- A. Permission to reproduce manuscript entitled “GABA_B Receptors and the development of the PVN vasculature”
- B. Permission to reproduce manuscript entitled “Endocan immunoreactivity in the mouse brain: method for identifying nonfunctional blood vessels”

A. Permission to reproduce manuscript entitled “GABA_B Receptors and the development of the PVN vasculature”



Via E-Mail

To: Krystle Frahm
Fort Collins, Colorado

Barbara Elias
Tel.: +49 (0) 711 8931 681
Fax: +49 (0) 711 8931 143
Barbara.Elias@thieme.de

Pages: 1

05. February 2014

License Permission

Permission granted by:

Publisher: Georg Thieme Verlag, Stuttgart

Contact person: Barbara Elias

Street: Rüdigerstr. 14

Postcode / City: 70469 Stuttgart, Germany

Phone / Fax: ++49 711 8931-681 / -143

E-mail: permission@thieme.de

As owner of the copyright we hereby grant permission to use the following material

Frahm et al., The Vasculature within the Paraventricular Nucleus of the Hypothalamus in Mice Varies as a Function of Development, Subnuclear Location, and GABA Signaling, Horm Metab Res 2012; 44(08): 619-624, DOI: 10.1055/s-0032-1304624, © Georg Thieme Verlag KG Stuttgart · New York

for use as part of the depositary copies of your PhD thesis entitled “The Vasculature within the Paraventricular Nucleus of the Hypothalamus” to be published at the Colorado State University.

We grant permission to use this material for the aforesaid publication in printed and electronic form to be stored in the electronic academic repository of the University. The article is to be used in the accepted WORD version without layout. Use of the final PDF version is explicitly excluded. Permission for further rights and for storage in any other repositories is explicitly excluded.

Credit is given to the original publication as above.

Stuttgart, 5. Feb 2014 
Date, place signature
Georg Thieme Verlag KG

Georg Thieme Verlag KG
Rüdigerstraße 14 · 70469 Stuttgart
P.O. Box 30 11 20 · 70451 Stuttgart
Germany

Tel.: +49(0)7 11/89 31-0
Fax: +49(0)7 11/89 31-298
Internet: www.thieme.com

Steuer-Nr. 97108/00604
Ust-Id-Nr. DE147638607
Registered offices
HR Stuttgart A 3499

Deutsche Bank Stuttgart
Account No.: 14 20017
Bank I.D. No.: 600 700 70
BIC: DEUTDE33
IBAN: DE49 6007 0070 0142 0017 00

B. Permission to reproduce manuscript entitled “Endocan immunoreactivity in the mouse brain: method for identifying nonfunctional blood vessels”

ELSEVIER LICENSE TERMS AND CONDITIONS

Feb 17, 2014

This is a License Agreement between krystle frahm ("You") and Elsevier ("Elsevier") provided by Copyright Clearance Center ("CCC"). The license consists of your order details, the terms and conditions provided by Elsevier, and the payment terms and conditions.

All payments must be made in full to CCC. For payment instructions, please see information listed at the bottom of this form.

Supplier	Elsevier Limited The Boulevard, Langford Lane Kidlington, Oxford, OX5 1GB, UK
Registered Company Number	1982084
Customer name	krystle frahm
Customer address	1625 W Elizabeth St L3 Fort Collins, CO 80521
License number	3331440715926
License date	Feb 17, 2014
Licensed content publisher	Elsevier
Licensed content publication	Journal of Immunological Methods
Licensed content title	Endocan immunoreactivity in the mouse brain: Method for identifying nonfunctional blood vessels
Licensed content author	Krystle A. Frahm, Connor P. Nash, Stuart A. Tobet
Licensed content date	15 December 2013
Licensed content volume number	398-399
Licensed content issue number	
Number of pages	6
Start Page	27
End Page	32
Type of Use	reuse in a thesis/dissertation
Portion	full article
Format	both print and electronic
Are you the author of this Elsevier article?	Yes

Will you be translating?	No
Title of your thesis/dissertation	THE VASCULATURE OF THE PARAVENTRICULAR NUCLEUS OF THE HYPOTHALAMUS: INFLUENCE OF DEVELOPMENT, GAMMA-AMINOBUTYRIC ACID (GABA) RECEPTORS, AND PRENATAL GLUCOCORTICOIDS
Expected completion date	May 2014
Estimated size (number of pages)	145
Elsevier VAT number	GB 494 6272 12
Permissions price	0.00 USD
VAT/Local Sales Tax	0.00 USD / 0.00 GBP
Total	0.00 USD
Terms and Conditions	

INTRODUCTION

1. The publisher for this copyrighted material is Elsevier. By clicking "accept" in connection with completing this licensing transaction, you agree that the following terms and conditions apply to this transaction (along with the Billing and Payment terms and conditions established by Copyright Clearance Center, Inc. ("CCC"), at the time that you opened your Rightslink account and that are available at any time at <http://myaccount.copyright.com>).

GENERAL TERMS

2. Elsevier hereby grants you permission to reproduce the aforementioned material subject to the terms and conditions indicated.

3. Acknowledgement: If any part of the material to be used (for example, figures) has appeared in our publication with credit or acknowledgement to another source, permission must also be sought from that source. If such permission is not obtained then that material may not be included in your publication/copies. Suitable acknowledgement to the source must be made, either as a footnote or in a reference list at the end of your publication, as follows:

"Reprinted from Publication title, Vol /edition number, Author(s), Title of article / title of chapter, Pages No., Copyright (Year), with permission from Elsevier [OR APPLICABLE SOCIETY COPYRIGHT OWNER]." Also Lancet special credit - "Reprinted from The Lancet, Vol. number, Author(s), Title of article, Pages No., Copyright (Year), with permission from Elsevier."

4. Reproduction of this material is confined to the purpose and/or media for which permission is hereby given.

5. Altering/Modifying Material: Not Permitted. However figures and illustrations may be

altered/adapted minimally to serve your work. Any other abbreviations, additions, deletions and/or any other alterations shall be made only with prior written authorization of Elsevier Ltd. (Please contact Elsevier at permissions@elsevier.com)

6. If the permission fee for the requested use of our material is waived in this instance, please be advised that your future requests for Elsevier materials may attract a fee.

7. Reservation of Rights: Publisher reserves all rights not specifically granted in the combination of (i) the license details provided by you and accepted in the course of this licensing transaction, (ii) these terms and conditions and (iii) CCC's Billing and Payment terms and conditions.

8. License Contingent Upon Payment: While you may exercise the rights licensed immediately upon issuance of the license at the end of the licensing process for the transaction, provided that you have disclosed complete and accurate details of your proposed use, no license is finally effective unless and until full payment is received from you (either by publisher or by CCC) as provided in CCC's Billing and Payment terms and conditions. If full payment is not received on a timely basis, then any license preliminarily granted shall be deemed automatically revoked and shall be void as if never granted. Further, in the event that you breach any of these terms and conditions or any of CCC's Billing and Payment terms and conditions, the license is automatically revoked and shall be void as if never granted. Use of materials as described in a revoked license, as well as any use of the materials beyond the scope of an unrevoked license, may constitute copyright infringement and publisher reserves the right to take any and all action to protect its copyright in the materials.

9. Warranties: Publisher makes no representations or warranties with respect to the licensed material.

10. Indemnity: You hereby indemnify and agree to hold harmless publisher and CCC, and their respective officers, directors, employees and agents, from and against any and all claims arising out of your use of the licensed material other than as specifically authorized pursuant to this license.

11. No Transfer of License: This license is personal to you and may not be sublicensed, assigned, or transferred by you to any other person without publisher's written permission.

12. No Amendment Except in Writing: This license may not be amended except in a writing signed by both parties (or, in the case of publisher, by CCC on publisher's behalf).

13. Objection to Contrary Terms: Publisher hereby objects to any terms contained in any purchase order, acknowledgment, check endorsement or other writing prepared by you, which terms are inconsistent with these terms and conditions or CCC's Billing and Payment terms and conditions. These terms and conditions, together with CCC's Billing and Payment terms and conditions (which are incorporated herein), comprise the entire agreement between you and publisher (and CCC) concerning this licensing transaction. In the event of any conflict between your obligations established by these terms and conditions and those

established by CCC's Billing and Payment terms and conditions, these terms and conditions shall control.

14. **Revocation:** Elsevier or Copyright Clearance Center may deny the permissions described in this License at their sole discretion, for any reason or no reason, with a full refund payable to you. Notice of such denial will be made using the contact information provided by you. Failure to receive such notice will not alter or invalidate the denial. In no event will Elsevier or Copyright Clearance Center be responsible or liable for any costs, expenses or damage incurred by you as a result of a denial of your permission request, other than a refund of the amount(s) paid by you to Elsevier and/or Copyright Clearance Center for denied permissions.

LIMITED LICENSE

The following terms and conditions apply only to specific license types:

15. **Translation:** This permission is granted for non-exclusive world **English** rights only unless your license was granted for translation rights. If you licensed translation rights you may only translate this content into the languages you requested. A professional translator must perform all translations and reproduce the content word for word preserving the integrity of the article. If this license is for use 1 or 2 figures then permission is granted for non-exclusive world rights in all languages.

16. **Posting licensed content on any Website:** The following terms and conditions apply as follows: Licensing material from an Elsevier journal: All content posted to the web site must maintain the copyright information line on the bottom of each image; A hyper-text must be included to the Homepage of the journal from which you are licensing at <http://www.sciencedirect.com/science/journal/xxxxx> or the Elsevier homepage for books at <http://www.elsevier.com>; Central Storage: This license does not include permission for a scanned version of the material to be stored in a central repository such as that provided by Heron/XanEdu.

Licensing material from an Elsevier book: A hyper-text link must be included to the Elsevier homepage at <http://www.elsevier.com>. All content posted to the web site must maintain the copyright information line on the bottom of each image.

Posting licensed content on Electronic reserve: In addition to the above the following clauses are applicable: The web site must be password-protected and made available only to bona fide students registered on a relevant course. This permission is granted for 1 year only. You may obtain a new license for future website posting.

For journal authors: the following clauses are applicable in addition to the above: Permission granted is limited to the author accepted manuscript version* of your paper.

***Accepted Author Manuscript (AAM) Definition:** An accepted author manuscript (AAM) is the author's version of the manuscript of an article that has been accepted for publication and which may include any author-incorporated changes suggested through the processes of

submission processing, peer review, and editor-author communications. AAMs do not include other publisher value-added contributions such as copy-editing, formatting, technical enhancements and (if relevant) pagination.

You are not allowed to download and post the published journal article (whether PDF or HTML, proof or final version), nor may you scan the printed edition to create an electronic version. A hyper-text must be included to the Homepage of the journal from which you are licensing at <http://www.sciencedirect.com/science/journal/xxxxx>. As part of our normal production process, you will receive an e-mail notice when your article appears on Elsevier's online service ScienceDirect (www.sciencedirect.com). That e-mail will include the article's Digital Object Identifier (DOI). This number provides the electronic link to the published article and should be included in the posting of your personal version. We ask that you wait until you receive this e-mail and have the DOI to do any posting.

Posting to a repository: Authors may post their AAM immediately to their employer's institutional repository for internal use only and may make their manuscript publically available after the journal-specific embargo period has ended.

Please also refer to Elsevier's Article Posting Policy for further information.

18. **For book authors** the following clauses are applicable in addition to the above: Authors are permitted to place a brief summary of their work online only. You are not allowed to download and post the published electronic version of your chapter, nor may you scan the printed edition to create an electronic version. **Posting to a repository:** Authors are permitted to post a summary of their chapter only in their institution's repository.

20. **Thesis/Dissertation:** If your license is for use in a thesis/dissertation your thesis may be submitted to your institution in either print or electronic form. Should your thesis be published commercially, please apply for permission. These requirements include permission for the Library and Archives of Canada to supply single copies, on demand, of the complete thesis and include permission for UMI to supply single copies, on demand, of the complete thesis. Should your thesis be published commercially, please apply for permission.

Elsevier Open Access Terms and Conditions

Elsevier publishes Open Access articles in both its Open Access journals and via its Open Access articles option in subscription journals.

Authors publishing in an Open Access journal or who choose to make their article Open Access in an Elsevier subscription journal select one of the following Creative Commons user licenses, which define how a reader may reuse their work: Creative Commons Attribution License (CC BY), Creative Commons Attribution – Non Commercial - Share Alike (CC BY NC SA) and Creative Commons Attribution – Non Commercial – No Derivatives (CC BY NC ND)

Terms & Conditions applicable to all Elsevier Open Access articles:

Any reuse of the article must not represent the author as endorsing the adaptation of the article nor should the article be modified in such a way as to damage the author's honour or reputation.

The author(s) must be appropriately credited.

If any part of the material to be used (for example, figures) has appeared in our publication with credit or acknowledgement to another source it is the responsibility of the user to ensure their reuse complies with the terms and conditions determined by the rights holder.

Additional Terms & Conditions applicable to each Creative Commons user license:

CC BY: You may distribute and copy the article, create extracts, abstracts, and other revised versions, adaptations or derivative works of or from an article (such as a translation), to include in a collective work (such as an anthology), to text or data mine the article, including for commercial purposes without permission from Elsevier

CC BY NC SA: For non-commercial purposes you may distribute and copy the article, create extracts, abstracts and other revised versions, adaptations or derivative works of or from an article (such as a translation), to include in a collective work (such as an anthology), to text and data mine the article and license new adaptations or creations under identical terms without permission from Elsevier

CC BY NC ND: For non-commercial purposes you may distribute and copy the article and include it in a collective work (such as an anthology), provided you do not alter or modify the article, without permission from Elsevier

Any commercial reuse of Open Access articles published with a CC BY NC SA or CC BY NC ND license requires permission from Elsevier and will be subject to a fee.

Commercial reuse includes:

- Promotional purposes (advertising or marketing)
- Commercial exploitation (e.g. a product for sale or loan)
- Systematic distribution (for a fee or free of charge)

Please refer to Elsevier's Open Access Policy for further information.

21. Other Conditions:

v1.7

If you would like to pay for this license now, please remit this license along with your payment made payable to "COPYRIGHT CLEARANCE CENTER" otherwise you will be invoiced within 48 hours of the license date. Payment should be in the form of a check or money order referencing your account number and this invoice number RLNK501228522.

Once you receive your invoice for this order, you may pay your invoice by credit card. Please follow instructions provided at that time.

Make Payment To:
Copyright Clearance Center
Dept 001
P.O. Box 843006
Boston, MA 02284-3006

For suggestions or comments regarding this order, contact RightsLink Customer Support: customercare@copyright.com or +1-877-622-5543 (toll free in the US) or +1-978-646-2777.

Gratis licenses (referencing \$0 in the Total field) are free. Please retain this printable license for your reference. No payment is required.
